

DISSERTATION

5-IODONAPHTHYL AZIDE LABELING OF SPECIFIC
MEMBRANE PROTEINS VIA ENERGY TRANSFER FROM DONOR
CHROMOPHORES

Submitted by

Bruce I. Meiklejohn

Department of Chemistry

In partial fulfillment of the requirements
for a Degree of Doctor of Philosophy
Colorado State University
Fort Collins, Colorado
Summer 1991

COLORADO STATE UNIVERSITY

July 6, 1991

WE HEREBY RECOMMEND THAT THE DISSERTATION PREPARED UNDER OUR SUPERVISION BY BRUCE IAN MEIKLEJOHN ENTITLED 5- IODONAPHTHYL AZIDE LABELING OF SPECIFIC MEMBRANE PROTEINS VIA ENERGY TRANSFER FROM DONOR CHROMOPHORES BE ACCEPTED AS FULFILLING IN PART REQUIREMENTS FOR THE DEGREE OF DOCTOR OF PHILOSOPHY.

Committee on Graduate Work

Robert A. Brown

Dale G. Coats

Braha Vadamp

Debra A. Rees

B. George Barinas

Advisor

Oren Anderson

Department Head

ABSTRACT OF DISSERTATION
5-IODONAPHTHYL AZIDE LABELING OF SPECIFIC
MEMBRANE PROTEINS VIA ENERGY TRANSFER FROM DONOR
CHROMOPHORES

The conditions required for activation of 5-iodonaphthyl-1-azide (INA) by energy transfer from donor chromophores have been examined and methods developed for identifying specific plasma membrane proteins proximal to known plasma membrane receptors. INA is hydrophobic and when inserted in the plasma membrane lipid bilayer, can be activated through energy transfer from the donor fluorochrome, eosin isothiocyanate (EITC). The energy transfer efficiency was greatly increased under anaerobic conditions; the triplet lifetime of EITC-conjugated to BSA increased from 10 μ sec to approximately 1 msec in solutions treated with glucose oxidase and catalase for 120 min. To determine whether [125 I]-INA would specifically label known membrane proteins, a μ -chain specific EITC-derivatized anti-murine IgM antibody was incubated with murine B-lymphocytes treated with 2.6×10^{-5} M [125 I]-INA. When B-lymphocytes were irradiated with 40 mW per centimeter 514 nm light from an argon ion laser, the 66 kDa IgM heavy chain was derivatized with INA and identified on autoradiographs of SDS-PAGE gels. In similar experiments, 2H3 rat basophilic

leukemia cells were incubated with EITC-IgE which bound to the monomeric Fc_ϵ receptor. Four [^{125}I]-INA derivatized plasma membrane proteins with molecular weights of 53, 38, 34, and 29 kDa were identified on autoradiographies of SDS-gels. When IgE was crosslinked with mouse anti-rat IgE three additional proteins with molecular weights of 60, 54, and 43 kDa, were labeled with the photoprobe. Under these conditions the receptor was known to be part of large molecular weight aggregates which contain non-receptor proteins. Collectively, these results suggest that INA may be useful in characterizing protein-protein interactions in the plasma membranes of intact cells under physiological conditions.

Bruce Ian Meiklejohn
Chemistry Department
Colorado State University
Fort Collins, CO 80523
Summer 1991

To my loving wife Susan, mother Mindy, and father Al.

ACKNOWLEDGMENTS

I wish to thank Professor George Barisas for his guidance and many suggestions during the completion of this work.

I would also like to thank Dr. Roess for her guidance and understanding in the rough times.

In addition I am indebted to the members of the Barisas group for their needed assistance. In particular , I would like to thank Tom Londo, Dr. Rahman, and Dr. Kenny for their helpfulness in completing this project.

Finally I would like to express my deepest appreciation to my wife Susan, mother Mindy, and father Al for their continued encouragement and support throughout my studies at Colorado State University.

TABLE OF CONTENTS

		<u>Page</u>
Chapter I	HISTORICAL BACKGROUND.....	1
I.1	Introduction.....	1
I.2	Membrane Probes.....	4
I.3	Photoaffinity Probes.....	6
I.4	Energy Transfer.....	9
Chapter II	MATERIAL AND METHODS	
II.1	Chemicals.....	15
II.2	Preparation of 5-Iodonaphthyl-1-azide	17
II.3	Preparation of Ester Derivative.....	17
II.4	Production of Anti-INA Antibodies....	20
II.5	Immunization.....	21
II.6	Rabbit Bleeding.....	22
II.7	Antibody Purification.....	22
II.8	ELISA for Anti-INA Antibodies.....	23
II.9	Eosin Triplet Lifetime Measurements..	25
II.10	INA Characterization.....	26
II.11	Red Blood Cell Experiment.....	28
II.12	Eosin Conjugation.....	29
II.13	Magnetic Beads.....	31
II.14	SDS-PAGE Electrophoresis.....	32
II.15	Immuno-transfer.....	33
II.16	Immunoblot for INA-derivatized Proteins.....	34
II.17	Gel Silver staining.....	34
II.18	Autoradiography.....	35
II.19	Gel Scanning.....	36
II.20	Gel Drying.....	36
II.21	INA Derivatization of sIgM on B-Cells	36
II.22	Immunoblot for IgM Heavy Chain.....	38
II.23	IgE Energy Transfer.....	38
Chapter III	Results	
III.1	Characterizing INA.....	42
III.2	Characterizing INA Derivative.....	46
III.3	Coupling INA to a Carrier Protein....	58

III.4	Anti-INA Antibody Production.....	61
III.5	Affinity Chromatography.....	63
III.6	Eosin Triplet Lifetime vs. Oxygen Depletion.....	64
III.7	INA Energy Transfer.....	76
III.8	Oxygen Tension vs. Transfer Efficiency	92
III.9	INA Labeling of RBC Proteins.....	92
III.10	INA Derivatization of sIgM on B-Cells.	96
III.11	Photoaffinity Labeling of Fc Receptor on 2H3 Cells.....	104
Chapter IV	Discussion.....	113
Chapter V	References.....	129

LIST OF TABLES

<u>Table</u>	<u>Title</u>	<u>Page</u>
I.	TLC Results of INA derivative Intermediates.....	51
II.	Anti-INA Antibody Specificity.....	62
III.	Oxygen Depletion Values.....	68
IV.	Eosin-BSA Triplet Lifetimes.....	77
V.	INA Converted vs. Time.....	83
VI.	Transfer Efficiency vs. Laser Power.....	86
VII.	Transfer Efficiency vs. [Eosin].....	89
VIII.	Transfer Efficiency vs. [INA].....	93
IX.	Summary Of Red Blood Cell Energy Transfer Experiments.....	98
X.	Molecular Weights of Proteins Labeled with INA in the IgE Energy Transfer Experiments.....	112

LIST OF FIGURES

<u>Figure</u>	<u>Title</u>	<u>Page</u>
1.	Schematic of the Biological Membrane....	2
2.	Possible Fates of Nitrenes.....	8
3.	Possible Energy Transfer.....	10
4.	Instrumental Block Diagram.....	41
5.	Synthesis of 5-Iodo-Naphthyl Azide.....	43
6.	Absorbance Spectrum For INA.....	44
7.	Photodecomposition of INA using U.V. Light.....	45
8a.	Synthesis of INA Derivative.....	48
8b.	Synthesis of INA Derivative (cont).....	49
8c.	Synthesis of INA Derivative (cont).....	50
9.	U.V. / Vis spectrum for INA carboxyl Intermediate.....	52
10.	NMR Spectrum for 1,5 dinitronaphthalene.	54
11.	NMR Spectrum for the compound 5-Iodo 1-nitro-naphthalene	55
12.	NMR Spectrum for 5-Iodo-naphthyl-1-amine	56
13.	U.V. Spectrum for the compound 5-Iodo-naphthyl-1-amine.....	57
14.	NMR Spectrum for Carboxyl INA-Derivative	59
15.	UV Spectrum for the INA Derivatized Protein	60
16.	Coupling Reaction of Protein to Affinity Column Reacti-Gel.....	65

17.	Affinity Chromatography Elution Profile.	66
18.	Percent Oxygen in Solution vs. Time.....	69
19.	UV / Vis. Spectrum for Eosin.....	70
20.	EITC Coupling Chemistry to Protein.....	72
21.	EITC-BSA Conjugate U.V./Vis Spectrum....	73
22.	Polarized Fluorescence Depletion Curve for 75% Oxygen in EITC-BSA Solution.....	74
23.	Polarized Fluorescence Depletion Curve for 7% Oxygen in EITC-BSA Solution.....	75
24.	EITC-BSA Lifetime vs. Percent Oxygen....	78
25.	Extraction Chemistry for Characterizing INA Energy Transfer Efficiency.....	80
26.	Spectrum for INA Conversion vs. Time....	81
27.	Plot of INA Conversion vs. Time.....	82
28.	Spectrum for INA Conversion vs. Power...	84
29.	Plot of INA Conversion vs. Laser Power.	87
30.	Spectrum for INA Conversion vs. [Eosin].	88
31.	Plot of INA Conversion vs. [Eosin].....	90
32.	Spectrum for INA Conversion vs. [INA]...	91
33.	Plot of INA Conversion vs. [INA].....	94
34.	Transfer Efficiency vs. Deoxygenation...	95
35.	Red Blood Cell Schematic Diagram.....	97
36.	B-Cell Schematic Diagram.....	100
37.	Photograph of B-Cell Autoradiograph.....	102
38.	Densitometer Scan of B-Cell Autoradiograph.....	103
39.	IgE Non-Crosslinking Schematic Diagram..	106

40.	IgE Crosslinking Schematic Diagram.....	107
41.	Photograph of a Silverstain of Proteins Present in Rat Basophile Membrane.....	108
42.	Densitometer Scan of the Crosslinking and Non-Crosslinking Energy Transfer Experiments.....	109
43	Gel Scan of the Autoradiograph for RBL Cells INA Labeled Cells by Energy Transfer.....	110
44	Enezyme Deoxygenation System.....	118
44	IgE Molecule.....	126

CHAPTER I

HISTORICAL BACKGROUND

I.1 Introduction

Cell membranes are composed of a phospholipid bilayer together with proteins that constitute various receptors and form the membrane architecture (Figure 1). These membrane proteins can be grossly classified as intrinsic proteins and peripheral proteins. Intrinsic proteins are hydrophobic and are embedded in the lipid bilayer. Peripheral proteins, on the other hand, are hydrophilic and bind to the polar surface of the membrane.

Several lines of evidence point to the involvement of receptor aggregation and interaction with additional membrane proteins as functional components of a variety of hormonal signal transduction systems. Thus aggregation of the receptors for insulin (1), epidermal growth hormone (2), and gonadotropin releasing hormone (3) has been proposed to be central to the transduction of signals mediated by these receptors, and elicitation of a biological response. Furthermore, associations between receptors and additional membrane proteins such as Major Histocompatible Class I antigen MHC I have been proposed to be involved in the

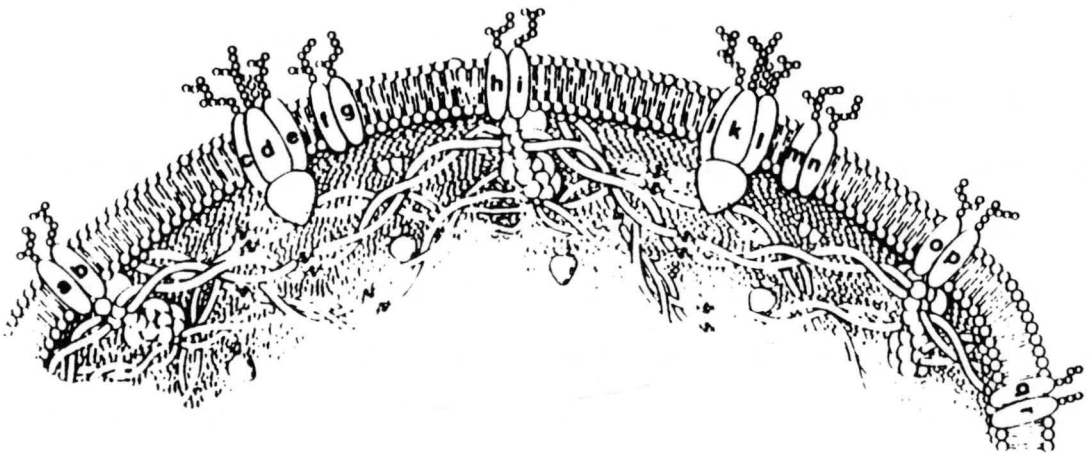


Figure 1. A schematic of a biological membrane depicting various structures and receptors.

function of the receptors for insulin, epidermal growth factor, and glucagon (4,5). Collectively, these observations indicate that simple ligand binding to a specific receptor may not be sufficient to produce a biological response. Therefore, characterizing the different proteins that constitute these membrane receptors would assist in understanding the receptors and cellular function. For example, the Fc_ϵ receptors on rat basophile for IgE have been structurally characterized to consist of 3 protein domains, the α , β , and γ domains (6,7). These proteins associate to form the portion of the Fc_ϵ receptor capable of binding the IgE molecule with high affinity (K_a of approximately 10^{10} liters/mole) (8). Bound IgE molecules then serve as receptors for binding of antigen which results in the release of vasoactive amines (9).

Because they are physically embedded in the lipid bilayer of the cell membrane, intrinsic proteins are more difficult to study. Typically, methods used for studying intrinsic proteins involve identifying and extracting the proteins, followed by out-of-membrane characterization. Antibodies that are specific to the intrinsic membrane protein of interest are usually employed for in-membrane identification (10). The antibody is labeled with a marker, for example a fluorophore, that can be detected (11-13). This is followed by solubilization of the these proteins. Harsh detergents such as CHAPS for the IgE receptor (6) and cholate for

acetylcholine receptor (14) have been used to extract such proteins.

Those conventional methods of intrinsic protein characterization, however, have limited success. Detergent solubilization can destroy the protein structure (14). Also, since the antibody is directed against one subunit of a receptor and not the entire receptor, any association between proteins within the receptor is lost once the proteins are removed from the membrane. Additionally, many antibodies are not capable of binding to the original protein once removed from the membrane. Thus, the *in vitro* identification is impossible. Because the ability to identify these membrane proteins out of the membrane is extremely important many different probes have been examined as well as techniques.

I.2 Membrane Probes

One class of protein probes are homo bifunctional reagents (15,16) that non-specifically and chemically crosslink proteins within the membrane. For example, glutaraldehyde (17) will crosslink the amine groups of lysine with an aldehyde, forming a Schiff base. This crosslinking occurs when the lysine and aldehyde are approximately 5-15 Å apart (18). Due to the large numbers of lysine residues on proteins, this method results in a high degree of crosslinking and a complex protein pattern observed on electrophoretic gels (19).

The complex patterns can be simplified by using homobifunctional reagents with a disulfide functional group (18,20), and a group such as di-methyl-3,3'-dithiobispropionimide dihydrochloride (21). In this case, intrinsic proteins are non-specifically crosslinked and analyzed on both reducing and non-reducing electrophoretic gels. The disulfide linkage will be cleaved on the reducing gels and no apparent protein crosslinking will be observed. On the other hand, bands present in the non-reduced gel (that are not present in the reduced gel) are attributed to nearest neighbor crosslinking.

Both methods make it possible to identify closely associated proteins throughout the membrane matrix and are not confined to a particular region or receptor on the cellular surface. It is known that various membrane proteins are able to traverse the membrane at approximately 200-1400 nm per sec at room temperature (16). During the time scale of these experiments, two proteins could diffuse together and crosslink, thus appearing to be nearest neighbors when, in actuality, they were not. Diffusional non-specific crosslinking of this type will be a small percentage of the overall labelling. Also, chemical coupling can alter the physical environment of the membrane and lead to poor representation of membrane structure.

I.3 Photoaffinity Probes

Another way of probing intrinsic membrane proteins is by using photochemical probes (22). One advantage of using a photochemical probe is that it will covalently label membrane proteins of interest under mild conditions (23). The probe reacts with functional groups on intrinsic proteins via carbon-hydrogen bonding (24). Fortunately, the conditions needed for this type of coupling reaction are compatible with membrane physiological conditions and because the probe is activated photochemically the length of the reaction can be controlled. This reduces non-specific diffusional crosslinking.

A majority of hydrophobic photochemical reagents are aromatic azides (22). Aromatic azides were first used by Knowles (24) to study the binding specificity of an antibody with an antigen. The hydrophobicity of the reagent allows for easy insertion of the probe into the lipid bilayer (25-27). Once embedded within the plasma membrane, photochemical probes can be activated when irradiated with the appropriate wavelength of light. Probes such as phenyl azides with alkyl substituents, e.g. azidophenylalanine, have activation wavelengths of approximately 250 nm (28,29). Unfortunately, the ultraviolet excitation wavelength causes decomposition of nucleic acids and proteins (30). If, however, the functional groups on the aromatic azides are modified, for example with nitro group or halogens, an increase in the activation

wavelength occurs. This, renders the probe more useful for membrane studies (31). Longer wavelengths of light are used to activate the photoprobes. This avoids degradation of the intrinsic protein during labeling (22).

Irradiation of aromatic azides with the proper wavelength of light causes the formation of an active nitrene (32-34). Once formed, the nitrene reacts indiscriminately with molecules within the membrane by a variety of mechanisms: carbon-hydrogen insertion, addition, hydrogen abstraction, rearrangement, and nucleophilic attack (Figure 2) (24). The most probable reaction is abstraction of a hydrogen molecule from the solvent. However, the mechanism of action that renders the nitrene useful as a photoprobe for in membrane protein is carbon-hydrogen or oxygen-hydrogen insertion (22). Carbon-hydrogen insertion has been shown to constitute only a small percent of the overall nitrene reaction (28). For example, phenylazides used to label proteins embedded in the membrane of artificial phospholipid vesicles (liposomes) were reported to label only approximately 3.3% of the highly unsaturated protein soybean lectin and only 0.25% of the saturated protein dimyristoyllectin present on the liposome (28). Therefore, aromatic azides are not useful for labeling proteins that do not contain a "hydrophobic pocket" (35). Addition of electron withdrawing substituents on the aromatic azide increases the reactivity of the nitrene and thus increases the number of molecules performing carbon-hydrogen

insertion (22). The efficiency of coupling is greater when the probe is held in close proximity to the protein of interest during the photo-activation process.

3.4 Energy Transfer

Besides direct irradiation of the aromatic azide at the maximum absorbance wavelength, aromatic azides can also be activated via an energy transfer mechanism which appears to be sensitized energy transfer (Figure 3) (36). Sensitized energy transfer requires an excited donor molecule to transfer its energy to a ground state acceptor molecule. Generally when a donor molecule, is excited to the excited singlet state, it can return to the ground state via fluorescence or non-radiative decay. Also, while in the excited singlet state, it can undergo intersystem crossing to the triplet state, followed by decay to the ground state by phosphorescence. However, in the presence of an acceptor molecule whose triplet energy levels are similar to the donor, energy transfer can occur (37, 38).

POSSIBLE NITRENE REACTIONS

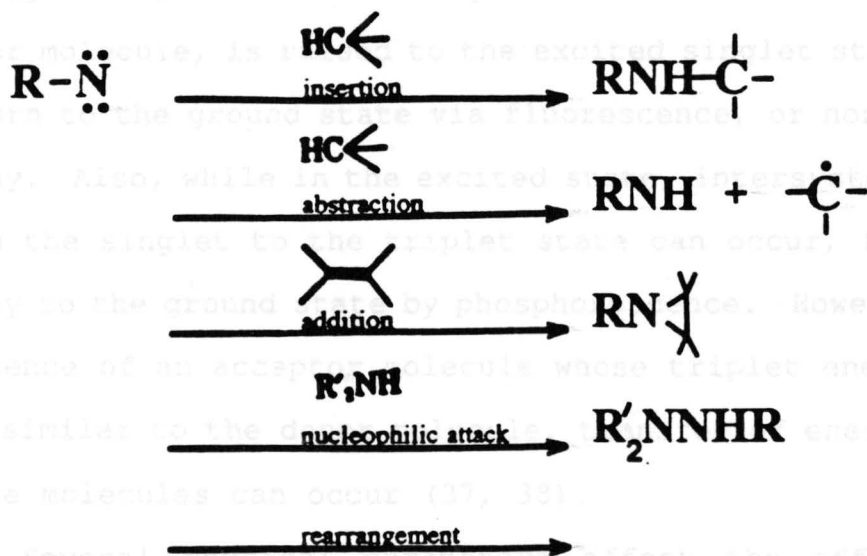


Figure 2. Upon activation the aromatic azide will form an active nitrene which may undergo several chemical reactions.

insertion (22). The efficiency of coupling is greater when the probe is held in close proximity to the protein of interest during the photo-activation process.

I.4 Energy Transfer

Besides direct irradiation of the aromatic azide at the maximum absorbance wavelength, aromatic azides can also be activated via an energy transfer mechanism which appears to be sensitized energy transfer (Figure 3) (36). Sensitized energy transfer requires an excited donor molecule to transfer its energy to a ground state acceptor molecule. Generally when a donor molecule, is raised to the excited singlet state, it can return to the ground state via fluorescence, or non-radiative decay. Also, while in the excited state, intersystem crossing from the singlet to the triplet state can occur, followed by decay to the ground state by phosphorescence. However, in the presence of an acceptor molecule whose triplet energy levels are similar to the donor molecule, transfer of energy between these molecules can occur (37, 38).

Several physical parameters affect the efficiency of transfer between two molecules. The efficiency of transfer is inversely proportional to the distance between the molecules (36). The overall efficiency of energy transfer is also dependent on the proper orientation of the two molecules that are within the transfer distance.

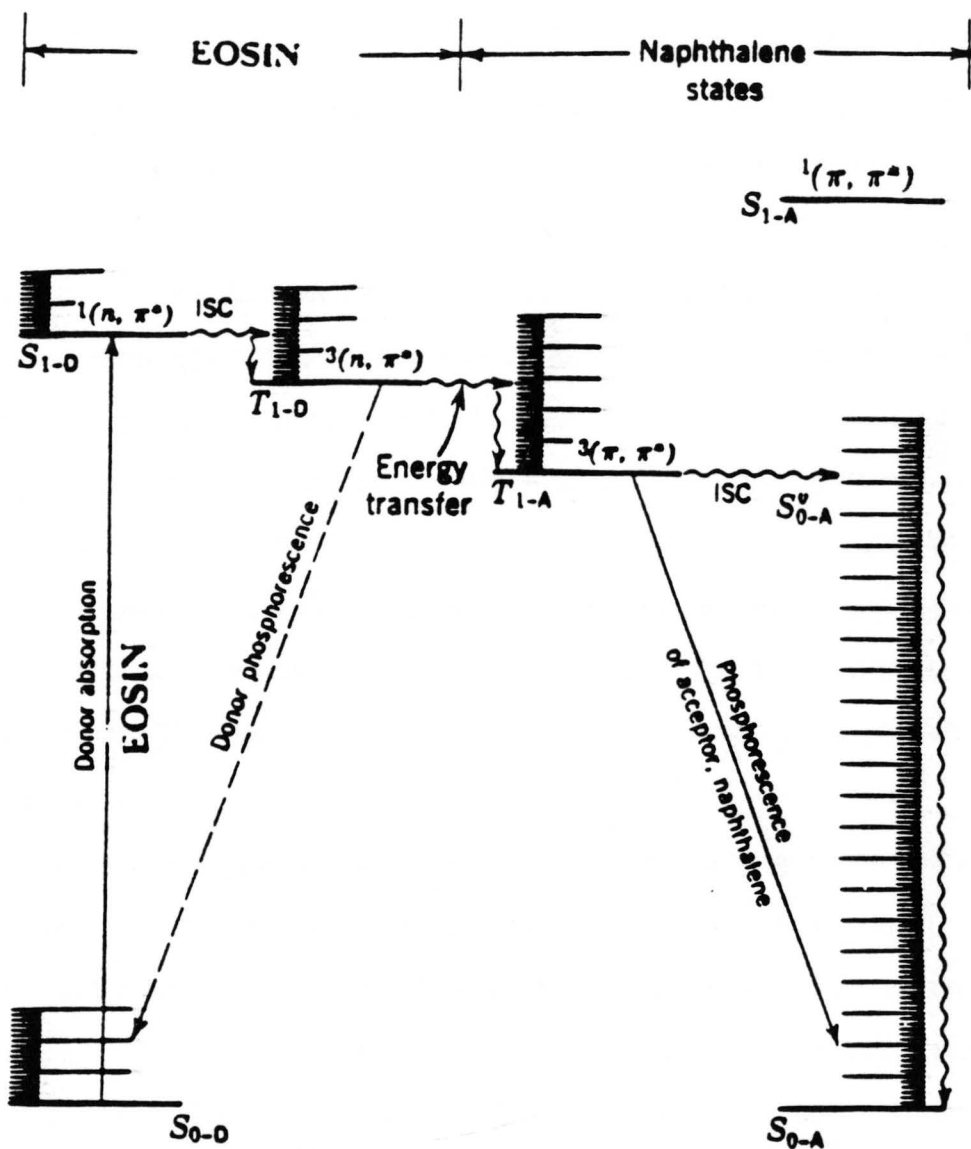


Figure 3. Possible sensitized energy transfer diagram of eosin donor to the naphthalene acceptor.

Additionally, there must be an overlap of the molecular orbitals between the donor and acceptor molecules for sensitized transfer to occur (37). The donor and acceptor molecules must have similar triplet energy levels. Also, a long triplet lifetime of the donor molecule is essential to increase the probability of interacting with an acceptor molecule. In sensitized energy transfer systems, excitation of the acceptor molecules occurs via the triplet state. Therefore, a high degree of intersystem crossing from the excited singlet state to the triplet state by the donor molecule is desirable. Benzophenone (donor) and naphthalene (acceptor) are good examples of properly matched triplet states (38). Chemical modification such as halogenation of the acceptor molecule can also increase the transfer efficiency (39-41).

To increase the effective lifetime molecules that quench the triplet state should be removed from the solution. One triplet quencher that is particularly problematic in solution studies is oxygen (42,43). Oxygen is a triplet energy acceptor (40) and can compete for energy transfer from the excited donor, thus decreasing the effective energy transfer to the acceptor molecule. Therefore removal of oxygen from the system is necessary. Naturally occurring enzymes such as glucose oxidase and catalase are mild deoxygenating systems that can be used to deoxygenate cellular systems (44-46).

Energy transfer can take place in the hydrophobic lipid bilayer if the donor and acceptor molecules are within 100 Å of each other. In biological systems this can be accomplished in two ways either by solubilizing the sensitizing molecule in the lipid bilayer or by holding the donor molecule in the proximity of the membrane surface (47,48). Localized regions on biological membranes can bind specific biomolecules such as hormones and antigens through the actions of in-membrane proteins (e.g. receptors and antibodies) (1). For example, the luteinizing hormone (LH) receptor contains seven transmembrane domains and is present on the surface of the Leydig cells can bind LH (49). Donor molecules can be attached to biomolecules that can bind to the intrinsic membrane proteins. This holds the donor molecule in regions of receptors.

In this study we have examined conditions under which the photochemical probe (50), 1-iodo-5-naphthyl azide (INA), originally synthesized by Gitler (35), can be used to measure the associations between specific receptors and adjacent membrane proteins. Our goal was to optimize this system and achieve maximum energy transfer and protein labeling efficiency. The acceptor hydrophobic azide is allowed to partition throughout the entire lipid bilayer. When irradiated with the appropriate wavelength of light the excited donor fluorochrome activates the azide molecules that are within the 100 Å of the donor. This selectively

crosslinks the membrane proteins of interest. Once energy transfer has taken place between the donor fluorophore and the aromatic azide, the latter can return to the ground state via phosphorescence or non-radiative decay or undergo intersystem crossing which generates an active nitrene. This activated nitrene can then react with a neighboring molecule such as solvent, lipid, or receptor protein. Upon extraction the proteins in which the probe is attached can be identified as associating with the receptor.

Previously, fluorescein has been employed to photosensitize INA (48,50). However, fluorescein has a relatively low quantum yield for triplet formation ($\Phi_t=0.05$) (40,41). This low yield of triplet fluorescein compromises the efficiency of energy transfer (22,40,42). As stated earlier, substitution of an aromatic compound with halogens usually increases the intersystem crossing from the excited singlet to the triplet state (dibromofluorescein $\Phi_t=0.49$, tetrabromofluorescein or eosin $\Phi_t=0.71$) (40,41). Therefore, in our experiments, we used eosin as the triplet donor. In the absence of oxygen, the lifetime of eosin's triplet state can extend to 1 to 2 ms (40,51), thus increasing the probability for triplet energy transfer.

Using energy transfer methods proteins comprising a particular receptor together with functionally associated proteins can be identified. This is an improvement over conventional techniques where the probe molecule is generally

incapable of identifying associated proteins once the proteins are extracted from the membrane. Our method allows for proteins to be labeled *in vivo*. The membrane proteins can then be separated and those having the probe attached are assumed to have existed in the region of the original receptor. Also, because the photoprobe can be identified through the use of radiolabeled. The identification of the proteins is not dependent on the three dimensional structure of the original protein or on the analysis of complex protein patterns on electrophoretic gels.

CHAPTER II

MATERIALS AND METHODS

II.1 Chemicals

1,5-diaminonaphthalene, potassium iodide, Triton X-100, and 1,5-dinitronaphthalene were purchased from Aldrich Chemical CO (Milwaukee, WI). Silica 60-200 mesh, hydrazine, succinic anhydride, rabbit IgG (Cohn fraction II,III), sephadex G-25-150, freunds complete adjuvant, freunds incomplete adjuvant, bovine serum albumin, succinamic acid, polyoxyethylene sorbitan mono laureate, p-nitrophenyl phosphate, 4-chloronaphthol, glucose oxidase, catalase, sodium azide, thiomerosol, agarose, L-glutamine, penicillin, streptomycin, and eosin Y were obtained from Sigma Chemical Co. (St. Louis, MO). Granular (tin 20) mesh was purchased from Mallinckrodt (Paris, KY). The Na- ^{125}I was obtained from ICN Biomedicals, INC. (Costa Mesa, CA). N-hydroxysulfosuccinimide, dicyclohexylcarbodiimide, and Reactigel 6X were obtained from Pierce Chemical Co. (Rockford, IL). The antibiotic ointment was purchased from Goldline Labs (Fort Lauderdale, FL). The sodium heparin was obtained from Solopak Labs (Franklin Park, IL). Goat anti-rabbit alkaline phosphatase, goat anti-rabbit horse radish peroxidase, and goat anti-mouse IgM (heavy chain and light chain) were obtained from American Qualex (La Mirada, CA). The eosin

isothiocyanate was purchased from Molecular Probes (Eugene, OR). Rat anti-mouse T-cell serum was obtained from Accurate Chemical Co. (Westbury, NY). Fetal calf serum was obtained from Hyclone Labs (Logan, UT). Delbecco's minimum essential medium was purchased from Irvine Scientific (Irvine, CA). Rat IgE was purchased from Chemicon International, Inc. (Temecula, CA). Mouse anti-rat IgE was purchased from Bioproducts for Science (Indianapolis, IN).

II.2 Preparation of 5-iodonaphthyl-1-azide

The synthesis of 5-iodonaphthyl-1-azide (INA) has been previously described by Gitler (35). 1,5-diaminonaphthalene¹ was dissolved in 50 % sulfuric acid with gentle heating. The solution was then cooled to 10°C and diazotized using two equivalents of sodium nitrite for 1 hour. It was necessary to lower the temperature to avoid making the diazo dye complex. After diazotization, one equivalent of sodium azide was added in the dark and allowed to react 24 hours to produce compound 1 in Figure 5. All steps after the addition of the azide were performed in the dark. One equivalent of potassium iodide was added and the mixture was allowed to react for an additional 24 hours to form compound 2 in Figure 5. The synthesis of radioactive INA required the use of [I¹²⁵]-NaI in this procedure. The brown reaction mixture was filtered and the precipitate extracted with n-hexane. The hexane extract was passed over a 60-200 mesh silica column (2 cm by 20 cm) packed into twenty times the reaction volume. The column was run at 0.5 ml per minute and monitored at 280 nm and the first peak was collected. The solvent was removed and the resulting pale yellow crystals (5-iodo-naphthyl-1-azide) dissolved in ethanol and stored at 4°C.

II.3 Preparation of INA Ester

To prepare the INA ester, 1,5-dinitronaphthalene was dissolved in 40% hydrazine (52) and stirred for one hour at

28°C. The solution was heated to 90°C for one hour, cooled to 25°C, and allowed to react for 23 hours. The solution was neutralized using 10% HCl and the resulting red precipitate, 1-amino-5-nitronaphthalene, was collected on Whatman #2 filter paper. This reaction produced a 95% yield and the compound was checked for purity using thin layer chromatography with silica as the stationary phase and 10% ammonium hydroxide in butanol as the mobile phase. 1-amino-5-nitronaphthalene was dissolved in 10% HCl in water and mixed for two hours. The solution was cooled to 10°C and mixed for one hour with 1.5 equivalents of sodium nitrite. Two equivalents of potassium iodide were added and allowed to react overnight to form a precipitate of 1-iodo-5-nitronaphthalene which was filtered on a Whatman #2 filter paper and dried. The steps to produce 1-iodo-5-nitronaphthalene produced a 88% yield. The 1-iodo-5-nitronaphthalene precipitate was dissolved in 70% acetic acid: 30% HCl. Ten equivalents of granulated tin (20 mesh) were added, the solution refluxed for two hours, then filtered and cooled to 10°C. Three parts of hot water were added to form a milky yellow solution which was then cooled, neutralized with sodium hydroxide and extracted with ether. The ether layer was filtered using Whatman #2 filter paper and extracted with an equal volume of 10% sulfuric acid. The green/brown precipitate, 1-iodo-5-aminonaphthalene sulfate salt, was collected and dried. The yield was 51% . This compound, which had a melting point of 212°C (53), was dissolved in 10%

methanol and made basic (pH > 10) with sodium hydroxide. The solution was heated to boiling and then cooled slowly to facilitate crystal formation. The brown/white 5-iodo-1-aminonaphthalene crystals were filtered and dried. The compound had a melting point of 75°C. It was tested for purity using thin layer chromatography and for correct symmetry by proton NMR.

5-iodo-1-aminonaphthalene was solubilized in dry THF followed by the addition of 10 equivalents of triethylamine and five equivalents of succinic anhydride. The reaction was allowed to proceed for 24 hours and the supernatant collected. Water was added until the solution turned a creamy brown. The solution was made basic (pH > 10) with sodium carbonate and extracted with ether to remove unreacted amines. The aqueous layer was collected and made acidic (pH < 4) with HCl. The solution was boiled and filtered hot to remove any di-acid formed during the acylation step. The precipitate was collected and dissolved in 20% methanol to crystallize the INA-acid derivative. The INA-acid, produced in 76% yield, was checked for purity using TLC, had a molar absorptivity at 296nm of $10,586 \text{ cm}^{-1}\text{M}^{-1}$, and a melting point of 213°C.

The active INA ester (54,55) was formed by adding one equivalent of n-hydroxysulfosuccinimide to the INA acid derivative, with a slight excess of dicyclohexylcarbodiimide in dry DMF and allowed to mix overnight. The mixture was cooled to 4°C for three hours to allow the urea side product

to precipitate out of solution. The urea was removed by filtration on Whatman #2 filter paper and the filtrate collected. The ester was precipitated by the addition of 20 volumes of ethyl acetate to the filtrate. The INA ester precipitate was collected and stored under nitrogen to prevent hydrolysis of the ester. This type of ester compound is known to react with primary amines to form amides (56) and, when added to proteins such as bovine serum albumin or rabbit immunoglobulin, reacts primarily with surface lysines.

II.4 Production of Anti-INA Antibodies

INA ester attached to a water-soluble carrier protein was needed for the immunization of animals. Direct attachment of INA to the protein was not possible due to the insolubility of the photo-probe in aqueous solution.

Cohn fraction II and III rabbit IgG, or bovine serum albumin, was dissolved in 0.1 M phosphate buffer pH 7.8 at 1 mg/ml. Fifteen equivalents of INA ester were added to these protein solutions, mixed for 30 minutes with gentle stirring, and then quenched with ten equivalents of 1.0 M TRIS. Protein-INA conjugates were separated from free INA by Sephadex G-25-150 size exclusion chromatography. The first protein peak was collected and extinction coefficients for INA, ($\epsilon_{296} = 10,586 \text{ cm}^{-1}\text{M}^{-1}$) and ($\epsilon_{278} = 6,840 \text{ cm}^{-1}\text{M}^{-1}$), were used to calculate INA:protein ratios.

II.5 Immunization

Three five week old New Zealand White rabbits were injected intramuscularly in the right thigh with 0.5 ml of 300 µg/ml INA-IgG (8:1 ratio) in Freund's complete adjuvant. Two weeks later the rabbits were injected with 0.5 ml of INA-IgG (300 µg/ml) in Freund's incomplete adjuvant and boosted 2 months later with 0.5 ml of INA-IgG (300 µg/ml) in Freund's incomplete adjuvant. After 10 days, the serum was collected and screened for anti-INA antibody by a dot blot assay. Nitrocellulose paper (Bio-Rad, Richmond, CA.) was divided into six equal squares, and a 1.5 x 100 mm capillary tube was used to apply 25 µl of each protein to individual squares on the nitrocellulose paper. After drying, the paper was placed in a bath of 2% dried milk in water for 15 minutes to block unreacted sites on the nitrocellulose paper, removed and washed with PBS containing 5% Tween (PBS-Tween). The paper was then placed in a 1:1000 dilution of anti-INA antibody serum (0.5 mg/ml) with PBS-Tween and allowed to incubate for one hour (or overnight if greater sensitivity was needed) (57). The paper was washed with PBS-Tween and placed in goat anti-rabbit horse radish peroxidase (0.5 mg/ml) (American Qualex, LaMirada, CA.) diluted 1:5000 with PBS-Tween, incubated for one hour at room temperature, and then washed with PBS-Tween followed by a wash with distilled water. The nitrocellulose paper was placed in a solution containing 3 mg/ml 4-chloronaphthol 1:5 dilution with 0.1 M tris buffer

0.9% saline pH 7.0 and 0.01% hydrogen peroxide and allowed to react for 20 minutes. A purple precipitate on the paper confirmed the presence of antibody.

II.6 Blood / Serum Collection

Animals that tested positive for circulating antibody were bled by venous puncture of the ear vein. Rabbits were placed in a restraining cage and hair removed from the ear over the vein of interest. The vein was wiped with isopropyl alcohol and placed under a heat lamp. The vein was cut along its length for about 1 cm. Antibiotic ointment (Goldline Labs, Fort Lauderdale, Florida 33309) was placed on the cut to avoid infection and clotting. Blood was collected into a 50 ml tube in which 1 ml of Sodium Heparin 1000 usp units/ml (SoloPak, SoloPak Labs, Franklin Park, Illinois) was added to avoid clotting. Approximately 50 ml of blood was collected from each rabbit. Blood was spun at 300 x g for 15 minutes at 10°C and the serum collected. Serum was frozen in 0.02% sodium azide or run over an affinity column for purification (see Antibody Purification). Rabbits were bled every three days until serum titer tested negative by ELISA.

II.7 Antibody Purification

The INA ester molecules was attached to a solid support matrix and the anti-INA antibody was purified from rabbit

serum by affinity chromatography. Acetone was removed from the (6X) Reacti-Gel carbonyldiimidazole-activated support (Pierce Chemical Company, Rockford Illinois). INA-ester was coupled to BSA (2.6 INA:BSA) and was dissolved in 0.1 M borate buffer pH 9.5 at a concentration of 2-10 mg/ml. Two ml of INA-BSA were added to 1 ml of settled gel. The protein-gel solution was gently mixed for 30 hours at 4°C and then stored in 0.1 M TRIS, pH 7.5 containing 0.02% sodium azide to prevent any organisms from growing in the buffer. On average, 15% of BSA-INA coupled to the gel was capable of binding anti-INA antibody. The gel was packed into a column, equilibrated with 0.01 M phosphate buffer pH 7.2, and the rabbit serum was applied to the column. Unbound proteins (i.e. albumin) were washed from the column with 0.01 M phosphate buffer, pH 7.2. The antibody was eluted from the column using 0.1 M phosphate buffer pH 2.2. Immunoblots showed that the affinity purified antibodies recognized the photoprobe and not the linker arm or carrier protein. The purified antibody solution was brought to pH 7 with a saturated solution of TRIS base, dialyzed overnight against 0.05 M phosphate buffer, pH 7.2 containing 0.02% sodium azide and stored at 4°C.

II.8 ELISA for Anti-INA Antibodies

Determination of presence of anti-INA antibodies required a series of controls. The controls included: 1) blank, for non-specific binding to the ELISA plate, 2) BSA to determine

presence antibodies directed against the carrier protein, 3) BSA-linker arm. The linker arm conjugation is the same procedure as the production of the INA ester from the acid derivative except that succinamic acid is used to form the ester. The succinamic ester was conjugated to BSA at a 8:1 ratio, 4) BSA-INA derivative to determine if antibodies were recognizing the INA molecule, 5) Rabbit antibody to determine if the secondary antibody was working correctly. Each protein solution was made up to a concentration of 1×10^{-5} M in 0.1 M carbonate buffer pH 9.5.

The wells of a 96 well ELISA plate (Costar) were coated with 0.15 ml of the respective protein solution and stored at 4°C overnight. The wells were washed with PBS/Tween 20 (0.1 M phosphate buffer pH 7.2, 0.9% NaCl, 5% polyoxyethylene sorbitan mono-laureate) three times. 0.15 ml of rabbit serum (diluted 1:100 with PBS/Tween 20) was added to each well and allowed to incubate for one hour. The ELISA plate was washed with PBS/Tween 20 three times. The wells were coated with 150 μ l of goat anti-rabbit alkaline phosphatase conjugate (American Qualex, LaMirada CA) (1 mg/ml diluted 1 to 5000 with PBS/Tween 20) and incubated for one hour. The wells were washed three times with PBS/Tween 20 and twice with distilled water to remove detergent that might inhibit the enzyme activity. The substrate solution (10% diethylamine, pH 9.2, 1 Mm $MgCl_2$, 1 mg/ml of p-nitrophenyl phosphate) was added and allowed to react for 20 minutes. The appearance of yellow

color (p-nitrophenol) indicated a positive test and was monitored at 405 nm.

II.9 Eosin Triplet Lifetime Measurements

The triplet lifetime for BSA-EITC was measured as a function of oxygen concentration. Glucose oxidase is a flavoenzyme that catalyzes the oxidation of β -D-glucose in the presence of oxygen to form δ -D-gluconolactone and hydrogen peroxide. Catalase catalyzes the reduction of hydrogen peroxide to water and oxygen. The overall reaction of the enzymes is the oxidation of two glucose molecules to remove one oxygen from solution. The relative levels of catalase (25,000 units per ml) were higher than glucose oxidase (50 units per ml) in order to instantaneously reduce formed peroxide. 0.1 ml of deoxygenating solution (50 units/ml glucose oxidase, 10,000 units/ml catalase), and 50 mM glucose, were placed in 25 ml of 0.1 M phosphate pH 7.4. The vial was sealed and the oxygen level measured using a YSI Model 55 Oxygen Monitor over two hours. At these enzyme levels the O_2 level was reduced to one-half its original level in 30.2 minutes. The solution was assumed to be at equilibrium with atmospheric oxygen at the start of the experiment (7.28 mg O_2 /L, 25°C, at 4896 ft). The triplet lifetime of eosin was determined as a function of O_2 concentration. A 2 mm wide precision rectangular glass capillary tube (Vitro Dynamics, Inc.) with a path length of 0.1 mm was fixed onto a slide with

epoxy for triplet lifetime measurements. The deoxygenating solution together with 10^{-5} M EITC-BSA conjugate with a 5:1 dye to protein ratio were placed into the capillary tube which was sealed. Measurements of eosin triplet lifetime were performed at various oxygen concentrations on the microscope-based polarized fluorescence depletion apparatus described by Yoshida and Barisas (58).

II.10 Characteristics of INA Activation by Energy Transfer

In each of the four experiments performed to characterize energy transfer, the samples were placed in a jacketed cuvette in which cold 0.1 M potassium ferricyanide, pH 12.0, was circulated through the jacket.

One ml eosin (1.0×10^{-6} M) solution in 70/30 ethanol/water at pH 3.0 was placed in the cuvette for irradiation. 0.1 ml of INA stock solution (1.0×10^{-3} M) was added to the cuvette in the dark. The samples were illuminated at 514nm, with a Coherent Radiation 100-10 argon ion laser at 72.5 mW per cm for 0, 5, 10, 15, and 30 minutes. Each sample was extracted with 1 ml hexane and diluted 1:5 with fresh hexane. The hexane solution was scanned from 360 nm to 260 nm in a Beckman DU 70 spectrophotometer to determine the amount of INA converted.

Dependence of INA Activation Rate on Laser Power

One ml eosin Y (1.3×10^{-5} M) solution in 70/30 ethanol/water V/V pH 3.0 and 0.10 ml of INA stock solution

(1.04×10^{-3} M) was added to the cuvette in the dark and exposed to the laser (514 nm) for 15 minutes at 4.5, 9, 18, 36, and 72 mW per cm. The solution was extracted with 1.0 ml of hexane in the dark and diluted 1:5 with fresh hexane. The hexane was scanned from 260 to 360 nm in a Beckman DU 70 spectrophotometer to determine the amount of INA converted.

Dependence of INA Activation Rate on Eosin Concentration

Eosin Y stock solution (4.3×10^{-5} M) in ethanol/water, 70/30 at pH 3.0 was diluted with ethanol/water 70/30 V/V at pH 3.0, 1:2, 1:5, 1:10, 1:20, 1:50. One ml of the eosin solution was added to the cuvette. In the dark 0.10 ml of INA (stock 1.04×10^{-3} M) was added to the cuvette with stirring. The cuvette was placed in the laser beam (514 nm at 72.5 mW per cm) for 30 minutes. Each solution was then extracted with 1 ml of hexane and diluted 1:5 with fresh hexane. The hexane was scanned from 360 nm to 260 nm in a Beckman DU 70 to determine INA converted.

Dependence of INA Activation on INA Concentration

One ml of 6.6×10^{-6} M eosin Y stock solution in 70% ethanol V/V in water was placed in a jacketed cuvette through which ice cold 0.10 M ferricyanide, pH 12.0, was circulated. In the dark, 0.025, 0.05, 0.1, or 0.20 mL of 1.0×10^{-3} M INA diluted to 0.20 mL with ethanol was added to the cuvette. The cuvette was placed in the beam path of a Coherent Radiation

100-10 argon laser tuned to 514 nm and producing 45.5 mW per cm power for 15 min. The sample was then acidified, extracted with 1.0 ml of hexane, and diluted 1:5 with fresh hexane, and was scanned from 360 nm to 260 nm in a Beckman DU 70 spectrophotometer to determine the amount of underivatized INA remaining in the sample.

II.11 INA Labeling of Red Blood Cell Protein

Human red blood cells were obtained and suspended at 1×10^5 cells per ml in 0.10 M phosphate buffer, 0.9% NaCl at pH 7.2. Samples were examined to determine the extent to which activation of INA by energy transfer could occur within a biological membrane. Samples were mixed end over end for one hour after the addition of 0.20 ml of INA (1.0×10^{-4} INA stock in ETOH) or 0.20 ml of ethanol for blank. The samples contained 1.0×10^{-6} M eosin Y in PBS as a non-specific fluorescence donor. Samples exposed to the laser light were irradiated for one hour at 514 nm and 100 mW per cm. Energy transfer samples were placed in a jacketed cuvette in which cold 0.10 M potassium ferricyanide pH 12.0 solution was circulated to avoid activation by ultraviolet or thermal decomposition of the photoprobe. The following energy transfer experiments were performed:

<u>Sample</u>	<u>Chromophore</u>	<u>Photoprobe</u>	<u>Light Source</u>
1) Blank	None	None	None
2) Dark	None	INA	None
3) Sun	None	INA	U.V. lamp
4) Eosin Blank	Eosin	None	None
5) No Eosin	None	INA	Laser 514 nm
6) Aerobic	Eosin	INA	Laser 514 nm
7) Anaerobic	Eosin	INA	Laser 514 nm

All samples were extracted with 9 volumes of cold toluene. One ml of the aqueous layer was removed and placed in a scintillation counter to detect I¹²⁵-INA groups on the proteins. INA attachment to RBC membrane proteins was also determined via immunoblot.

II.12 Eosin Conjugation to Protein

Method 1. 10.0 mg of eosin-isothiocyanate (EITC) were dissolved in 0.10 ml of DMSO and diluted to 1.0 ml with 0.050 M borate buffer pH 9.5, and mixed for 10 minutes in the dark. 2.0 mg of antibody or bovine serum albumin was dissolved in 1.0 ml of 0.050 M borate buffer pH 9.5. Eosin solution was added to the protein and mixed gently overnight. The reaction was stopped by adjusting the pH to 6.0 with saturated TRIS-HCl. To remove unbound dye, a Sephadex G 25-150 column was packed with eight times the reaction volume and equilibrated with 0.050 M phosphate pH 7.2 before adding the protein-dye

mixture. The column was run at 0.50 ml per minute and monitored at 280 nm. The first peak containing the EITC-protein conjugate was collected and then dialyzed against 0.05 M phosphate buffer pH 7.2 for 24 hours. The protein:eosin ratios were determined (ϵ_{533} [Eosin] = 83,000 $\text{cm}^{-1}\text{M}^{-1}$ and ϵ_{280} = 21,600 $\text{cm}^{-1}\text{M}^{-1}$). The reaction conditions were adjusted to obtain a ratio of five eosin molecules per protein for both BSA (eosin triplet lifetime measurements) and goat anti-mouse IgM (murine B-lymphocyte experiment), while the IgE molecules were adjusted to a ratio of three to one for the rat basophil Fc receptor experiments. The protein solutions containing 0.02% sodium azide were stored in the dark at 4°C.

Method II. This was used when conjugating larger amounts of protein or a specific conjugation ratio was required. 10.0 mg of EITC were dissolved in one ml DMSO and diluted with 0.050 M borate pH 9.5 to a total volume of 5.0 ml. The eosin solution was placed in dialysis tubing (cut-off 12 kDa). The protein to be conjugated was dissolved in 0.050 M borate pH 9.5 at a concentration of 2.0 mg/ml.

The EITC dialysis tubing was placed in the protein solution with stirring. After 1 hour 0.10 ml of protein solution was removed and passed through a 5 ml pasteur pipet G-25 size exclusion column. The column was monitored at 280 nm and the first peak was collected and conjugation ratio determined. The reaction was allowed to continue until the desired conjugation ratio was achieved. The reaction was

stopped by the addition of saturated TRIS-HCl bringing the pH down to 6.0. The protein conjugate was passed over a G-25 column size exclusion column. The column was packed to eight times the volume of protein solution and equilibrated with 0.050 M phosphate buffer pH 7.0, run at 0.5 ml per minute, monitored at 280 nm, and the first peak was collected. The protein-eosin conjugate was stored at 4°C in dark and with 0.02% sodium azide.

II.13 Magnetic Beads for Isolation of Mouse B-Cells

Preactivated magnetic beads (Dynal, Fort Lee, N.J.) were washed in distilled water. Rat anti-mouse T-cell serum (Accurate Chemical CO., Westbury, N.Y.) was dissolved in 0.2 M borate buffer pH 9.5 at a concentration of 0.15 mg/ml. Dynal beads were supplied at a concentration of 4×10^8 beads per ml (30 mg/ml). 0.005 mg of rat anti-mouse T-cell antibody were added per ml of magnetic beads. Water was added (equal volume of the antibody solution) to the desired amount of beads. The beads and antibody solution were mixed for 24 hours at 22°C. Using a magnet the beads were removed from the solution. The beads were washed with 0.1 M PBS pH 7.2 for 15 minutes and again the solution removed.

Any unreacted functional groups on the beads were blocked with 1M ethanolamine HCl pH 9.5 and 0.1% Tween-20 for 20 minutes. The beads were then washed in 0.05 M Tris, 0.1 M NaCl, 0.1% BSA, 0.01% thimerasol, 0.1% Tween-20 at pH 7.5 and

incubated for 12 hours. The beads were washed again in ethanolamine buffer for two hours. Beads were stored at 4°C in 0.05 M Tris buffer pH 7.2, 0.1 M NaCl, 0.1% BSA, 0.01 thimerosal (or 0.02% Na-Azide).

II.14 SDS-PAGE Electrophoresis

Electrophoresis was accomplished following the Laemmli SDS-PAGE system (59). Cells from energy transfer experiment were pelleted by centrifugation for 10 minutes at 300 x g. The supernatant was discarded and the pellet resuspended in 0.3 ml of 1% Triton X-100 in the dark. The cell suspension was placed in a sonicator for one hour. To complete solubilization of membrane proteins 0.3 ml of Laemmli SDS sample buffer was added to the cell membrane preparation.

Glass gel casting plates were washed with absolute ethanol and sealed together with approximately 4 ml of 2% agarose at 100°C. Agarose was applied to the plates and allowed to cool to prevent linkage of the separating gel solution before polymerization can occur. Separating gel (9% crosslinking) was poured to approximately 4 cm from the top of the plate and allowed to polymerize for six hours. The separating gel solution was overlaid gently with water to aid the polymerization process. After polymerization the water was poured off and the a stacking gel (3% crosslinking) solution was poured and allowed to polymerize 45 minutes. A

15 well Teflon comb was placed in the solution during the polymerization to form the sample wells.

Samples were applied to the gel and run at 80 Volts for five hours in the dark. The gel was run in the dark to allow separation of free photoprobe from unlabelled membrane proteins.

II.15 Transfer of Proteins from SDS Gel to Nitrocellulose

Twenty sheets of filter paper (Munktell filter paper, grade 1F. Pharmacia, Uppsala, Sweden) and one piece of nitrocellulose paper (trans-blot transfer medium) were cut into 11 x 14 cm pieces. All filter paper and nitrocellulose were handled using gloves. The filter paper was soaked for 30 minutes in transfer buffer (20% methanol, 48 mM Tris base, 0.0375% w/v SDS, and 39 mM glycine). The transfer unit (LKB, 2117 Multiphor II, Bromma, Sweden) anode was washed with distilled water. Nine sheets of filter paper were stacked on the anode making sure not to trap any air bubbles. The nitrocellulose was placed on top of the filter paper stack again avoiding trapped air bubbles. The SDS-gel to be transferred was placed on top of the stack followed by an additional nine sheets of filter paper. The cathode was wetted with distilled water and placed on top of the transfer stack. The transfer was accomplished at 123 mA (0.8 mA per cm²) for one hour. The gel was removed and placed in 45% methanol, 10% acetic acid, and 45% water for 30 minutes. The

nitrocellulose paper was placed in 1% w/v Carnation dry milk for 20 minutes with gentle agitation.

II.16 Immunoblot for INA-Labelled Proteins

Nitrocellulose paper (Bio Rad, Richmond, CA.) was removed from the milk solution, washed with PBS-Tween three times, and then incubated for two hours in a solution of 1×10^{-6} M rabbit anti-INA antibody in PBS-Tween. The paper was washed with PBS-Tween to remove unbound proteins, and then incubated in the secondary antibody solution, goat anti-rabbit horse radish peroxidase (0.5 mg/ml) (American Qualex, LaMirada, CA.) diluted 1:2000 with PBS-Tween, for one hour and then washed with PBS-Tween followed by one wash with distilled water. Paper was then incubated for 20 minutes in 3 mg/ml 4-chloro-1-naphthol (Sigma) diluted 1:5 with 0.1 M tris pH 7.2, 0.9% saline, and 0.01% H_2O_2). A purple precipitate was indicative of a positive test for INA-labelled protein.

II.17 Silver Staining of SDS Gels

The gel to be stained was incubated for one hour in 10% glutaraldehyde to fix the proteins. The gel was washed for 24 hours in four changes of distilled water to facilitate the removal of unreacted glutaraldehyde from the gel. The gel was placed in silver stain solution for 15 minutes. The silver stain solution was prepared by dissolving 2 g $AgNO_3$ in 10 ml of distilled water, and while stirring 4 ml of concentrated

ammonium hydroxide was added drop wise. 53 ml of 0.36% sodium hydroxide was added and brought up to a final volume of 250 ml with distilled water.

The gel was washed three times, 15 minutes each, with distilled water and placed in developing solution (2.5 ml of 1% citric acid, 0.2 ml 37% formaldehyde, to a final volume of 500 ml with distilled water) for three to fifteen minutes depending on desired development. To avoid over-development, the gel was removed from the solution at about 50% total desired color development and washed repeatedly in distilled water.

II.18 Autoradiography

Nitrocellulose paper was removed from the immunotransfer blocking solution (1% carnation dry milk), dried and placed in plastic bag and transfer to a tray exposure cassette. The exposure cassette was lined with Dupont Cronex intensifying screens (Lighting Plus). The film (Kodak X-Omat AR) was placed in contact with the nitrocellulose immunoblot paper and the cassette placed in a -70°C freezer. Due to relatively low levels of I¹²⁵ on the protein, 10 to 14 days was the average exposure time.

Film was removed in the dark from the cassette and placed in Dektol solution (Dektol developer was diluted 1:1 with water) for five minutes. The film was washed for five-minutes in a water bath and placed in an acid fixer bath for five

minutes followed again by a five-minute wash in the water bath. The film was dried and analyzed for labeled protein.

II.19 Scanning Autoradiographs

Autoradiographs were scanned at 300 dot per inch resolution on an Hewlett Packard Scan Jet Plus white light scanner. The system was interfaced with a Microscan 2000 video image analyzer (Technology Resources, Inc., Nashville, TN.).

II.20 Gel Drying

The slab gel dryer (Hoffer Scientific Inst., Drygel Jr., Model SE540) was attached to a vacuum pump with a liquid nitrogen cold trap. On the gel dryer two sheets of filter paper were placed on the 18-gauge stainless steel screen. The gel was placed on top of the filter paper, avoiding trapping pockets of air. The gel was thoroughly washed with water before drying. One sheet of wet cellophane was placed on the gel, again avoiding trapping air bubbles. The porous polyethylene sheet was placed on top of the gel stack followed by the silicon rubber flap. The gel was dried for 50 minutes and then removed from the apparatus for permanent storage.

II.21 INA Derivatization of sIgM on B-Cells

B-cells were isolated 6-8 week old female BALB/c mice. Cells were washed in balanced salt solution (BSS) (60) and

centrifugation at 300 x g for 5 minutes. To lyse red blood cells, the pellet was suspended in 5 ml of 0.87% ammonium chloride, 0.1 M Tris pH 7.2 for three minutes. Intact cells were isolated by centrifugation at 300 x g for 5 min and resuspended in 0.1 M phosphate buffer, 0.9% w/v sodium chloride, pH 7.2. Polyclonal antibodies specific for mouse T cells were conjugated to Dynabeads (Dynal Inc., Fort Lee, N.J.) as described earlier. A 40-fold excess of beads were added to the cell suspension and incubated for 20 minutes. T cells bound to the anti-T cell antibody were removed with a magnet. The remaining cell suspension depleted of T-cells was collected and centrifuged at 300 x g for 5 minutes and the cell pellet was resuspended in 6 ml BSS. 0.6 ml of 26.4 mM [¹²⁵I]-INA was added to the cell suspension and incubated for one hour in the dark with gentle mixing. Cells were centrifuged at 300 x g for 10 minutes and suspended in 6 ml of BSS. [¹²⁵I]-INA activity was determined by counting 1 ml of cell suspension was placed in a Beckman LS 1701 counter.

Three samples were prepared. Sample 1 was incubated with underivatized goat anti-mouse IgM antibody (American Qualex, LaMirada CA.), deoxygenated with 0.1mg/ml glucose oxidase, 0.1mg/ml catalase and 25 mM glucose for 60 minutes, and then exposed to 40 mW per cm 514 nm light for 30 minutes. The beam was filtered using a 514nm band pass filter and expanded to approximately 1 cm in diameter using a 8x Galilean telescope. This telescope was used for all experiments involving the

energy transfer in RBC's, B-cells, and 2H3 cells. Two 1 ml samples were labeled with 0.04 ml of EITC-goat anti-mouse IgM (0.5 mg/ml) for one hour at 21°C in the dark. The cell suspension was washed with BSS to remove unbound antibody and suspended in 1 ml of BSS. After deoxygenation, Sample 2 received no further treatment while Sample 3 was exposed to 40 mW of 514 nm laser light for 30 min.

II.22 Immunoblot for IgM Heavy Chain in B-Cell Energy Transfer

Nitrocellulose was placed for one hour in a solution containing goat anti-mouse IgM horse radish peroxidase conjugate (0.5 mg/ml) specific for the heavy and light chain (American Qualex, LaMirada CA.), diluted 1:2000 with PBS-Tween. The paper was washed with PBS-Tween followed by one wash with distilled water and then placed for 20 minutes in 3 mg/ml 4-chloronaphthol in methanol diluted 1:5 with 0.1 M Tris buffer pH 7.2, 0.9% saline and 0.01% hydrogen peroxide. Immunoblots were photographed and the amount of color development was determined visually.

II.23 Derivatization of INA on Rat Basophilic Leukemia Cells

The 2H3 cells used in these experiments are a subclone of a rat basophil leukemia. 2H3 cells were grown in culture media containing 10% fetal calf serum, 1% L-glutamine, 1 IU/ml penicillin, 1 µg/ml streptomycin, and 88% Dulbecco's minimum essential medium at 37°C and 5% CO₂ in air. Cells

were harvested by centrifugation for 10 minutes at 300 x g and resuspended in 10 ml of BSS. 0.01 ml of 26.4 mM [¹²⁵I]-INA in ethanol was added to the cell suspension in the dark which was incubated for two hours with gentle mixing (ethanol concentration did not exceed 1%). The cell suspension was centrifuged for 10 minutes at 300 x g and the resulting pellet was resuspended in 500 µl BSS.

INA-labeled cells were incubated with 250 µl of 1.4 x 10⁻⁷M EITC-rat IgE in 0.1 M phosphate buffer, pH 7.2 (Chemicon International, Inc., Temecula, CA). The EITC-IgE had a dye to protein ratio of 3 to 1. After 1 hr, cells were obtained by centrifugation at 300 x g for 10 minutes, washed twice with BSS and divided into two 0.5 ml samples. One sample received no further treatment. The second sample was treated with 0.05 ml of a 25 mg/ml stock solution containing mouse anti-rat IgE specific for the IgE heavy chain (Bioproducts for Science, Indianapolis, IN.). Both samples were then incubated for two hours in the dark, washed 3 times with BSS, and finally deoxygenated in one ml of solution containing 0.1 mg/ml glucose oxidase, 0.1 mg/ml of catalase and 25 mM glucose in 0.1 M phosphate buffer pH 7.2 for one hour.

Samples were then placed in a jacketed cuvette through which a solution of 0.1 M ferricyanide pH 12.5 was circulated. The laser beam was passed through a 514 nm band pass filter and a telescope (8x) to expand the beam to approximately 1 cm in diameter prior to the cuvette (Figure 4). The samples were

exposed for two hours to the laser beam (514 nm, 40 mW). The cell samples were collected and membrane preparations were run on SDS gels and autoradiographed for analysis of labeled proteins.

Instrumentation For Energy Transfer System

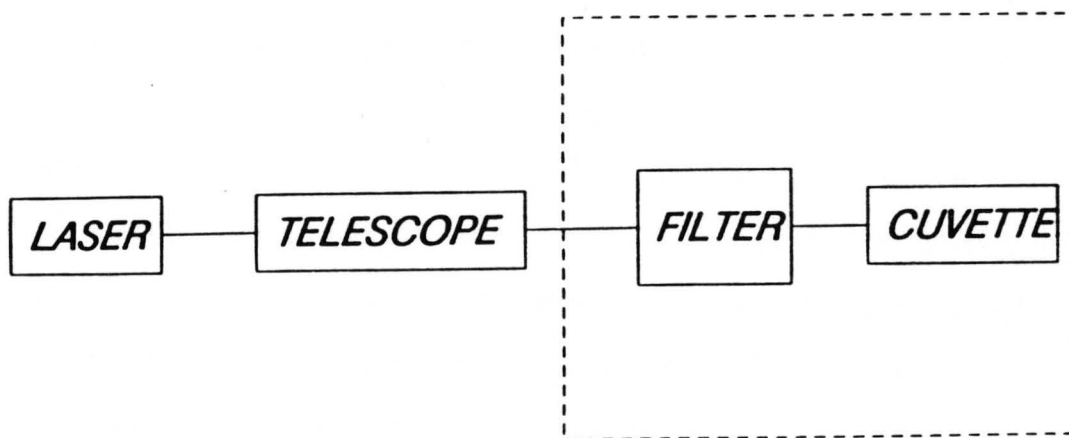


Figure 4. A block diagram of the instrumentation for the energy transfer experiments. A 514 nm laser beam is passed through a 8x Galilean expansion telescope and a 514 nm band pass filter. The beam is then directed into a jacketed cuvette to expose the sample.

Chapter III

RESULTS

III.1 Characterization of INA

Our first objective was to demonstrate that we could conveniently synthesize the photoprobe 5-iodo-1-naphthyl azide, INA, and that we could photoactivate this compound by irradiation with ultra violet light.

INA was synthesized using a modification of Gitler's method (35). Figure 5 depicts the specifics of this synthesis. Typical experiments produced a 68% yield of INA from the 1,5 dinitronaphthalene starting material (the purity of which was tested by melting point analysis).

INA was characterized photochemically by use of U V spectrophotometry (Figure 6). U.V. spectra were obtained for both non-irradiated and irradiated INA solutions. These spectra demonstrated the physical differences of the two resulting compounds. For example, curve A of Figure 7 shows the characteristic absorption maximum at 310 nm for a non-irradiated INA solution. The calculated molar absorptivity for this species is $21,400 \text{ cm}^{-1}\text{M}^{-1}$. Curve C in this figure is a spectrum of the same solution after irradiation with broad band ultraviolet light for three minutes. Here, the

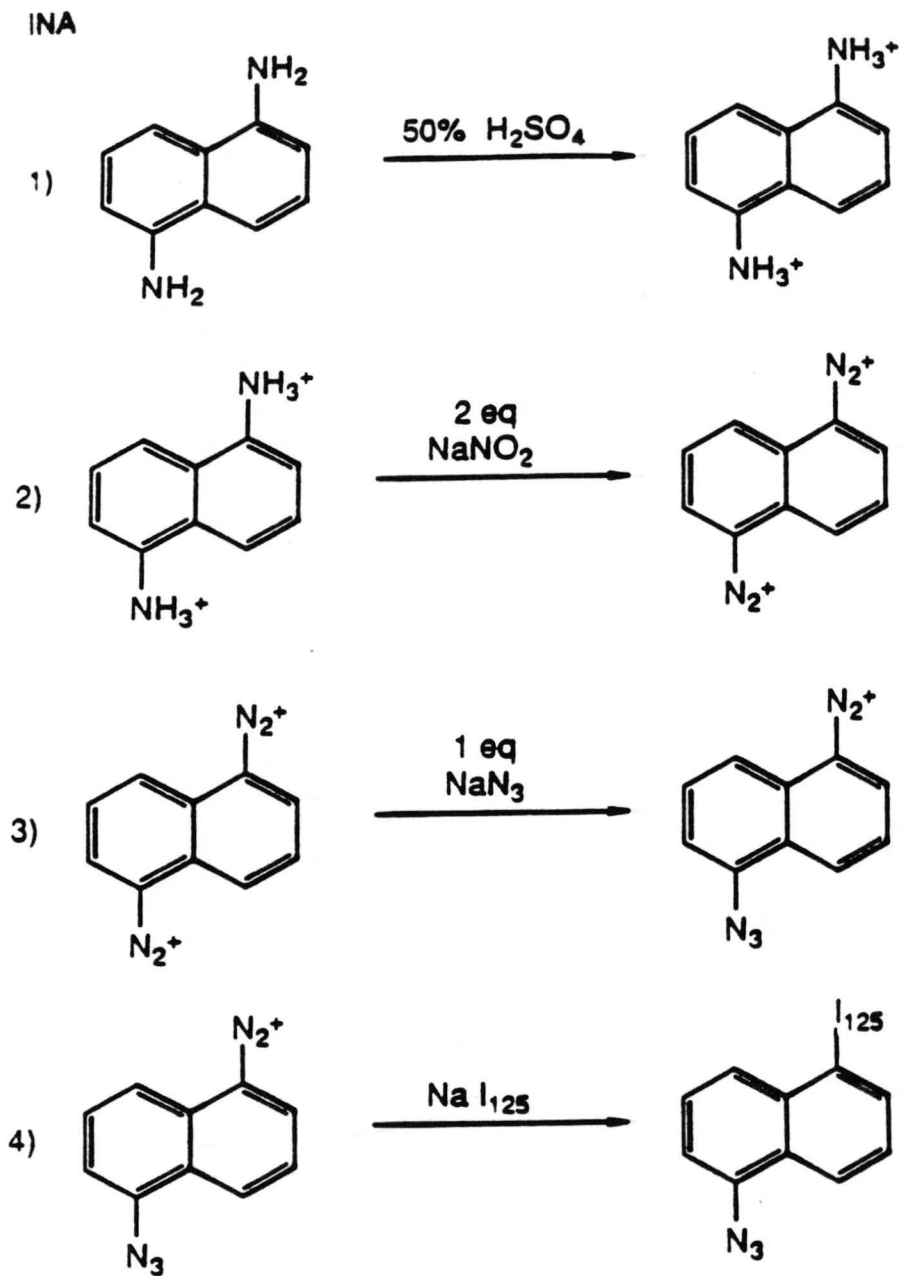


Figure 5. The overall synthesis of the photoprobe 5-iodo-naphthyl-1-azide.

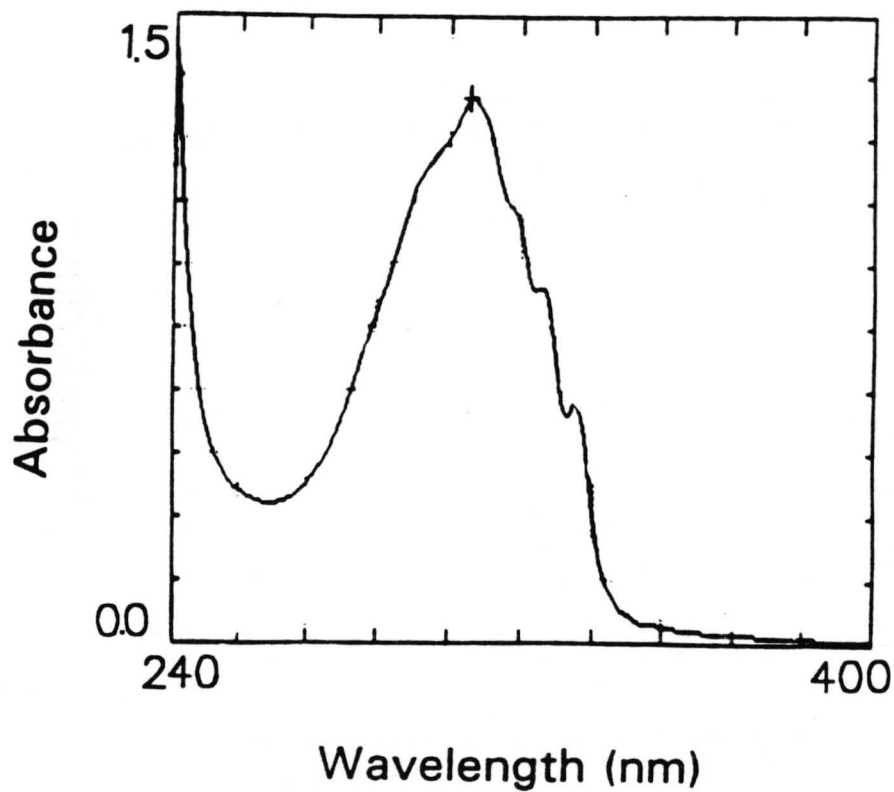


Figure 6. The absorbance spectrum of the photoprobe 5-iodonaphthyl-1-azide. The compound has an absorbance maximum at 310 nm with an extinction coefficient of $21,400 \text{ cm}^{-1}\text{M}^{-1}$.

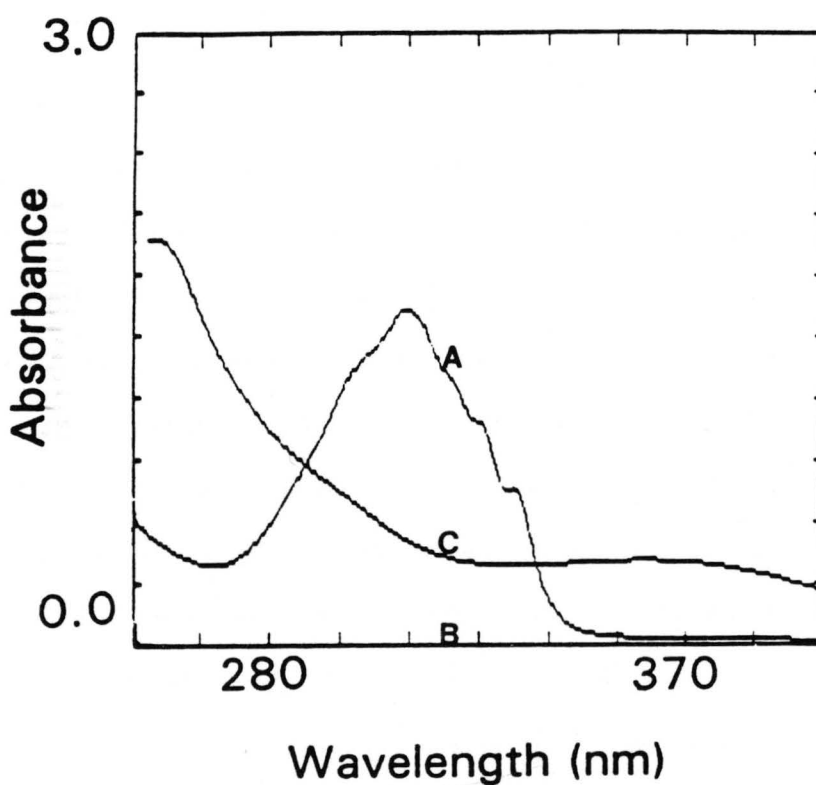


Figure 7. The spectrum shows the disappearance of photo-probe after irradiation with ultraviolet light for three minutes. Trace A is the original sample, B is background ethanol solvent, and trace C is after exposure.

absorption peak at 310 nm has disappeared indicating that the compound was indeed photolyzed by short wavelength (high energy) light. Curve B in the figure is a background spectrum of the solvent and shows no discernable absorption in the wavelength range of interest.

These results demonstrated that the modified Gitler method was capable of generating useful amounts of INA and that the INA molecule possessed the desired photochemical properties.

III.2 Synthesis of INA Derivative

Our next objective was to characterize INA with respect to its usefulness as a biological photoprobe. To be of any value, INA must possess three properties (in addition to its photoactive characteristics). Firstly, to be used as a photoprobe in biological systems, it must be able to imbed into the lipid bilayer. Secondly, once activated, it must be capable of indiscriminately coupling to proteins in the cell membrane. Thirdly, it must be coupled to a water soluble protein for production of anti-INA antibodies. These antibodies were used to assay the INA after completion of each experiment. Unfortunately, for this last application, INA in its normal state was useless. Our next objective was to derivatise the molecule into a more useful form.

Figures 8 a, b, and c illustrate the strategy used to accomplish the derivatization. We wanted to convert the 1,5-

dinitronaphthalene to the active succinimide ester. The first part of the process is illustrated in Figure 8a. Conversion of 1,5-dinitronaphthalene to 5-amino-1-nitronaphthalene (compound 1 to 2) proceeded with a 95% yield.

The steps to produce the 5-iodo-1-nitronaphthalene (compound 4) proceeded with 88% yield, while reduction by tin to make compound 5 resulted in only 51% yield. Further to make the 1-iodo-carboxyl compound (Figure 8b, compound 6) produced in 76% yield. The absorption spectrum of this compound is given in Figure 9. The physical properties of the compound were determined for identification purposes. The molar absorptivity at 296 nm was determined to be $10,586 \text{ cm}^{-1}\text{M}^{-1}$, while its melting point was found to be 213°C . The overall yield up to, and including this step was calculated to be 31%. At this point dicyclohexylcarbodiimide was added to make compound 7 which in turn was reacted with N-hydroxysuccinimide to produce the active ester compound 8 (Figure 8c). This type of ester is known to react with primary amines to form amides (56). Thus, when this ester was added to a protein solution it produced compound 9 (the proteins used were bovine serum albumin and rabbit immunoglobulin G). For characterization of the synthesis, the intermediate compounds 1, 3, 6, and 7 were run on a 200 mesh silica TLC and the colors and R_f values were recorded

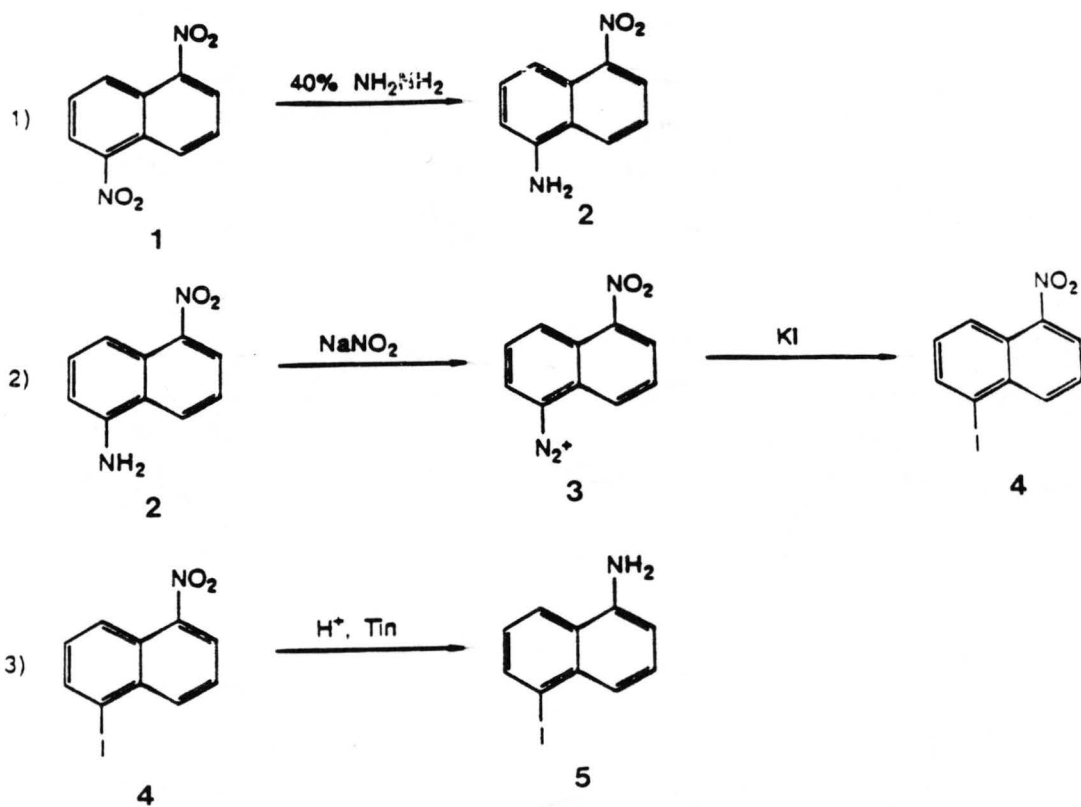


Figure 8a.

The synthesis of the photoprobe derivative. The synthesis involved the conversion of 1,5 dinitronaphthalene to the active succinimide ester. The first series of reaction steps involved the formation of an aromatic amine.

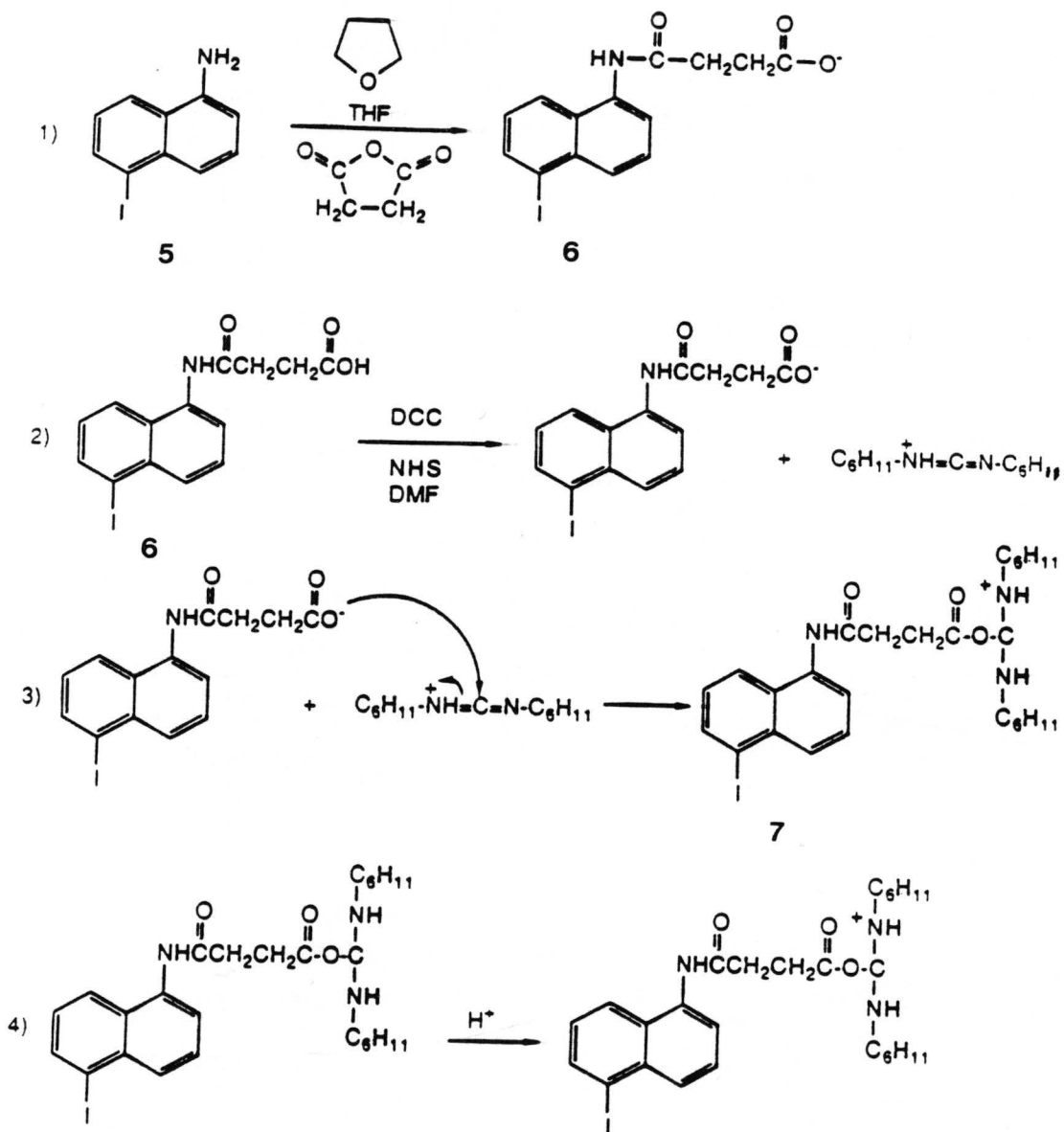


Figure 8b. INA derivative synthesis continued. Acylation of the aromatic amine and further addition of dicyclohexylcarbodiimide.

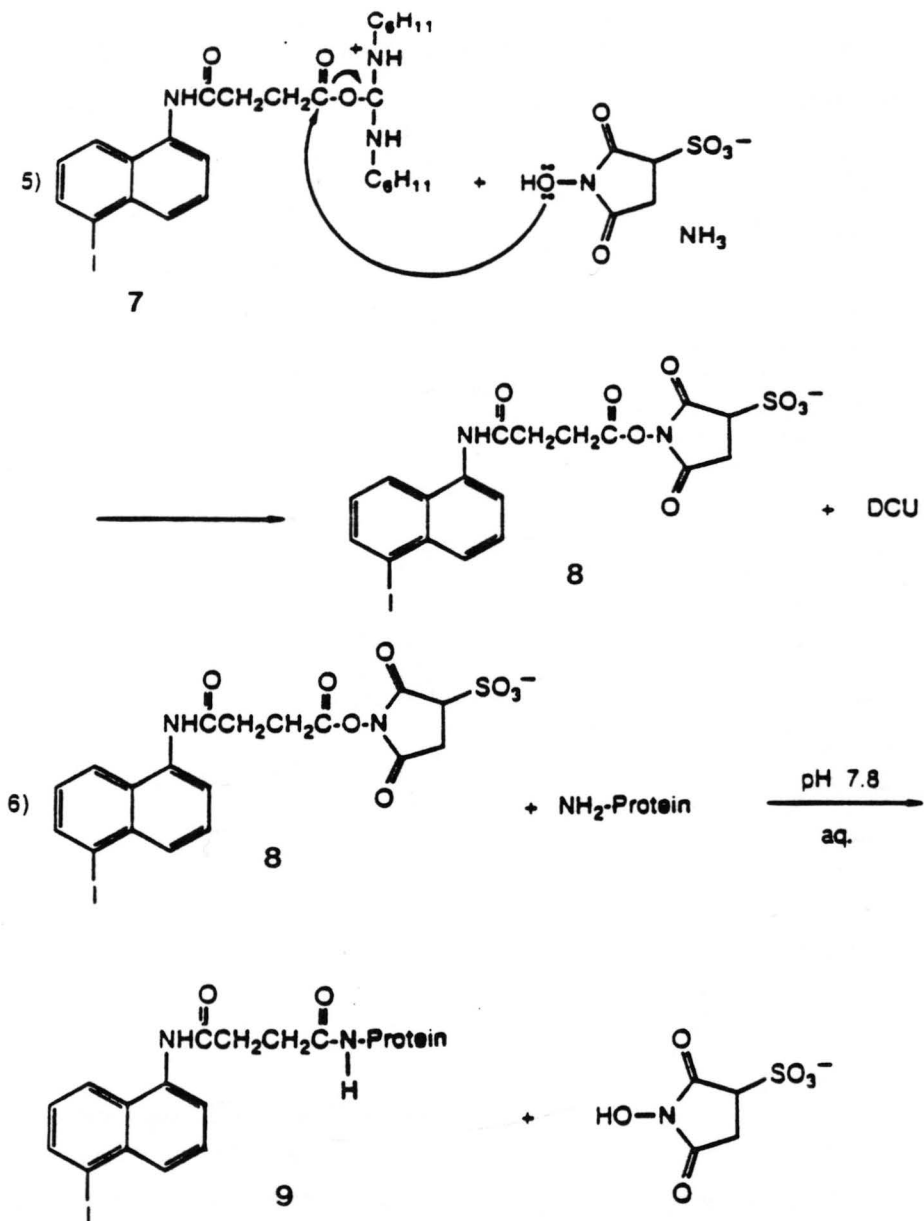
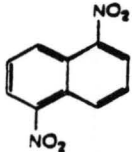
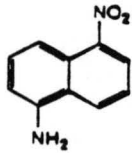
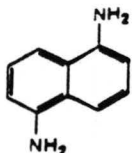
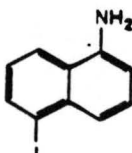
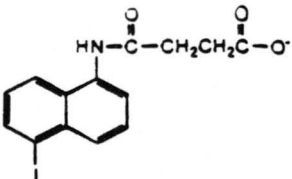


Figure 8c. Synthesis of the active INA ester derivative. The ester will react with the polar side chain of lysine to form the corresponding amide linkage.

Table I

TLC of INA Derivatives.

LANE	Rf	COLOR	COMPOUND
1	.92	Light Blue	
2	.82	Brown	
3	.77	Purple	
4	.82	Orange	
5	.22	Red	

**** Veiwed using short wave U.V. lamp

The five compounds were run on a TLC plate and Rf values calculated. The compounds had the reported colors when viewed under a shortwave ultraviolet lamp.

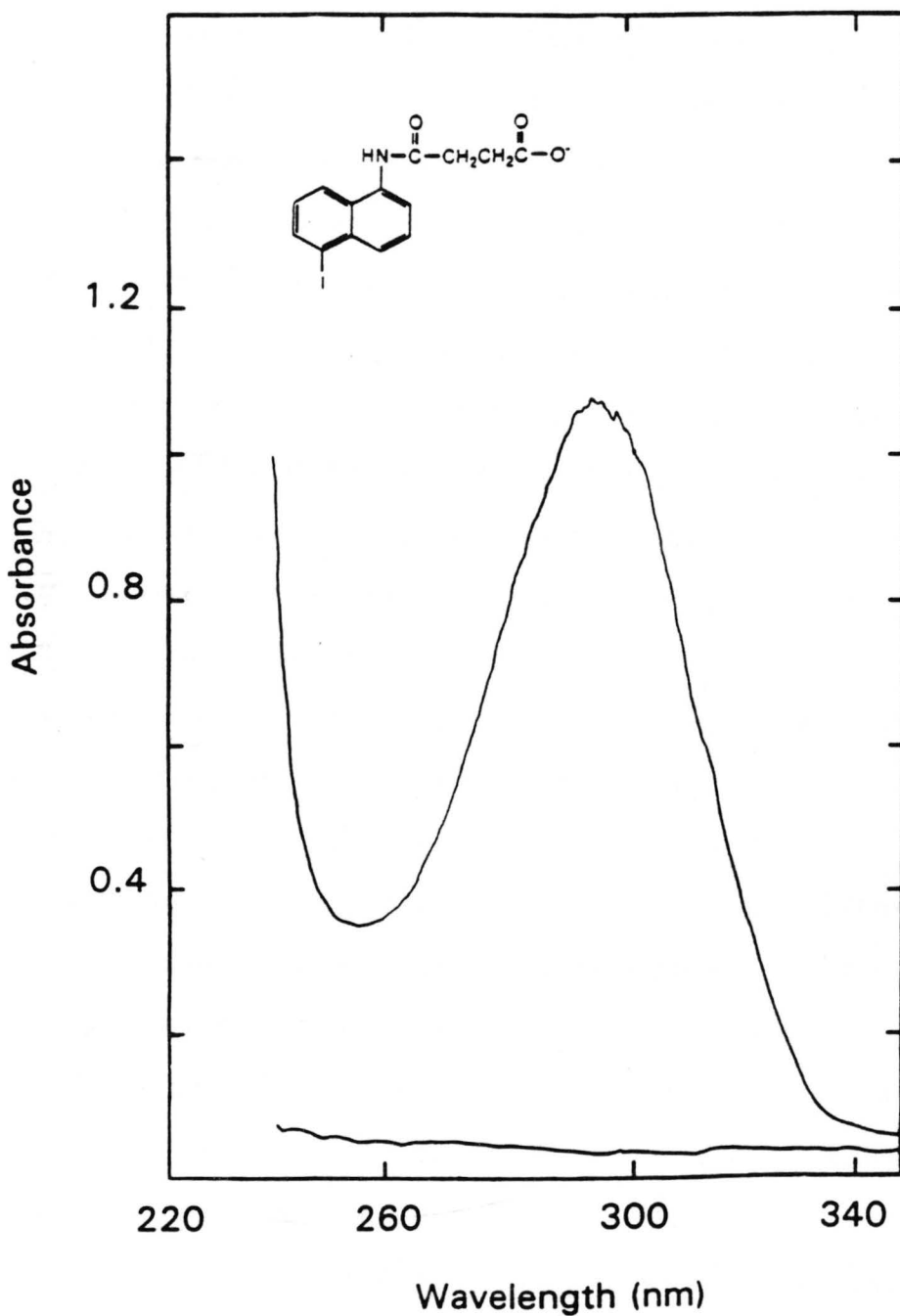


Figure 9. The ultraviolet spectrum of the carboxyl derivative of the photoprobe. It has an absorbance max at 296 nm and an extinction coefficient of $10,586 \text{ cm}^{-1}\text{M}^{-1}$

(Table 1). Subsequent production of conjugated proteins used the values from this table as guidelines for success.

Additionally, the intermediate compounds of the first synthetic attempt were characterized using NMR to confirm the process. First, the NMR spectrum for the starting material 1,5-dinitronaphthalene (Figure 10) had, as was expected, three aromatic proton peaks appearing as two doublets and one triplet between 7.0 to 9.0 ppm. Second, the 5-iodo-1-nitronaphthalene compound had a more complex spectrum due to the six non-equivalent aromatic protons (Figure 11). These protons show up between 6.9 and 8.2 ppm. Next the NMR spectrum for 5-iodo-1-aminonaphthalene (Figure 12) also contained six non-equivalent aromatic protons (two triplets and four doublets). These also give a complex spectrum between 6.8 and 8.2 ppm. In addition, the 1-iodo-5-aminonaphthalene contained two protons as determined by integration which appear in the broad peak at 4.2 ppm. These protons arise from the addition of the amine group versus the nitro group of the preceding compound. Note, the peaks at 7.2 ppm and 1.5 ppm in the NMR spectra are due to acetone which was used as the solvent.

The absorbance spectrum for 1-amino-5-iodonaphthalene (compound 5) was found to have an absorption peak at 333 nm (Figure 13). This is indicative of a halogenated aromatic ring structure. The last intermediate to be analyzed was the

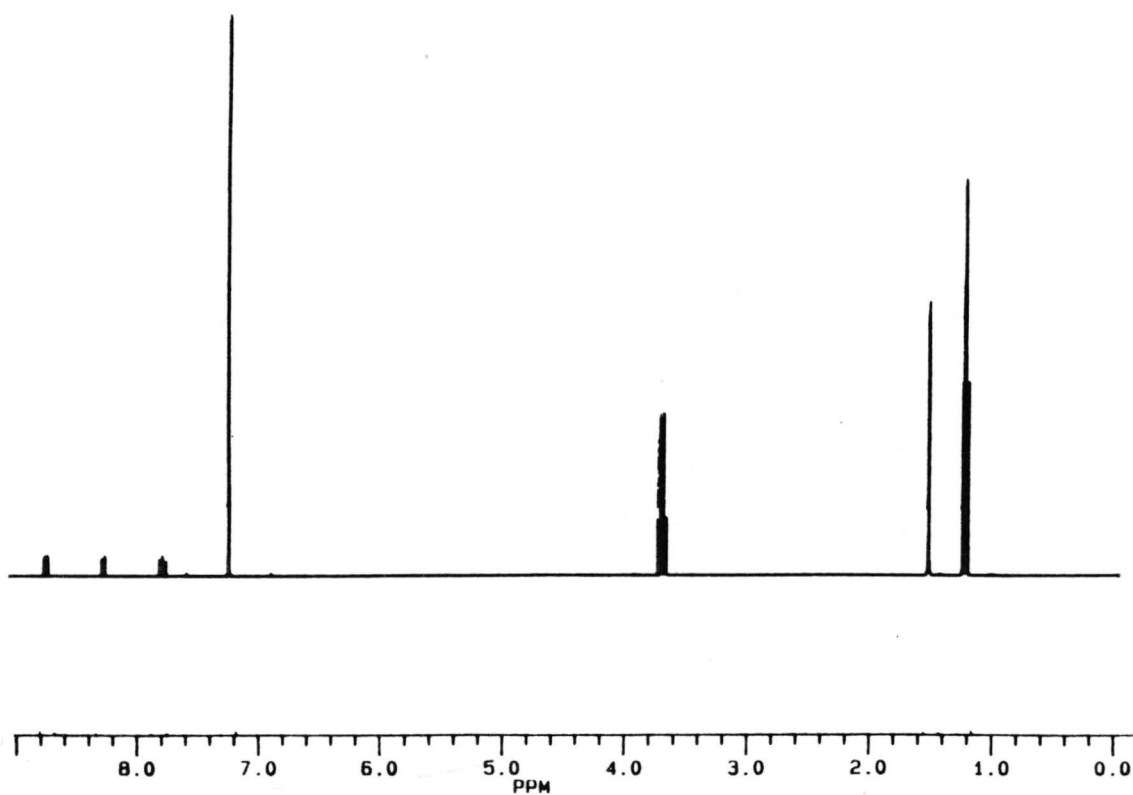


Figure 10. The NMR spectrum for 1,5-dinitronaphthalene.

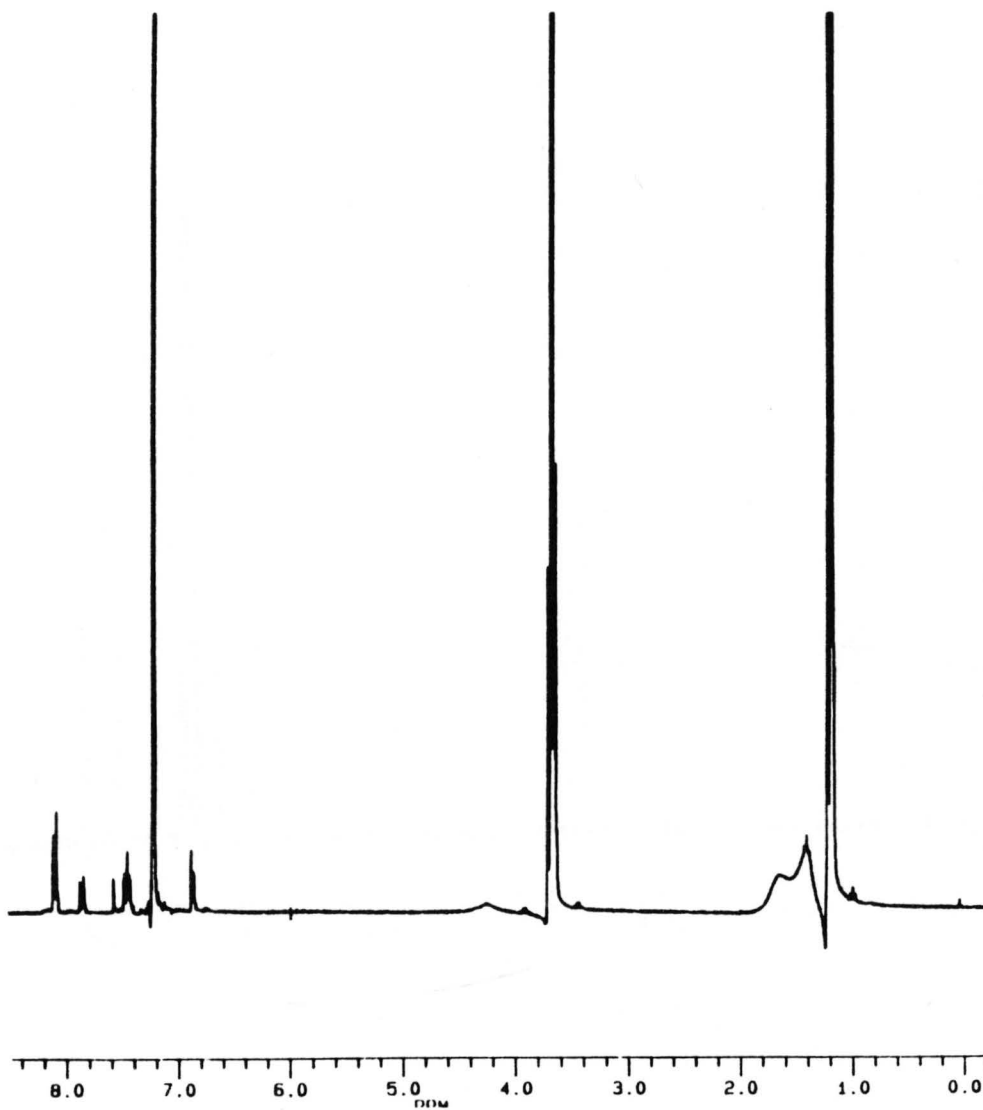


Figure 11. The NMR spectrum for 5-iodo-1-nitronaphthalene.

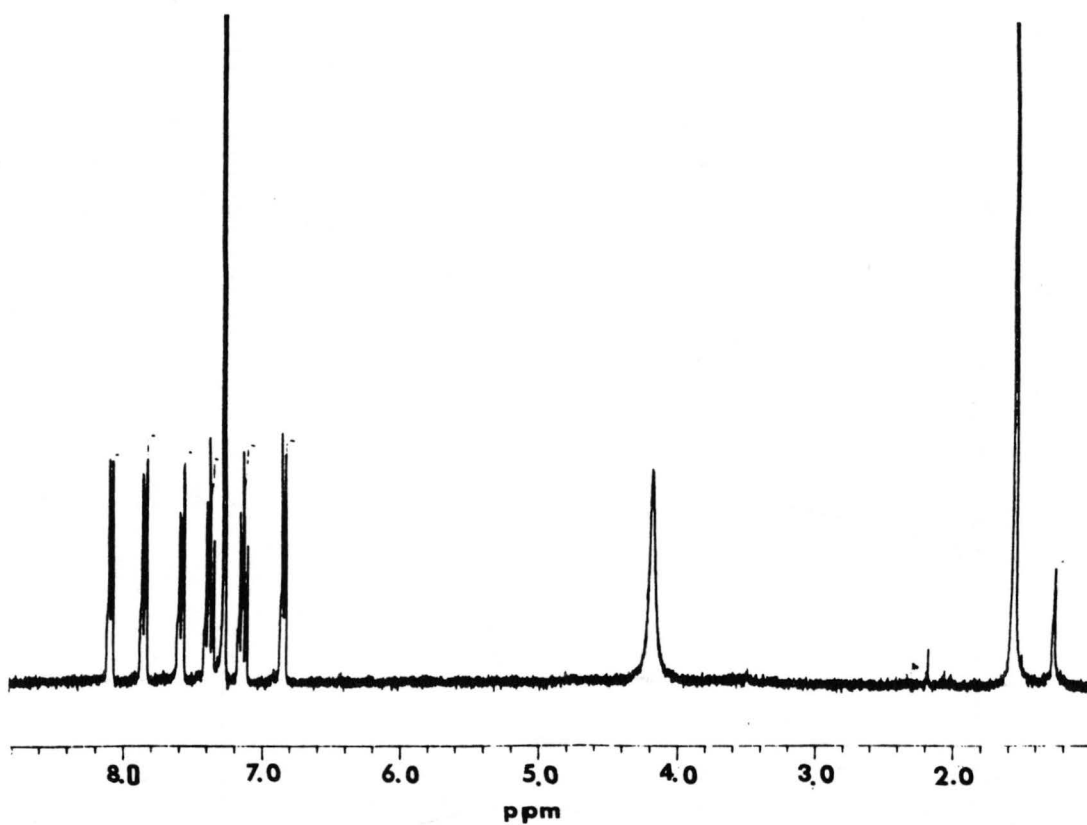


Figure 12. The NMR spectrum for 5-iodo-naphthyl-1-amine.

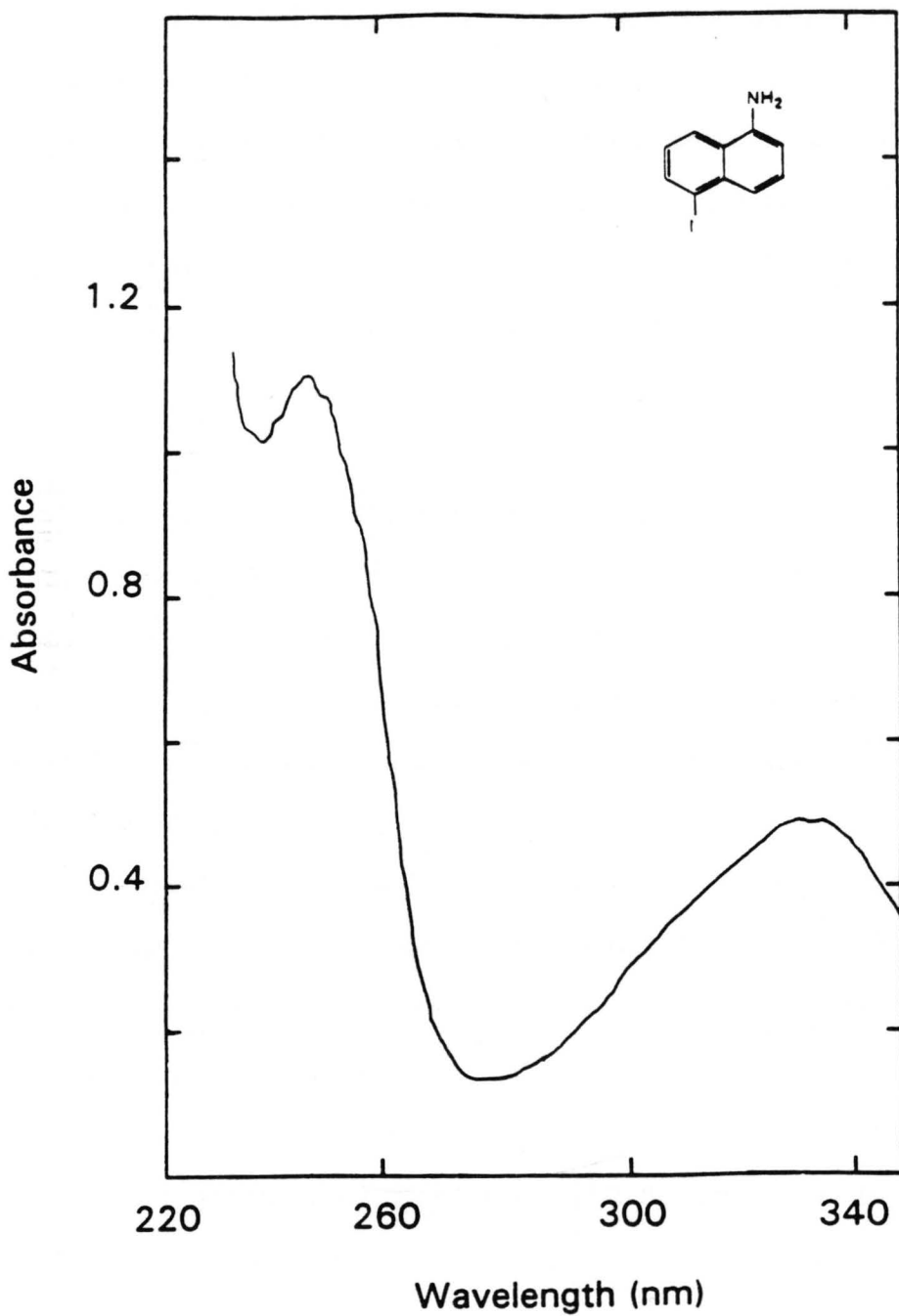


Figure 13. The ultraviolet spectrum of the 5-iodo-naphthyl-1-amine.

carbonyl derivative (compound 6). The NMR spectrum for this intermediate produced bands at 10 ppm due to the COOH, aromatic protons at 7.2 ppm to 8.4 ppm, acyl protons 2 ppm to 3 ppm, and an amide proton at 3.3 ppm (Figure 14). These peaks are consistent with the structure of 1-amine-5-iodonaphthalene. The strong peak at 2.5 is due to the DMSO solvent.

III.3 Coupling INA to Carrier Proteins

The INA amide derivative was coupled to a carrier protein (rabbit immunoglobulin G) for antibody production. An ultraviolet spectrum of the compound, shown in Figure 9, demonstrated an absorbance maximum at 296 ($\epsilon_{296} = 10,586 \text{ cm}^{-1}\text{M}^{-1}$) and melted at 213°C.

The spectrum shown in Figure 15 demonstrated that derivatized INA did attach to protein. These INA derivatized proteins were used in immunization of rabbits against INA, anti-INA antibody screening, and affinity chromatography. The amount of INA conjugated to protein was determined by the ratio of the absorbance peaks at 280 nm and 296 nm using the following equation:

$$[\text{INA}] = \frac{[\text{Abs}^{278} \times \epsilon^{296}(\text{protein})] - [\text{Abs}^{296} \times \epsilon^{278}(\text{protein})]}{[\epsilon^{278}(\text{INA}) \times \epsilon^{296}(\text{protein})] - [\epsilon^{296}(\text{INA}) \times \epsilon^{278}(\text{protein})]}$$

$$[\text{Protein}] = \frac{[\text{Abs}^{296} \times \epsilon^{278}(\text{INA})] - [\text{Abs}^{278} \times \epsilon^{296}(\text{INA})]}{[\epsilon^{278}(\text{INA}) \times \epsilon^{296}(\text{protein})] - [\epsilon^{296}(\text{INA}) \times \epsilon^{278}(\text{protein})]}$$

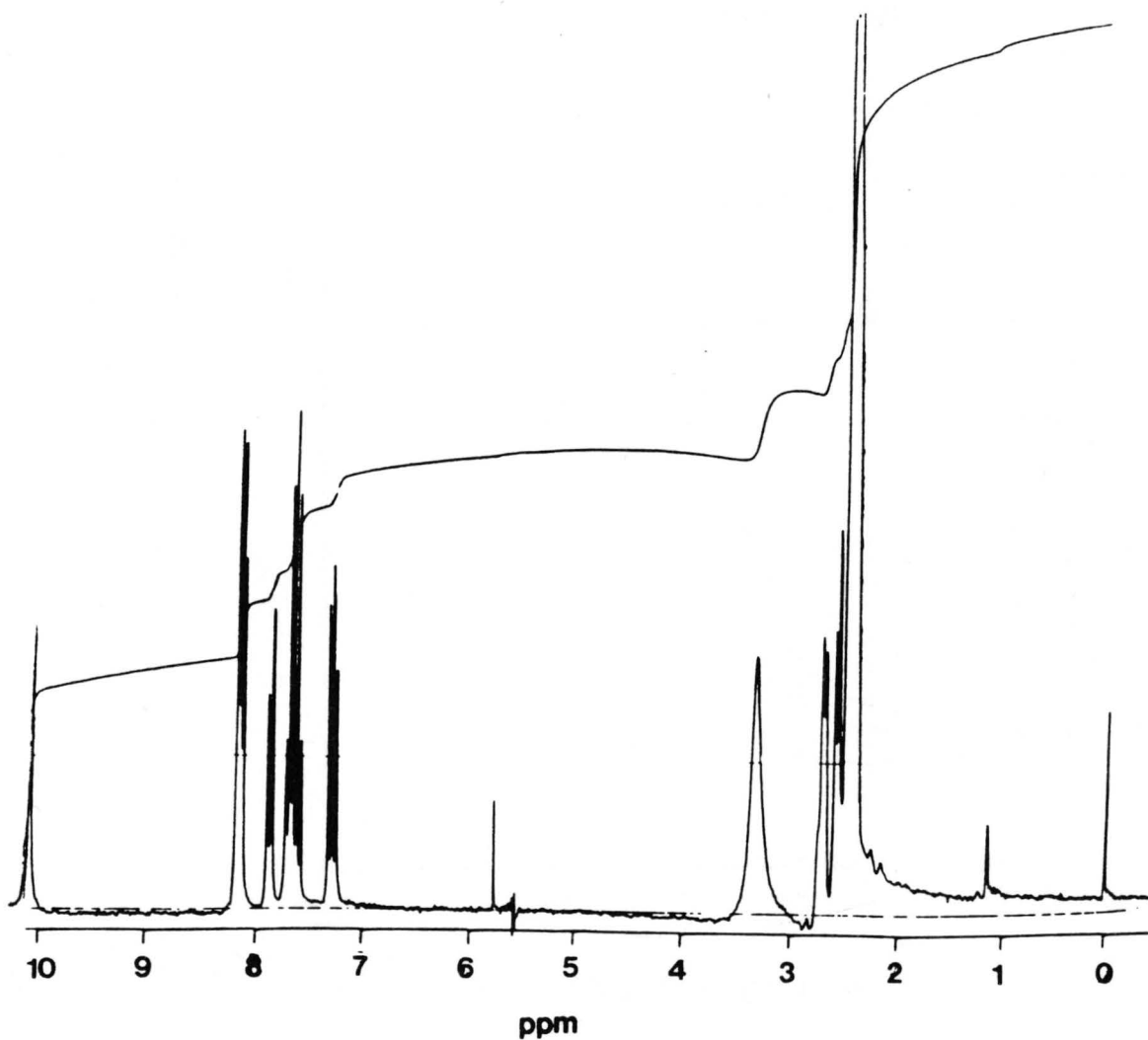


Figure 14. The NMR spectrum of the INA carboxyl derivative. The salt of the compound had a melting point of 213°C.

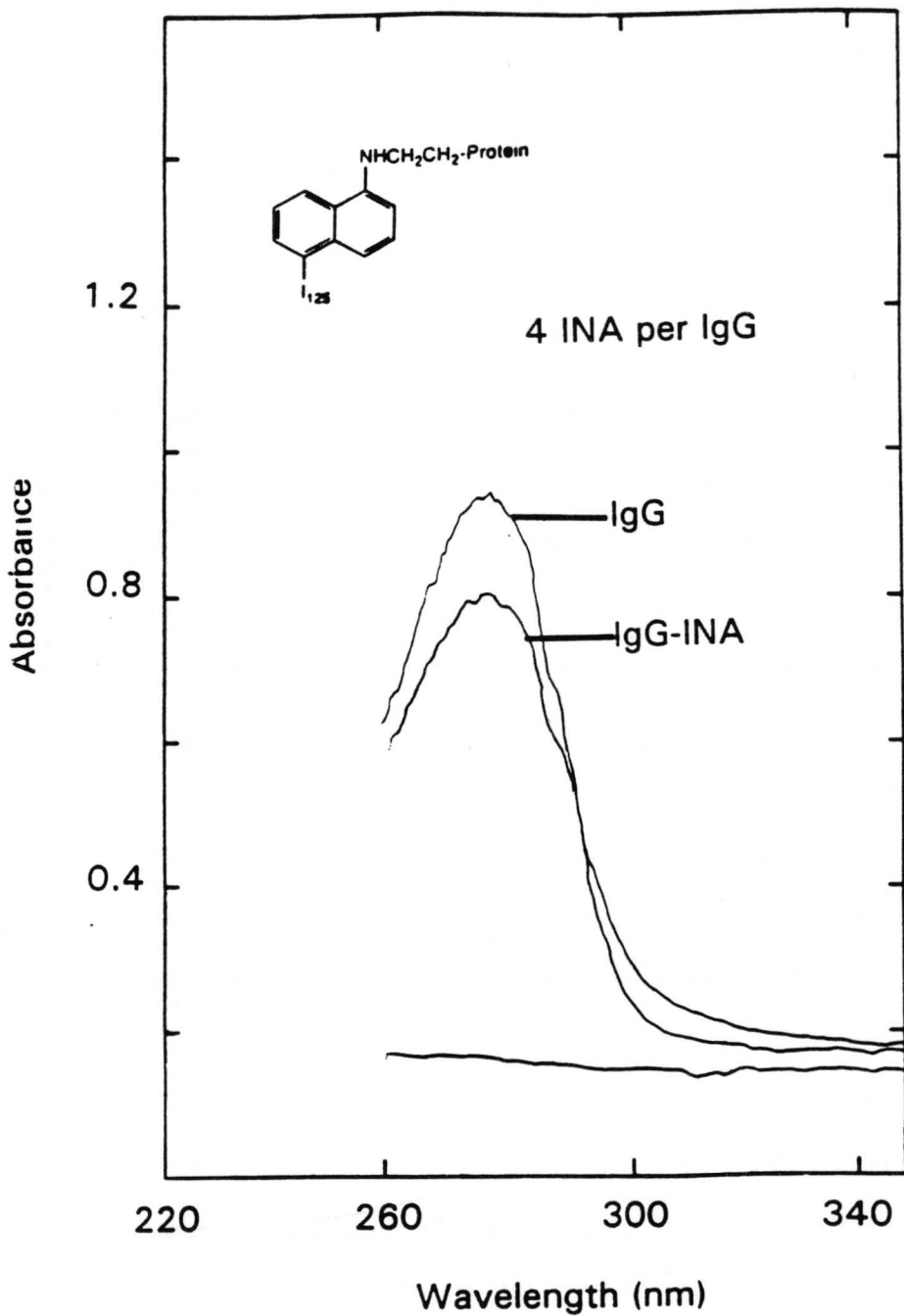


Figure 15. The ultraviolet spectrum of the photoprobe derivative covalently attached to a rabbit IgG molecule. Four probes were attached on average per protein.

The protein we used contained four INA molecules per protein. The shoulder on the protein absorbance spectrum (Figure 15) and the broadening of the absorbance from 290 nm to 400 nm is due to conjugation of INA to the protein through the amide linkage.

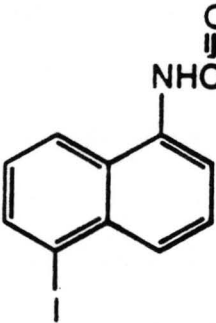
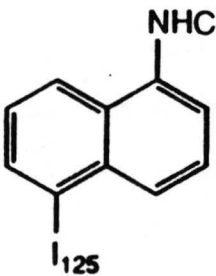
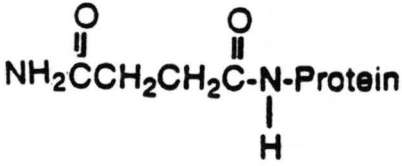
III.4 Anti-INA Antibody Production

Our next objective was to quantitatively measure the amount of INA that was incorporated onto the cell membrane proteins. This required the production of anti-INA antibodies. Antibodies generally exhibit both high specificity and high binding affinity toward their target molecule. These were the properties we hoped to observe in the anti-INA antibodies.

To stimulate anti-INA antibody production, INA was coupled to rabbit IgG molecules. We used rabbit immunoglobulin (Ig) as the carrier protein to minimize the number of antibodies directed against the carrier backbone since rabbit Ig is not immunogenic to rabbits. The ratio of INA to rabbit IgG was about 4 to 1. Three hundred micrograms were injected into each of the three rabbits. After roughly a month, the rabbit serum was affinity purified and tested for specificity against INA using ELISA and immunoblot methods. We determined that the rabbits had an average purified antibody titer of 0.75 mg/ml of blood. To assess specificity, immunoblots were performed and the results of these experiments are shown in Table 2. Row one revealed that

Table II

Summary of the Specificity of the Purified Rabbit Anti-INA Antibody.

Sample	Antibody Detection
BSA-INA (Chemically)	 <p data-bbox="916 850 1071 883">Positive</p>
BSA-INA (Photo-chemically)	 <p data-bbox="916 1103 1071 1136">Positive</p>
BSA-Linker arm	 <p data-bbox="1023 1550 1182 1583">Negative</p>

the purified antibody was not specific for the BSA protein used as the affinity column backbone. The entries in rows 2 and 3 prove that the anti-INA purified antibody was specific for both chemically coupled and photo-chemically activated INA derivatized protein. However, the chemically coupled INA and the photo-chemically activated INA products were slightly different as seen in the relative strengths of responses. The difference is that the chemically coupled INA contained an amide constituent, whereas the photo-activated product had a secondary amine functional group. The amine was not used for immunization of the animals. It has been established that amides are more strongly immunogenic as compared amine counterparts. Thus, the amide gave a more intense blot. To further illustrate the anti-INA antibody specificity for INA, it was tested against the succinic acid linker arm. As can be seen in row four, there was no reaction between the anti-INA antibodies and the succinic linker arm.

III.5 Affinity Chromatography of Rabbit Serum

The antibody was affinity purified to assure the highest purity. These purified antibodies were used as monospecific reagent in protein labeling assays. To accomplish this, INA was conjugated to a backbone protein which in turn was attached to a solid support. The protein also acted as a spacer arm to extend the INA molecule away from the solid support matrix and into the solution. The protein we used

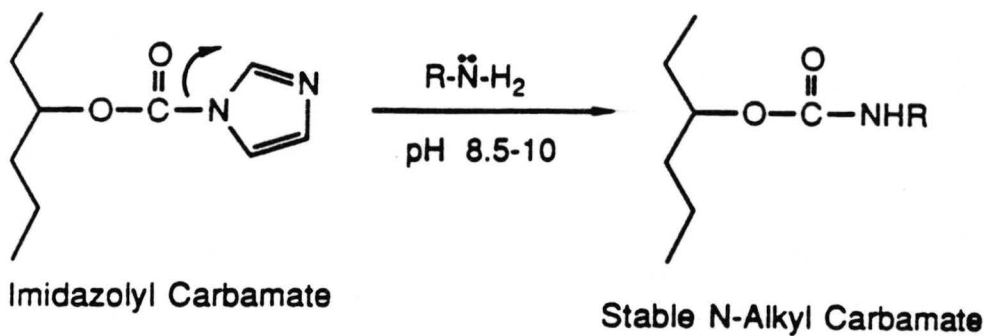
bovine serum albumin (BSA). The INA derivative was coupled to the protein through the amine on the side chain of the lysine residues. BSA is known to have 56 lysines approximately 35 of which are capable of coupling to INA (61). The remainder are used for coupling of the BSA to the solid support matrix. Here, the amines attached to the imidazolyl carbamate on the solid support (6 x crosslinked agarose) to form a stable N-Alkyl carbamate linkage (Figure 16). Once attached to the column, we assumed that approximately 20% of the protein-INA conjugate would retain its ability to bind anti-INA antibodies. This assumption was based on other affinity columns of this type (62). A conjugation ratio of 2.6 INA molecules per BSA was used for antibody purification.

A typical elution profile of the protein purification experiment is shown in Figure 17. The solution that eluted at pH 7.2 contained free serum proteins that did not bind (i.e. albumin) to the INA-BSA; whereas the peak that eluted at pH 2.2 was the anti-INA antibodies.

III.6 Eosin Triplet lifetime vs. O₂ Concentration

We used eosin as the donor molecule in energy transfer experiments. Therefore, we wanted to characterize its triplet lifetime. Oxygen interferes with the energy transfer process by reacting with triplet state molecules and thus facilitating deactivation via methods other than energy transfer

React Gel - Carbonyldiimidazole Activated Support



- Optimal pH 9-11.
- Use non-primary amine buffer.

Figure 16. The coupling of the derivatized protein to the reacti-gel solid support. The primary amines on the protein will couple to the (6X) crosslinked agarose to form a stable N- Alkyl carbamate linkage.

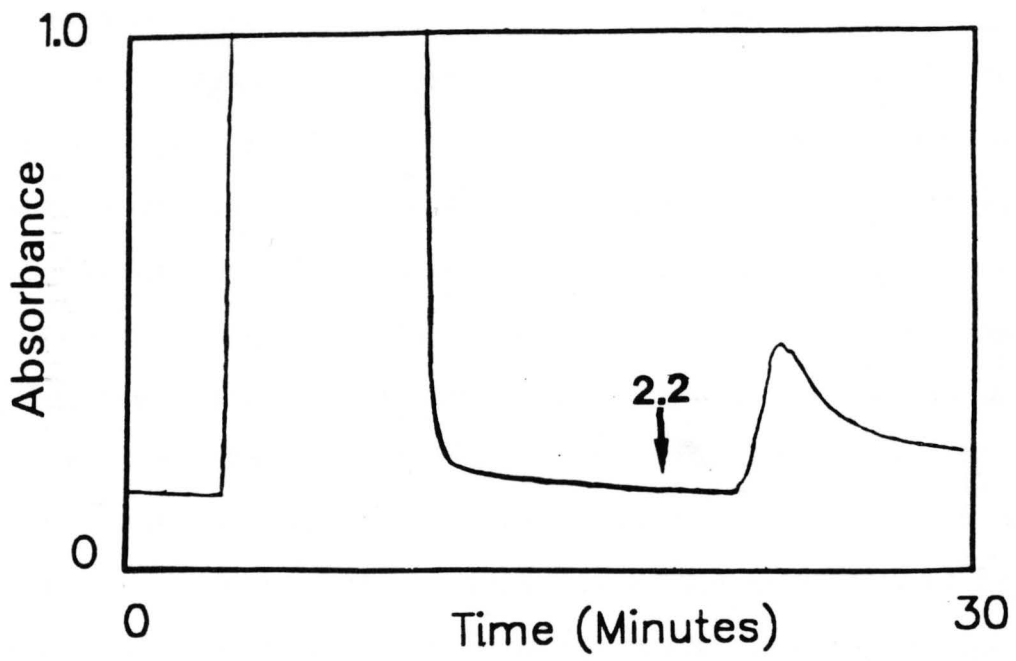


Figure 17. A typical elution profile for an antibody purification. The first peak is free serum proteins. The second peak eluting at pH 2.2 is the specific anti-INA antibody.

mechanisms. Therefore, it was essential to remove O_2 from the system. This was accomplished by use of a glucose oxidase and catalase enzyme system. Glucose oxidase produces H_2O_2 from O_2 . H_2O_2 is toxic to cells and must be removed by the use of catalase (Catalase produces H_2O and H_2 from H_2O_2). In these experiments, the concentration of catalase was high relative to glucose oxidase to destroy hydrogen peroxide quickly upon its formation.

Oxygen levels were measured using a Yellow Springs Instrument (YSI) type 55 oxygen probe. Table 3 lists the values for both the calculated and measured levels of oxygen in a solution containing the enzyme mixture. Column two depicts percent O_2 for the measured O_2 levels. Whereas, columns three enumerate percent of atmospheric O_2 remaining in the system for the fitted line. The values in the fourth column are the differences between the measured O_2 and the calculated O_2 levels. The O_2 depletion data were fitted to a single exponential that had a time constant (the depletion of $[O_2]$ to $1/e$ of the initial values) 30.2 minutes. A plot of both the calculated and measured O_2 levels are shown in Figure 18.

The fluorochrome eosin has an excitation maximum at 524 nm and an emission maximum at 548 nm (Figure 19). An argon laser at 514 nm was used to excite the fluorochrome. In the absence of oxygen, free eosin had a long-lived triplet state of 2 msec. This stable triplet state stands a much better

Table III

Removal of Oxygen as a Function of Time Using the Enzymes Glucose Oxidase and Catalase.

Time (min)	Measured (% oxygen)	Calculated (% oxygen)	Difference
2	87.52	91.05	3.58
4	84.47	85.44	.97
6	79.53	80.18	.65
8	75.81	75.25	.54
10	71.81	70.66	1.15
12	67.95	66.35	1.59
14	64.18	62.31	1.86
16	60.50	58.54	1.95
18	56.01	55.00	1.00
20	53.14	51.70	1.43
22	49.46	48.60	0.85
24	46.68	45.71	0.97
26	43.36	43.00	0.35
28	39.86	40.46	0.60
30	38.15	38.09	0.06
32	35.64	35.86	0.22
34	33.93	33.78	0.14
36	31.42	31.83	0.42
38	29.44	30.02	0.58
40	27.65	28.31	0.66
42	26.03	26.71	0.68
44	24.60	25.22	0.62
46	23.07	23.82	0.75
48	21.63	22.51	0.88
50	20.38	21.28	0.91

Values for the calculated and measured levels of oxygen in the solution. In column one is the time. Column two is the percent O₂ calculated using enzyme kinetics. Column three is measured O₂. Column four is the difference between the calculated and measured values.

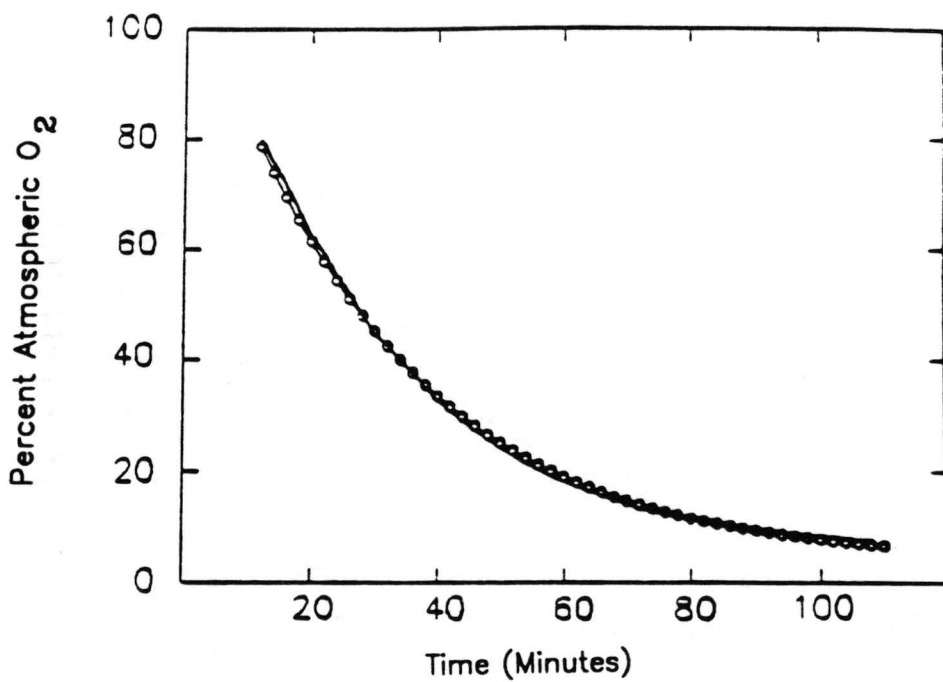


Figure 18. Percent Atmospheric Oxygen versus Time. The hollow points are the measured oxygen and the line is the calculated.

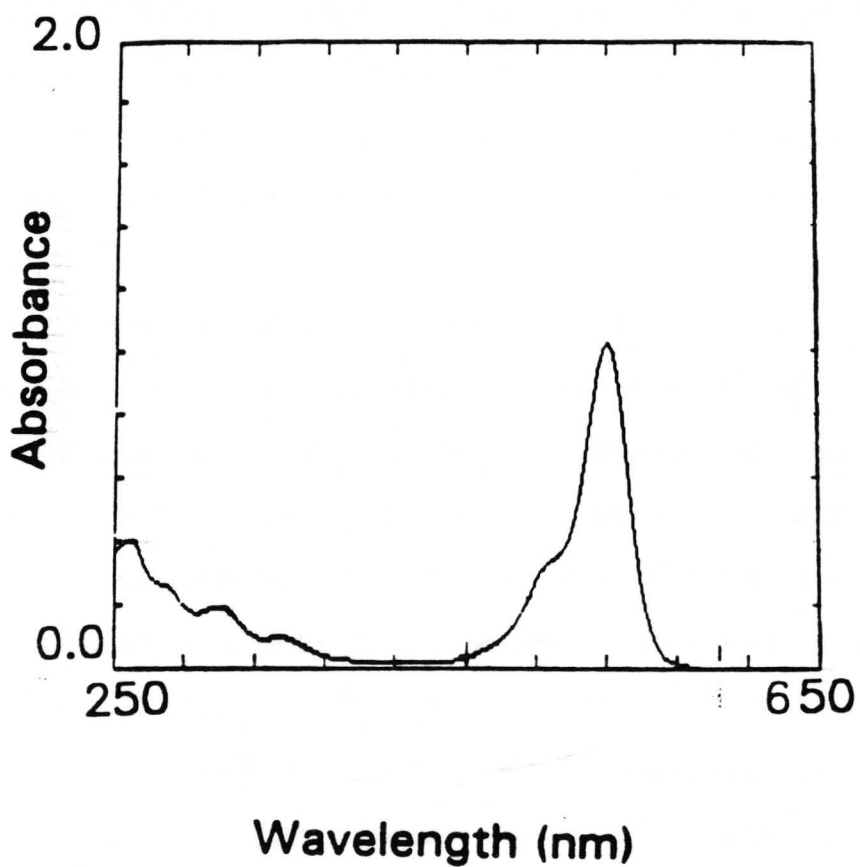


Figure 19. The UV/VIS spectrum for eosin. The molecule has a excitation maximum at 524 nm and a emission maximum at 548 nm.

chance of energy transfer than the eosin triplet in an aerobic solution whose triplet lifetime is only 0.02 msec. As a result, we designed experiments to measure the removal of oxygen from the system. In these experiments, eosin was covalently bound to BSA to mimic normal reaction conditions in which the eosin will be attached to some probe molecule (i.e. hormone, antibody, etc.). Eosin was attached through its isothio-cyanate group to one of the free amines on BSA to form a covalent thiourea linkage (Figure 20). The reaction conditions were adjusted to obtain a ratio of five eosin molecules per BSA (Figure 21, Eosin $\epsilon^{524} = 83,000 \text{ cm}^{-1}\text{M}^{-1}$, $\epsilon^{280}=21,600 \text{ cm}^{-1}\text{M}^{-1}$).

Fluorescence depletion recovery curves for various oxygen concentrations were constructed. The extent of triplet conversion of the probe increased with decreasing amounts of O_2 in the solution. Next, the rate at which the eosin conjugate's fluorescence returned to its original intensity after exposure to a high intensity laser beam was measured. Depletion curves Figures 22 and 23, illustrate the two extremes of O_2 tension that were measured in these experiments. Figure 22 represents a solution that was 75% of atmospheric oxygen, while Figure 23 was a solution at 7% of atmospheric Oxygen. It can be seen from these figures that the lifetime increased from 104.8 μsec for 75% O_2 to 947.7 μsec for a solution of 7% O_2 . This indicates that the longer

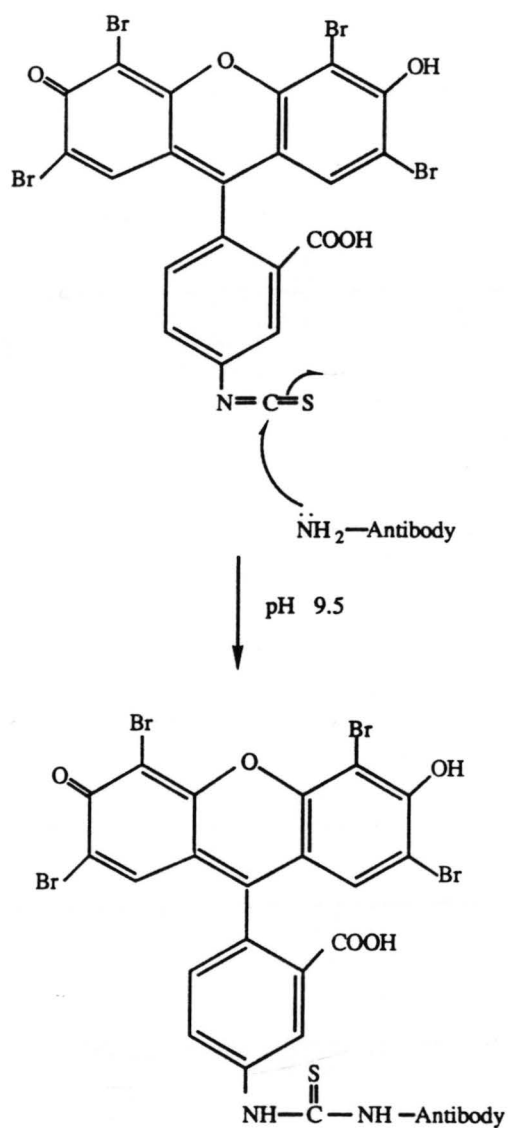


Figure 20.

Eosin will attach to proteins covalently through its isothiocyanate group. It will react with the amine side chain of lysine to form a thiourea.

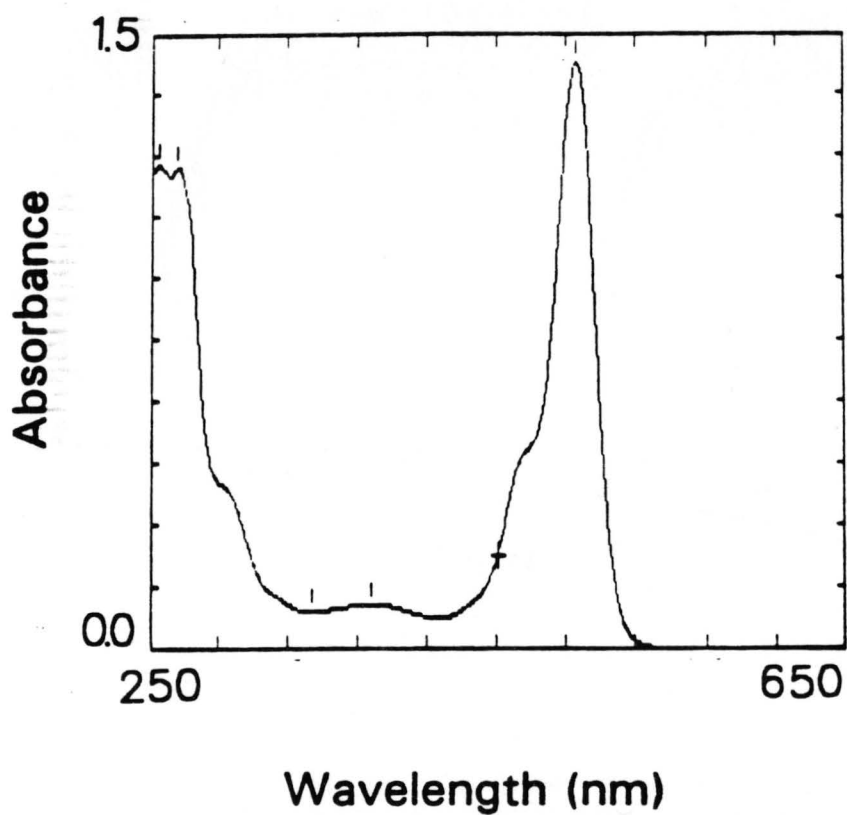


Figure 21. BSA in which five eosin molecules have been covalently attached. The shoulder at 530 nm is due to eosin. The peak at 280 nm is due to both eosin and protein.

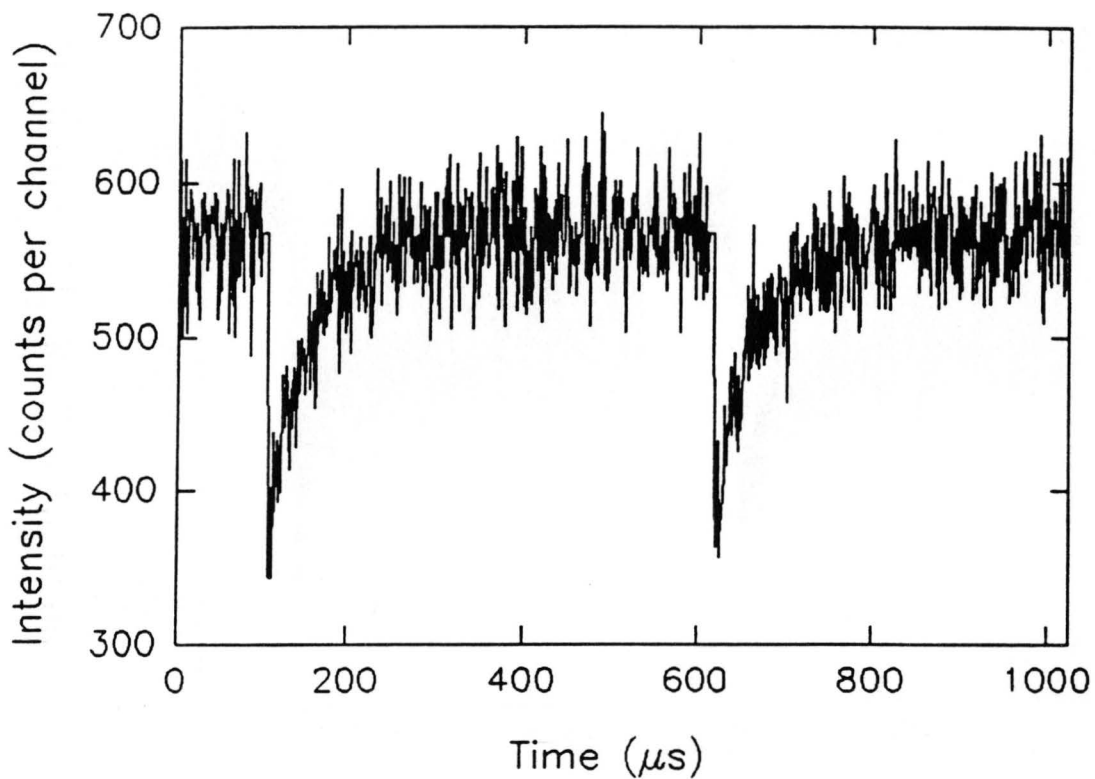


Figure 22. The polarized fluorescence depletion trace for a solution of BSA-Eosin in which the oxygen level is 75% of solution at equilibrium with atmospheric oxygen.

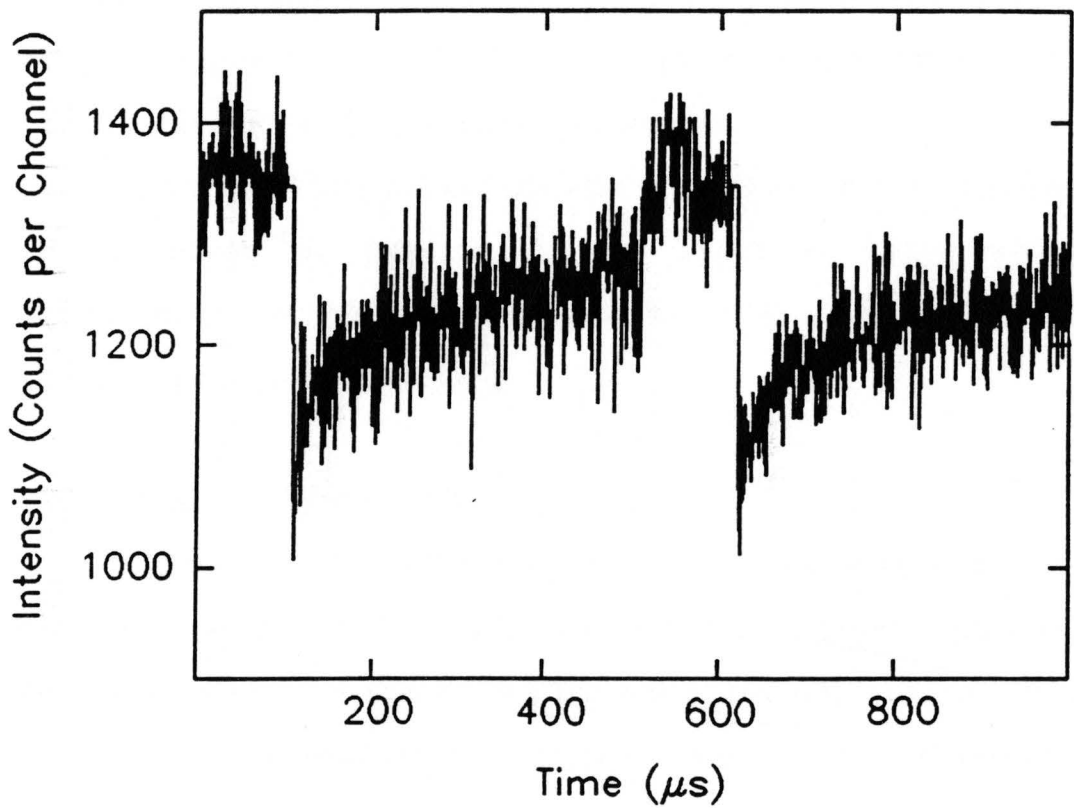


Figure 23. The polarized fluorescence depletion trace for a solution of BSA-Eosin in which the oxygen level is 7% of solution at equilibrium with atmospheric oxygen.

the triplet lifetime the slower the rate of fluorescence recovery. Table 4 illustrates triplet lifetimes for eosin solutions containing varying amounts of O_2 . Using this data we calculated that in a completely deoxygenated system, the triplet lifetime of eosin bound to BSA would have a lifetime of approximately one msec. A graph of the triplet lifetime versus oxygen concentration is presented in Figure 24. From this graph one can determine the lifetime of the fluorophore for a given O_2 tension. The lifetime value would be subsequently used as a parameter in the determination of energy transfer efficiency.

III.7 INA Energy Transfer

The parameters affecting the sensitized energy transfer between the donor fluorochrome and the acceptor photo-probe were analyzed. In the following experiments, eosin Y (2', 4', 5', 7'-tetrabromofluorescein) was used as the fluorochrome. Laser light at 514 nm was passed through a 514 nm band pass filter before it irradiated the sample. This was to avoid any decomposition of the photoprobe due to ultraviolet plasms glow from the laser. The sample was contained in a jacketed cuvette that had cold 0.1 M ferricyanide solution in the envelope. This acted as a liquid filter to aid in the elimination of ultraviolet light. Ferricyanide was chosen because it absorbs light at 310 nm. The ferricyanide solution was constantly circulated to avoid thermal decomposition.

TABLE IV

Triplet Lifetime of EITC Bound to BSA at Various Oxygen Concentrations.

PERCENT OXYGEN	LIFETIME (μ SEC)	1 / LIFETIME
7	947.7 \pm .027	1.06 X 10 ⁻³
8	931.1 \pm 49.3	1.07 X 10 ⁻³
11	848.6 \pm 39.7	1.80 X 10 ⁻³
12	789.1 \pm 15.5	1.27 X 10 ⁻³
19	622.7 \pm 36.7	1.61 X 10 ⁻³
22	500.9 \pm 15.5	2.00 X 10 ⁻³
30	324.7 \pm 11.4	3.08 X 10 ⁻³
36	220.5 \pm 11.9	4.54 X 10 ⁻³
48	163.4 \pm 4.4	6.12 X 10 ⁻³
75	104.8 \pm 3.1	9.55 X 10 ⁻³

The triplet lifetime was measured as a function of the percent oxygen in solution at equilibrium with the atmosphere. The lifetime is reported as micro-seconds and 1/microseconds.

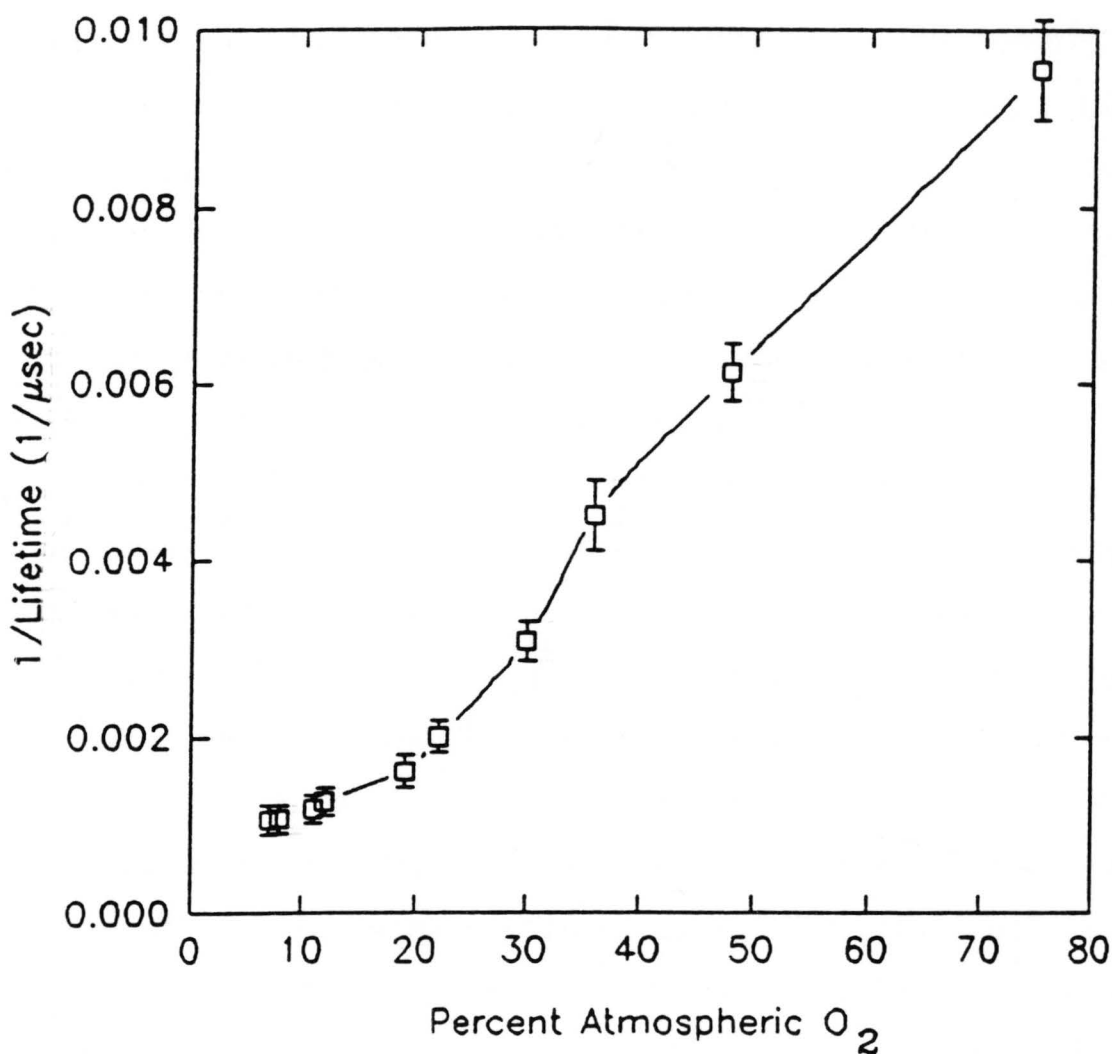


Figure 24.

The percent oxygen in a solution versus the lifetime (1/microseconds) of eosin was plotted. The triplet lifetime increased from 10 μ sec to 1 msec as the oxygen concentration decreased in solution.

When irradiated with 310 nm light (or 514 nm light when in the presence of the donor eosin) the 5-iodo-naphthyl-1-azide, forms an active nitrene which performs hydrogen abstraction from the surrounding environment. After reaction, the solution was acidified to produce the ammonium cation and the product, 1-iodo-5-aminonaphthalene cation, was extracted from the cell suspension into an aqueous solvent (Figure 25). The amount of photoprobe remaining in the organic layer was measured to determine the conversion efficiency.

The first parameter to be observed was the time dependence of irradiation on the efficiency of energy transfer. As shown in Figure 26 the amount of INA that was converted via energy transfer increased with increased exposure time. For example, at 30 minutes approximately 50% of the INA was converted. Whereas at 60 minutes we also observed that the differential rate of conversion of INA decreased with increased exposure time. To illustrate this point, the extent of conversion as a function of time is graphed in Figure 27 and shown in Table 5. It can be seen that at 15 minutes of exposure, 38.2% of the probe was converted. While from 15 minutes to 30 minutes only an additional 14.5% of the photo-probe was converted.

Next, the effect of laser power on energy transfer was determined. In these experiments, all of the solutions were exposed for 15 minutes. Figure 28 is a graphical representation of the data. At 36 mW the system was capable

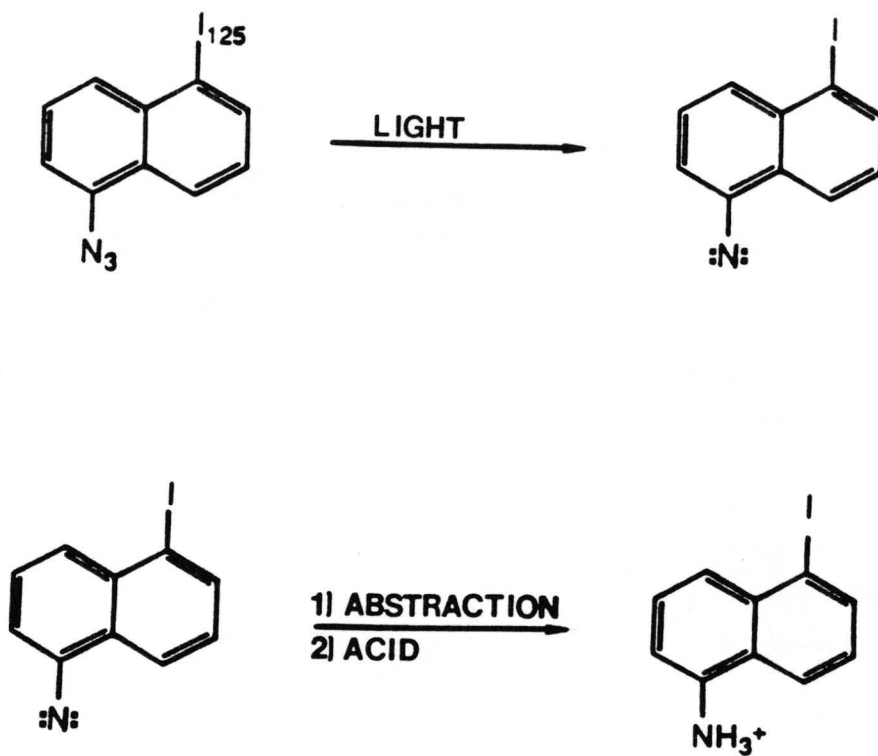


Figure 25.

The photoprobe (5-iodo-1-naphthylazide) when irradiated with the proper wavelength of light will form an active nitrene. The nitrene will abstract a proton from solution and from the amine. Upon acidification it will form the change species and can be extracted into the aqueous phase.

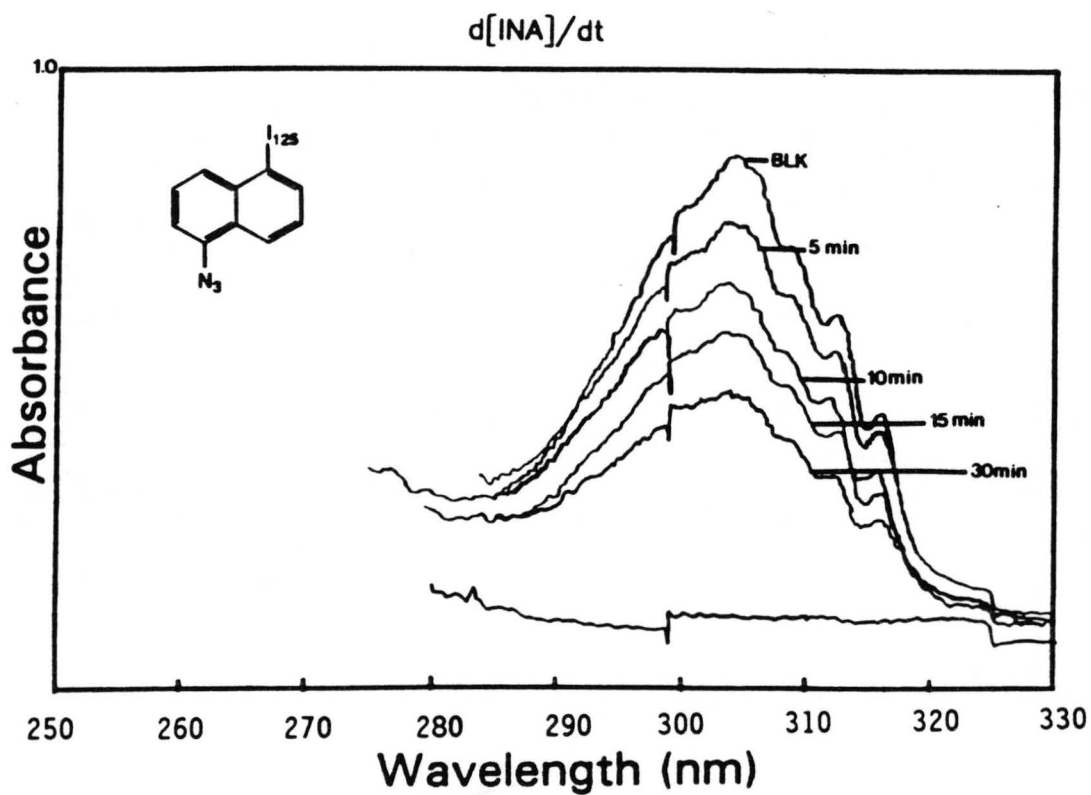


Figure 26. The spectrum for the photoproduct (INA) remaining in solution after a given amount of time. The laser beam was at 514 nm and 36.4 mW.

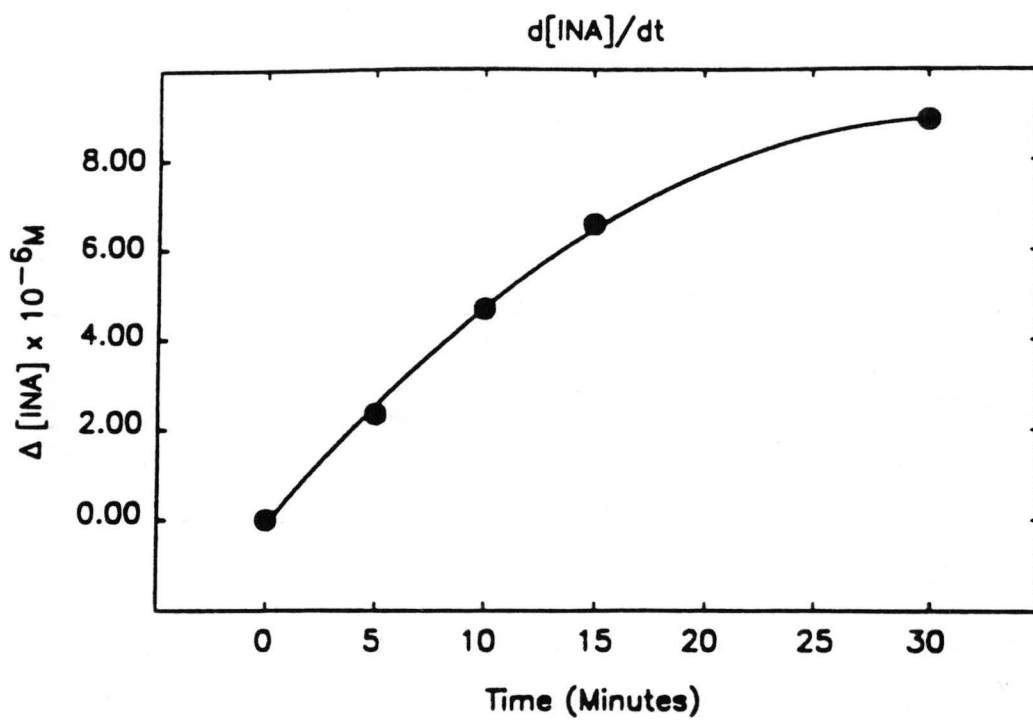


Figure 27. The amount of INA converted versus exposure times to the laser are plotted. The laser is at 514 nm and 36.4 mW.

Table V

Conversion of INA via Energy Transfer as a Function of Time.

TIME (MIN)	INA REMAINING	PERCENT CHANGE
0	$1.73 \times 10^{-3} \text{ M}$	0
5	$1.50 \times 10^{-3} \text{ M}$	13.3
10	$1.26 \times 10^{-3} \text{ M}$	27.2
15	$1.07 \times 10^{-3} \text{ M}$	38.2
30	$8.18 \times 10^{-4} \text{ M}$	52.7

The amount of photoprobe (INA) remaining after a given time. The percent change is also calculated for the rate of photoprobe conversion.

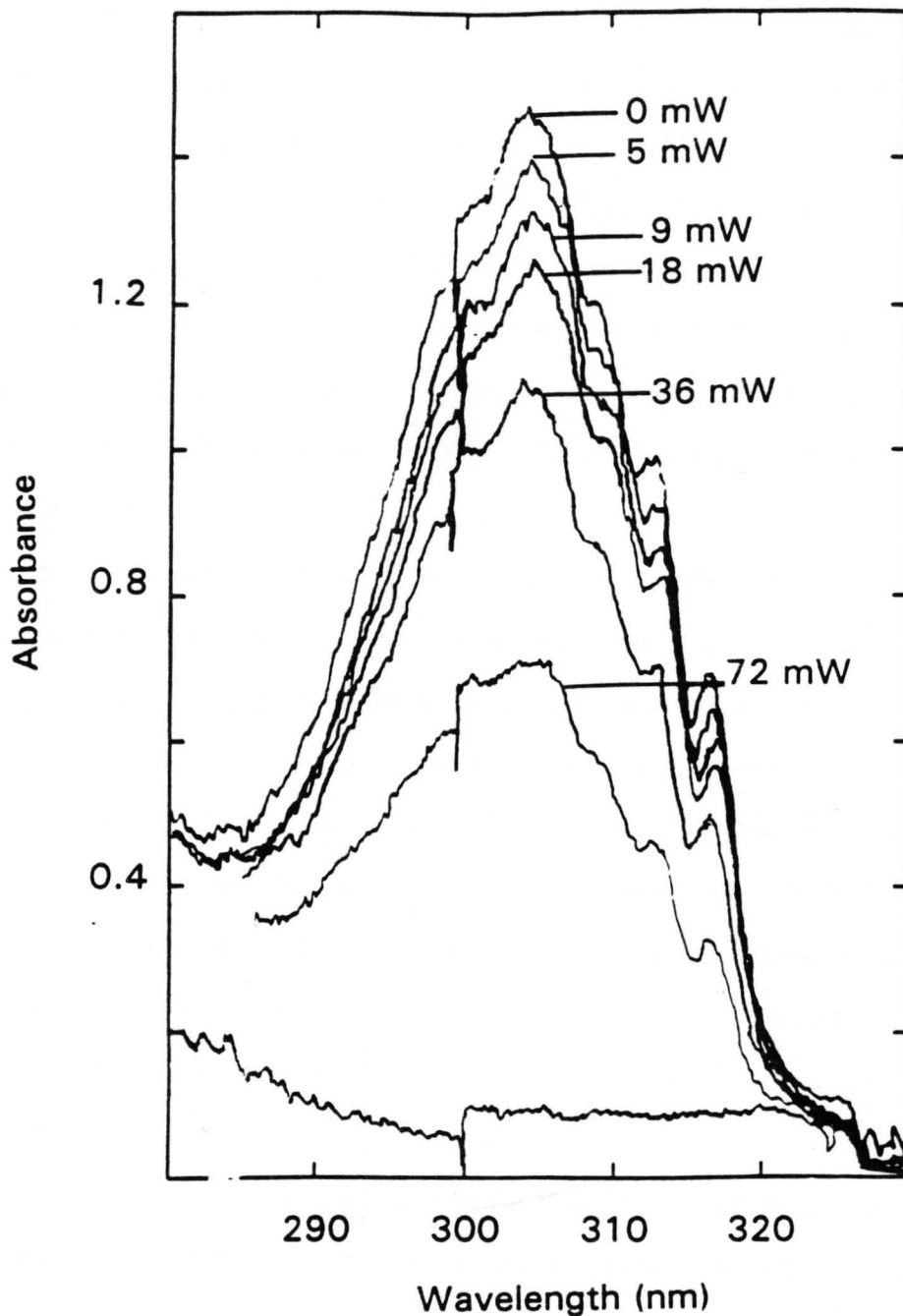


Figure 28.

The amount of photoprobe (INA) converted was measured as a function of laser power. The samples were exposed for 15 minutes each to a 514 nm laser beam.

of reducing 1/2 of the original photoprobe in 15 minutes. This can be seen by the reduction of the absorption peak at 310 nm. However, the amount of eosin in the solution had to be corrected for as a function of the number of photons it was physically capable of absorbing (Table 6). The number of photons is dependent on the fluorochrome concentration and the rate at which the molecules are promoted to the triplet state. We concluded that the most efficient power for conversion of photoprobe was 36.4 mW under these experimental conditions (Figure 29).

The concentration of eosin donor, affected the efficiency of energy transfer. We observed that lowering the eosin concentration caused a decrease in the amount of INA converted (Figure 30). In these experiments the amount of INA, power, and exposure time were held constant. Again, the energy transfer efficiency had to be normalized relative to the number of photons absorbed at a given concentration of eosin (Table 7). The result of normalization indicated that INA conversion has a maximum efficiency at 1.0×10^{-5} M eosin (Figure 31).

Finally, studies were performed to determine what effect the concentration of INA had on energy transfer efficiency. The amount of eosin, power, and exposure time were kept constant. The process was monitored at 310 nm to determine the rate of INA conversion (Figure 32). After correction for

Table VI

The Amount of INA Converted via Energy Transfer Measured as a Function of Laser Power.

Laser Power (mW)	Moles Photons Absorbed	INA Converted	Transfer Efficiency (10 ⁻⁴)
0	0	0	0
9	3.31 X 10 ⁻⁵	3.37 X 10 ⁻⁸	9.88
18	6.62 X 10 ⁻⁵	5.14 X 10 ⁻⁸	7.79
36	1.32 X 10 ⁻⁴	8.87 X 10 ⁻⁸	6.73
72	2.64 X 10 ⁻⁴	1.77 X 10 ⁻⁷	6.70

[EOSIN] = 1.32 X 10⁻⁵ M

EOSIN ABSORBANCE AT 514 nm = 1.33

.95 = 1 X 10^{-A}

[INA] STOCK = 1.04 X 10⁻³ M

Efficiency = $\frac{\text{Moles INA Converted}}{\text{Moles of Photons Absorbed}}$

LASER EXPOSURE 15 MINUTES

The amount of INA converted as a function of laser power was measured. The number of photons emitted, and the number of photons absorbed by the eosin solution in a 15-minute period. The amount of INA converted was measured and the transfer efficiency calculated.

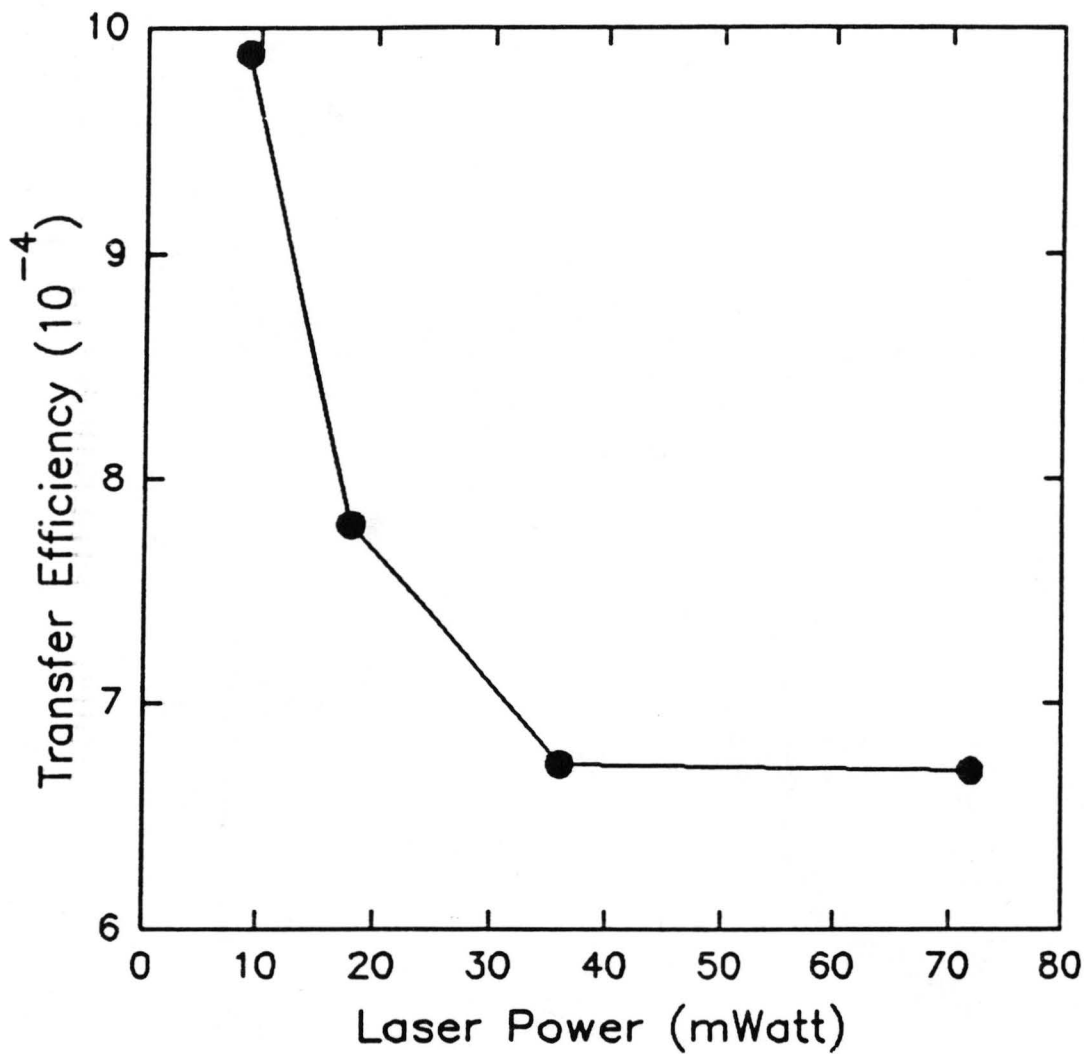


Figure 29. Energy transfer efficiency as a function of laser power.

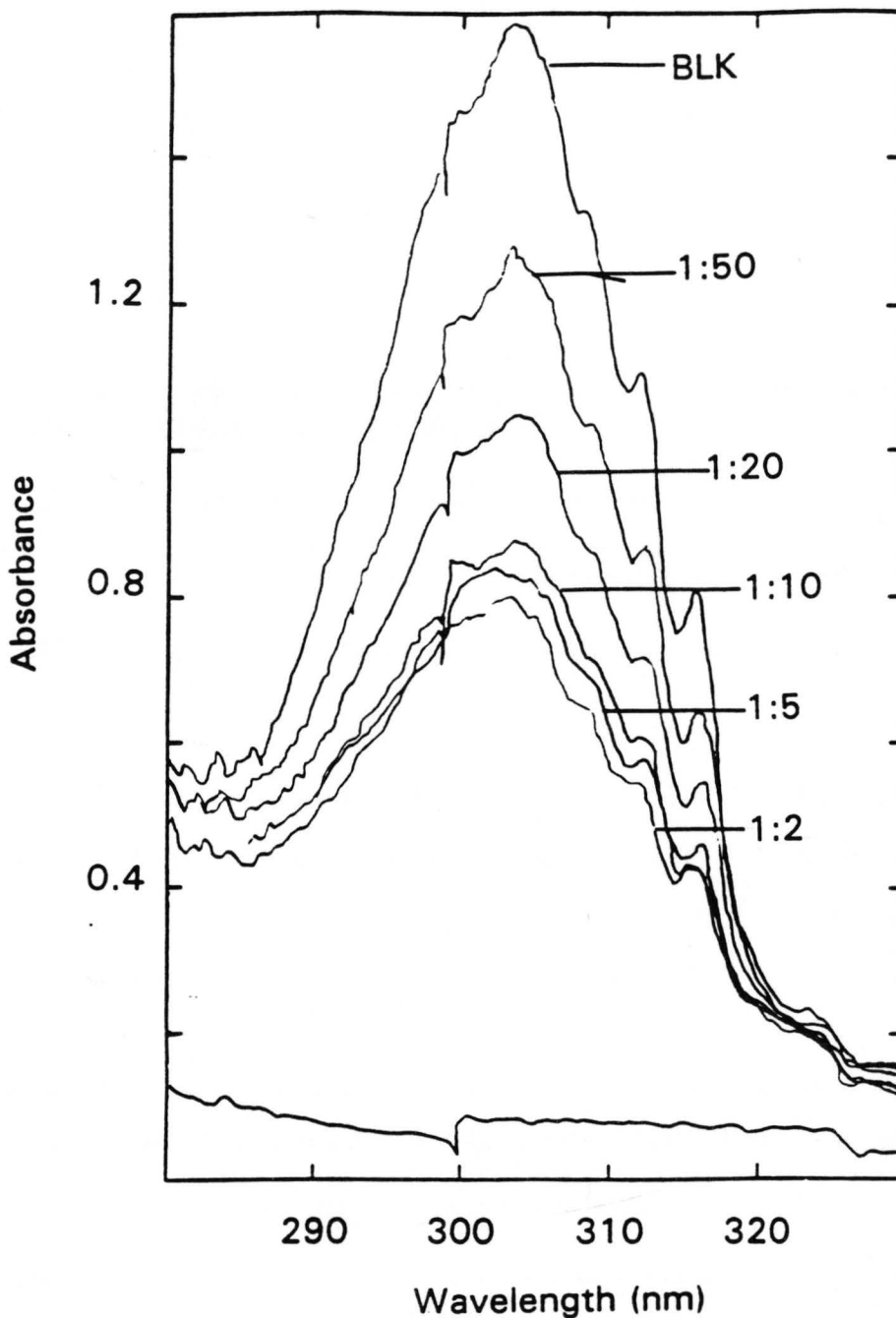


Figure 30. Energy transfer efficiency as a function of eosin concentration. Various dilutions were made of the original eosin solution (4.3×10^{-5} M). The samples were exposed to the laser (514 nm) for 30 minutes at 45.5 mW.

Table VII

The Amount of INA Converted via Energy Transfer Measured as a Function of Eosin Concentration.

[Eosin]	Moles Photons Absorbed	Moles INA Converted	Transfer Efficiency
$1.3 \times 10^{-6} \text{ M}$	2.41×10^{-5}	1.9×10^{-8}	7.75×10^{-4}
$3.3 \times 10^{-6} \text{ M}$	4.94×10^{-5}	3.2×10^{-8}	6.34×10^{-4}
$6.6 \times 10^{-6} \text{ M}$	7.31×10^{-5}	4.2×10^{-8}	5.75×10^{-4}
$1.3 \times 10^{-5} \text{ M}$	8.88×10^{-5}	4.6×10^{-8}	5.10×10^{-4}
$3.3 \times 10^{-5} \text{ M}$	9.36×10^{-5}	4.9×10^{-8}	5.21×10^{-4}

Transfer Efficiency = INA Converted/ Photons absorbed
 2.41 eV per photon at 514 nm
 $1 - 10^{-A}$ = photons absorbed correction
 [INA] = $1.04 \times 10^{-4} \text{ M}$

The amount of INA converted was calculated as a function of eosin concentration. The sample was exposed to the laser for 30 minutes at 45 mW. The number photons absorbed at given eosin concentration.

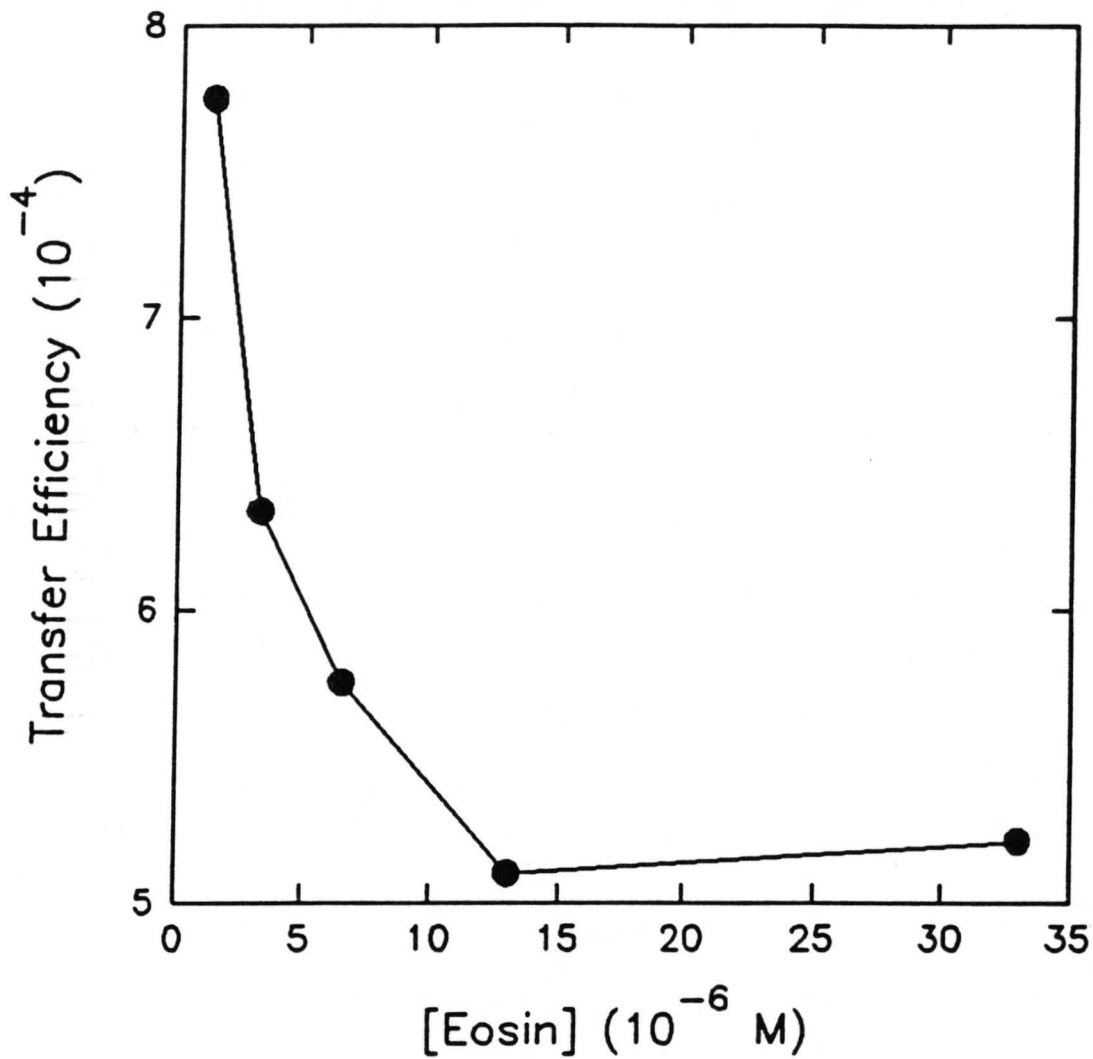


Figure 31. The efficiency of energy transfer as a function as a concentration of eosin. They were exposed for 30 minutes to 514 nm (45 mW) light.

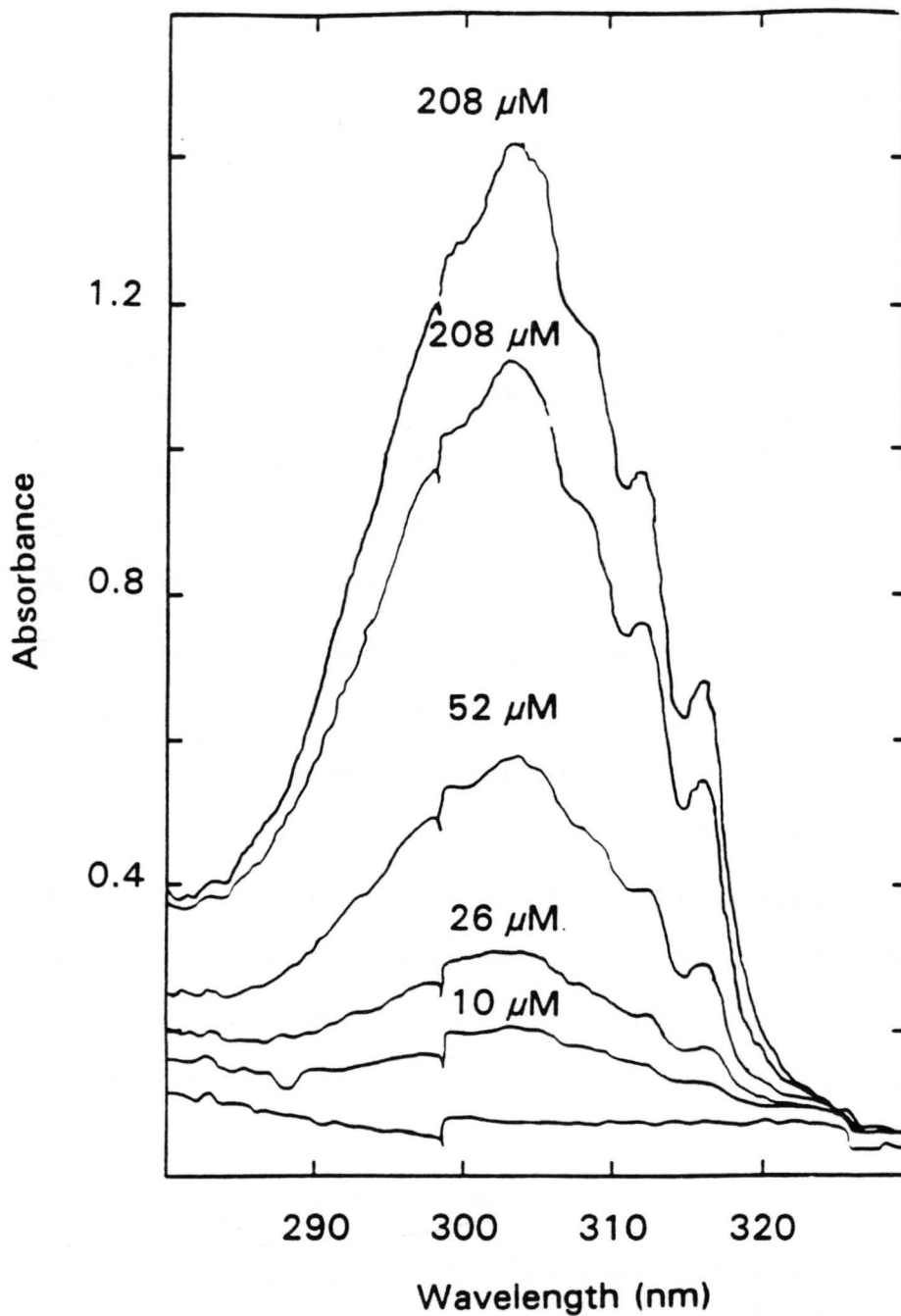


Figure 32.

The transfer of energy was measured as a function of INA concentration. Various amounts of INA were added and the depletion measured. The eosin concentration was 6.6×10^{-6} M. The experiment was exposed to 514 nm and 45 mW laser beam for 15 minutes.

photons absorbed (Table 8) the energy transfer was found to be was most efficient at $1 \times 10^{-5}M$ INA (Figure 33). INA conversion efficiency at this concentration was approximately one INA molecule was converted per 10_3 photon absorbed.

III.8 Deoxygenation vs. Time

If triplet-triplet transfer of energy was actually occurring, the removal of oxygen from the system should cause an increase in the efficiency of energy transfer and in fact this was the case. These experiments were designed to monitor the extent of increase in efficiency. Sample A was not deoxygenated, or irradiated with any light and was used as the reference, Figure 34, curve A. Curve B of this figure is data from a solution that was the exposed to 514 nm laser light for 15 minutes. Curve C is a deoxygenated sample that was irradiated for 15 minutes. This sample resulted in a 34 % increase over the non-deoxygenated sample. These results suggest that deoxygenation of the sample increase the energy transfer efficiency and results in better protein labeling.

III.9 INA Labeling of RBC Proteins

With the preceding characterization experiments completed, we were ready to apply energy transfer activation of INA to specific cell systems. The first of these systems was a suspension of RBC's. We chose RBC's because we could

Table VIII

The Amount of INA Converted Due to Energy Transfer was Measured as a Function of the INA Concentration in the presence of oxygen.

[INA] (10^{-5} M)	Δ ABSORBANCE	Δ INA MOLES (10^{-8})	Transfer Efficiency (10^{-4})
20.8	.21	4.91	8.73
10.8	.19	4.40	7.81
5.20	.11	2.57	4.56
2.60	.04	0.93	1.65
0	0	0	0

INA STOCK = 1×10^{-3} M

[Eosin] = 6.6×10^{-6} M

EXPOSED 15 MINUTES = 7.31×10^{-5} Moles of Photons Absorbed

Transfer Efficiency = $\frac{\text{INA CONVERTED (moles)}}{\text{PHOTONS ABSORBED (moles)}}$

The energy transfer efficiency is calculated as a function of the photoprobe concentration. The donor (eosin) was at 6.6×10^{-6} M. The samples were exposed to a 514 nm laser beam at 45 mW for 15 minutes.

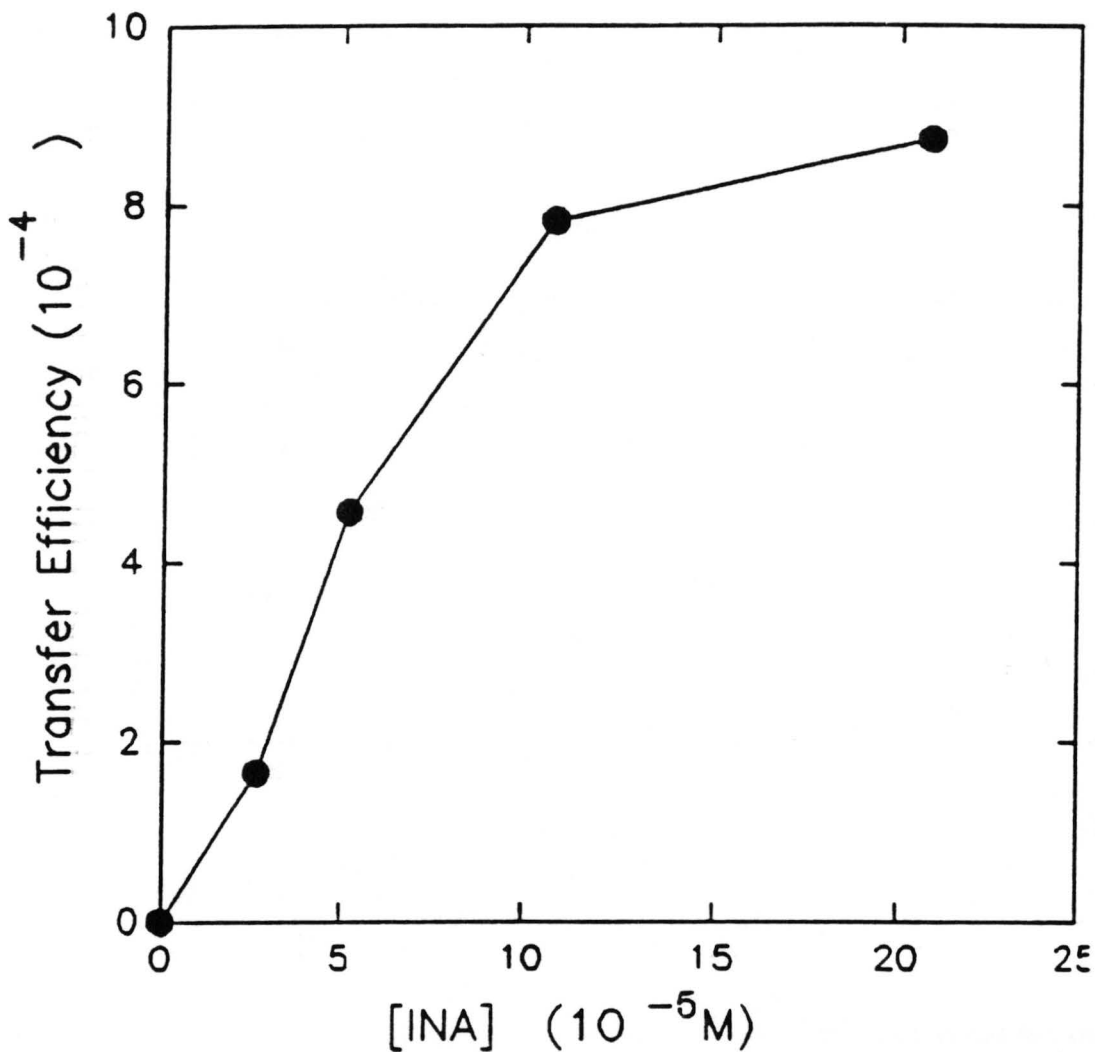


Figure 33. A plot of efficiency of energy transfer versus concentration of photoprobe (INA). The experiment conditions are stated in Table 8.

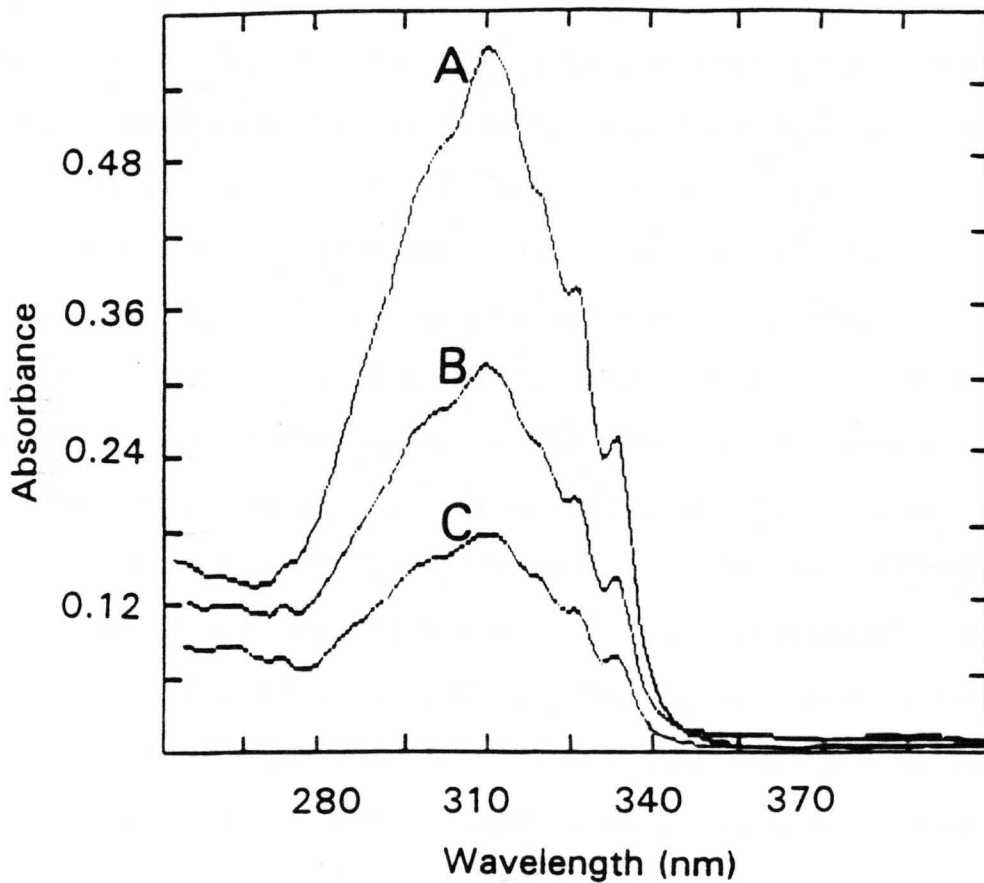


Figure 34. The energy transfer efficiency was measured as a function of deoxygenation.

obtain large numbers of these cells. Experiments were designed to determine the efficiency of energy transfer across the cell membrane (Figure 35). Here, RBC's were suspended in a solution of eosin Y and exposed to different wavelengths of light. The results obtained are summarized in Table 9. When the solution was exposed to direct ultraviolet light the INA that was already in membranes became activated. This is shown in sample 3 of the table. This condition produced the highest number of counts (18411) and the strongest intensity on the dot blot (using the anti-INA antibodies produced earlier). On the other hand, when the sample was irradiated with 514 nm light in the absence of eosin (sample 5) there was no detectable conversion of photoprobe. When eosin was present and the solution irradiated at 514nm, INA was converted via energy transfer. This can be seen through the increased number of counts and the positive immunoblots for samples 6 and 7 of table IX. The efficiency of energy transfer was observed to increase 4-5 fold as the sample was deoxygenated (sample 7). These experiments indicate that energy transfer was capable of working as predicted on a biological system.

III.10 INA Labeling of sIgM on B-cells

Next we performed the energy transfer experiments on a suspension of B lymphocytes. B lymphocytes were used because commercially available antibodies that recognize surface IgM molecules are available. The heavy chain of IgM molecules on

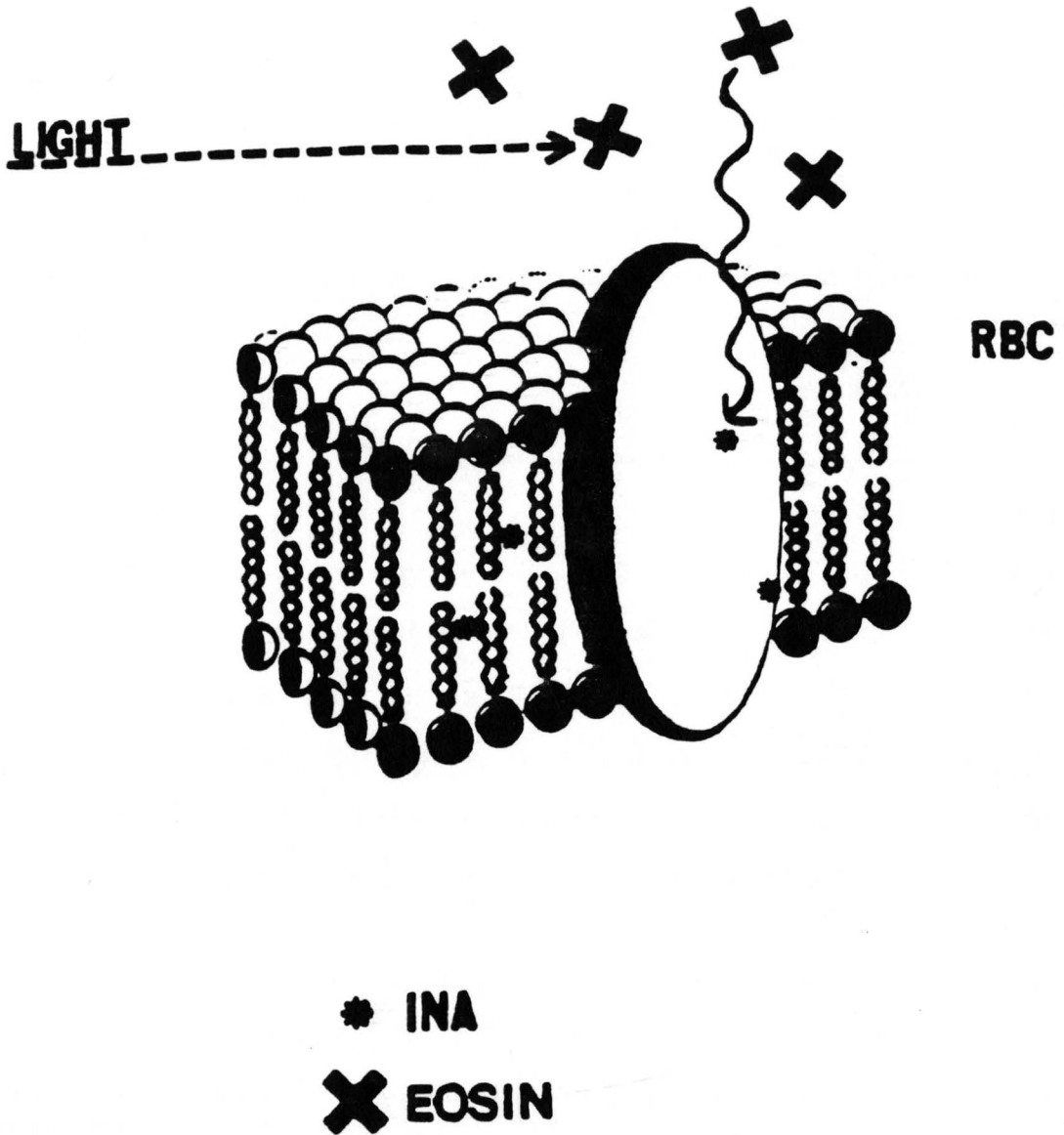


Figure 35. Labeling RBC proteins by energy transfer activation of INA. The photoprobe (INA) embeds into the lipid bilayer and becomes activated by donor molecules outside the cell.

Table IX

INA Labeling of RBC Proteins

SAMPLE	COUNTS (per min)	ANTIBODY
1 Blank	142	Neg
2 Dark blank (not exposed to any light)	251	Neg
3 UV (direct conversion at 310 nm)	18411	Pos
4 Eosin blank (not exposed to any light)	131	Neg
5 514 nm Light (no eosin in solution)	120	Neg
6 514 nm Light (Eosin solution)	255	Pos
7 514 nm Light (eosin solution deoxygenated)	904	Pos

**** LASER LIGHT ONE HOUR 514 nm, 36 mW

Summarized results from red blood cell energy transfer experiments. The amount of INA incorporation into membrane protein was detected using ^{125}I (counts) and immunoblotting with anti-INA antibodies (antibody).

mouse B lymphocytes is known to traverse the lipid bilayer anchoring the molecule on the surface. It should, therefore, be possible to label selectively this trans membrane segment using our energy transfer method. Figure 36 is a schematic diagram of the B cell energy transfer experiment. The B cells were incubated with INA allowing it to partition into the membrane. We propose that once the photoprobe was embedded in photoprobe was embedded in the membrane, it should be possible to photochemically form the nitrene and label the segment of the heavy chain of the IgM that traverses the membrane. In these experiments, eosin molecules were attached to a goat anti-mouse IgM heavy chain at a ratio of 5 fluorochromes per protein (data not shown). The antibody was allowed to bind to the cell thus holding the eosin in close proximity to the IgM heavy chains. We expected to observe INA labeling of these regions of these IgM's.

Silver staining was the method used to non-selectively identify all of the proteins on SDS gels. These gels were analyzed by the use of an immunoblot in which proteins were labeled with a goat anti-mouse IgM (heavy chain) horse radish peroxidase conjugate. The purpose of the antibody conjugate was used to determine which of the bands on the silver stain corresponded to the IgM heavy chain. When the enzyme substrate was added to the immunoblot all four lanes gave a positive result for the band corresponding to a molecular weight of 66 kDa.

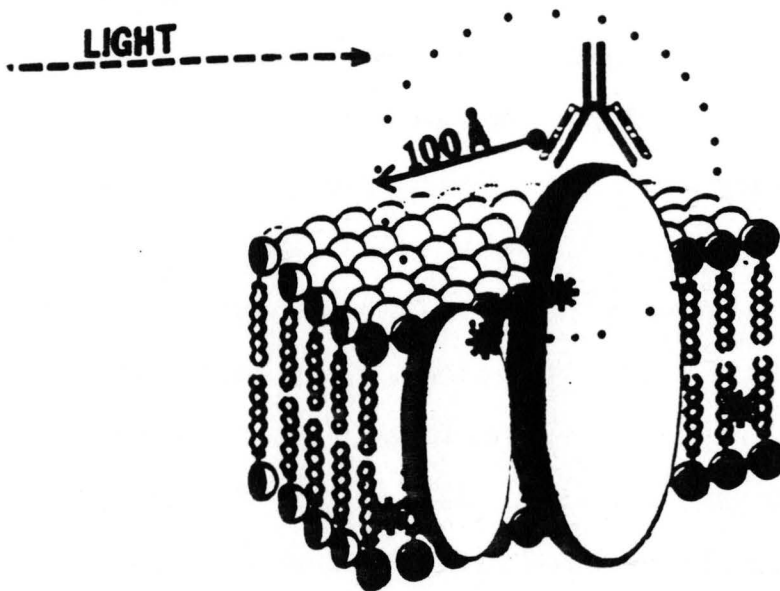


Figure 36. Schematic of a mouse B-cell. The eosin donor is covalently attached to the antibody that recognizes the IgM molecule. The donor will transfer energy to the photoprobe embedded in the membrane in the region of the heavy chain.

Four samples were analyzed on SDS-PAGE followed by autoradiography (Figure 37) to determine if energy transfer activation of INA had occurred in the region of the heavy chain. The autoradiographs were analyzed on a gel scanner for molecular weight determination. The results are shown in Figure 38. In this representation, lane A contained standard IgM that had been labeled with ^{125}I . On SDS-PAGE reducing gels this antibody dissociated into heavy chains (66 kDa) and light chains (23 kDa) and were then used as molecular weight markers for the other lanes.

Lane B contained the photoprobe and eosin-antibody conjugate that were not exposed to light. This lane had no autoradiograph bands indicating that no energy transfer activation of INA had taken place and that non-specific absorption of the photoprobe onto the membrane proteins did not occur. The third lane contained sample that was similar in composition to lane two except that this solution was deoxygenated and exposed to 514 nm light for one hour. We observed a single autoradiographic band at 66 kDa. This band corresponds to the selectively labeled heavy chain that traverses the lipid bilayer. This was the same band observed in lane 3 of the immunoblot and silver stain. This confirmed the prediction that the heavy chain of IgM could be selectively labeled with the INA photoprobe via energy transfer.

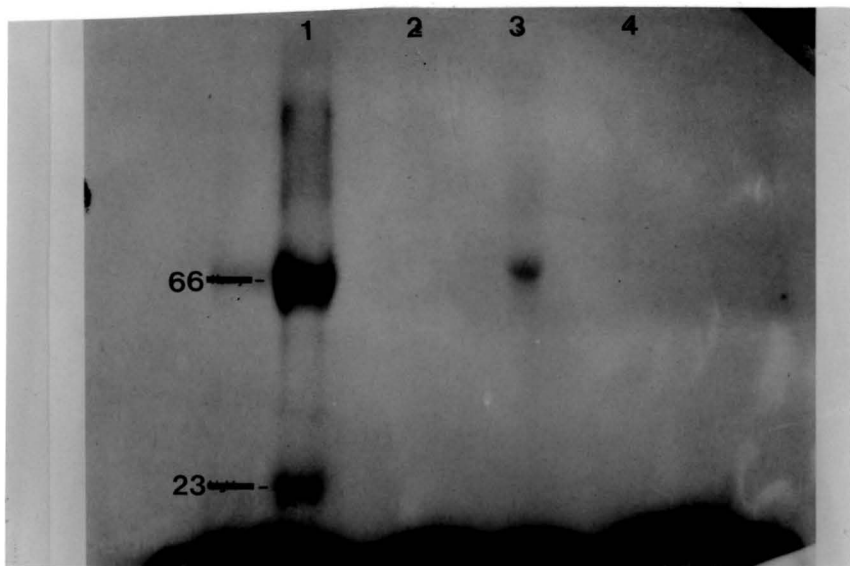


Figure 37. Autoradiograph of B cell sIgM labeled by INA using energy transfer. The samples in the four lanes are: 1) Std IgM, 2) dark blank, 3) eosin, 4) eosin blank.

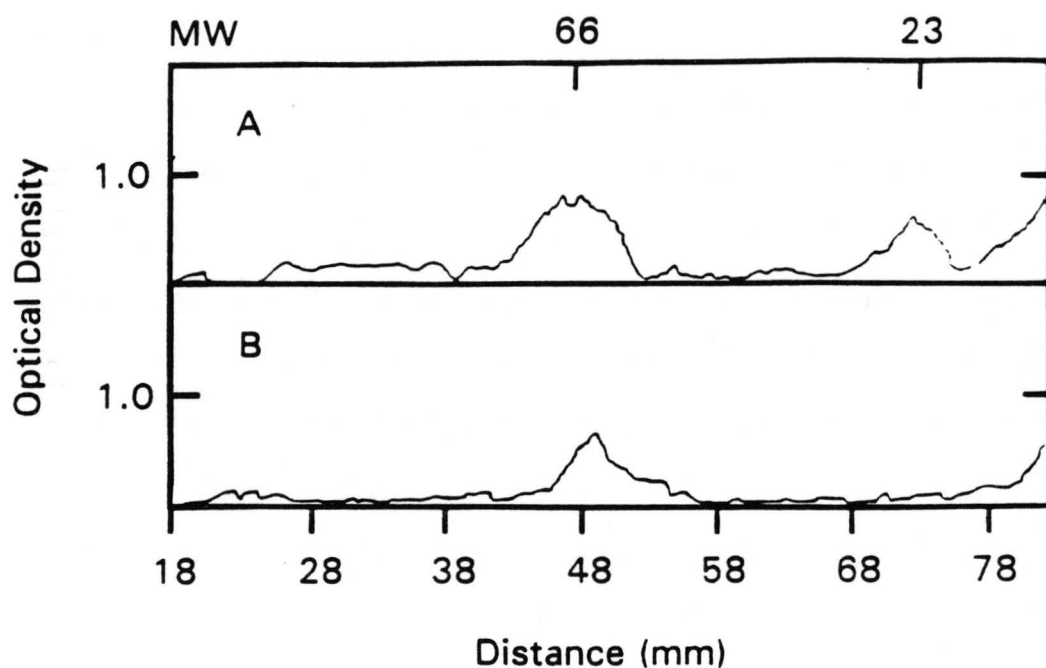


Figure 38: The densitometric scans of lanes 1 and 3 B cell energy transfer autoradiograph shown Figure 37. The top scan shows the IgM standard in which the 66 kDa heavy chain and 23 kDa light chain are labeled. The bottom scan is of lane 3 where only the 66 kDa heavy chain is labelled.

Lane four held a sample of the photoprobe and antibody but no eosin. This solution was exposed to 514 nm laser light for one hour. The absence of bands in the autoradiograph indicated that no conversion of the photoprobe occurred due to UV plasma glow or thermal decomposition. Thus, we effectively filtered the unwanted wavelengths of light from the laser.

III.11 INA Labeling of the IgE Fc Receptor on 2H3 Cells

Another cell line we were interested in studying was the 2H3 rat basophilic leukemic cell line. These mucosal mast cells express type I Fc_ε receptors on their surface and are capable of binding IgE molecule through its ε-chain. When these bound IgE molecules are crosslinked with antigen they exocytose granules containing vasoactive amines. This is characteristic of allergic responses. We were interested in probing these Fc_ε receptors and determining the changes that occur upon crosslinking.

The INA activation by energy transfer of 2H3 rat basophilic leucemic cells (RBL) required two different immunoglobulins, rat IgE and mouse anti-rat IgE. Rat IgE-eosin conjugate (2 eosin per protein) was added and allowed to bind to the non-crosslinked RBL cell surface. This allowed the eosin donor to be held in close proximity to the Fc_ε receptor on the surface. The number of eosins bound per antibody was kept low so as to not modify the epitope recognized by the mouse anti-rat IgE. Antibody binding was

confirmed by observation of the cells under a fluorescence microscope (524 nm excitation light). The cells exhibited specific fluorescence if antibody was bound.

The second antibody was a monoclonal mouse anti-rat IgE heavy chain. This antibody was used to crosslink the IgE molecules on the surface of the basophil cell. This mimics the binding of naturally occurring antigens. Both the non-crosslinked (Figure 39) and crosslinked (Figure 40) systems were irradiated with 514 nm light and INA activation by energy transfer was allowed to occur.

The extent of protein labeling was analyzed by SDS-PAGE (Figure 41) followed by autoradiography (Figure 42). Lanes one and four contained molecular weight standards which included bovine albumin serum (66 kDa) egg albumin (45 kDa) and carbonic anhydrase (29 kDa). The standards were labeled with ^{125}I for further examination by autoradiography. Lanes two (non-crosslinked) and three (crosslinked) contained proteins isolated from the IgE (RBL cells) experiments. The polyacrylamide gel was silver stained using the Oakly method shown in Figure 41. Many different proteins were found to be present in the gel. This was indicative of the total amount of protein present in the basophil membrane.

The autoradiograph was scanned (Figure 43) to determine the molecular weights of the proteins contained on it. Radio-labeled BSA and carbonic anhydrase were used as standards for

IgE

LIGHT
514nm →

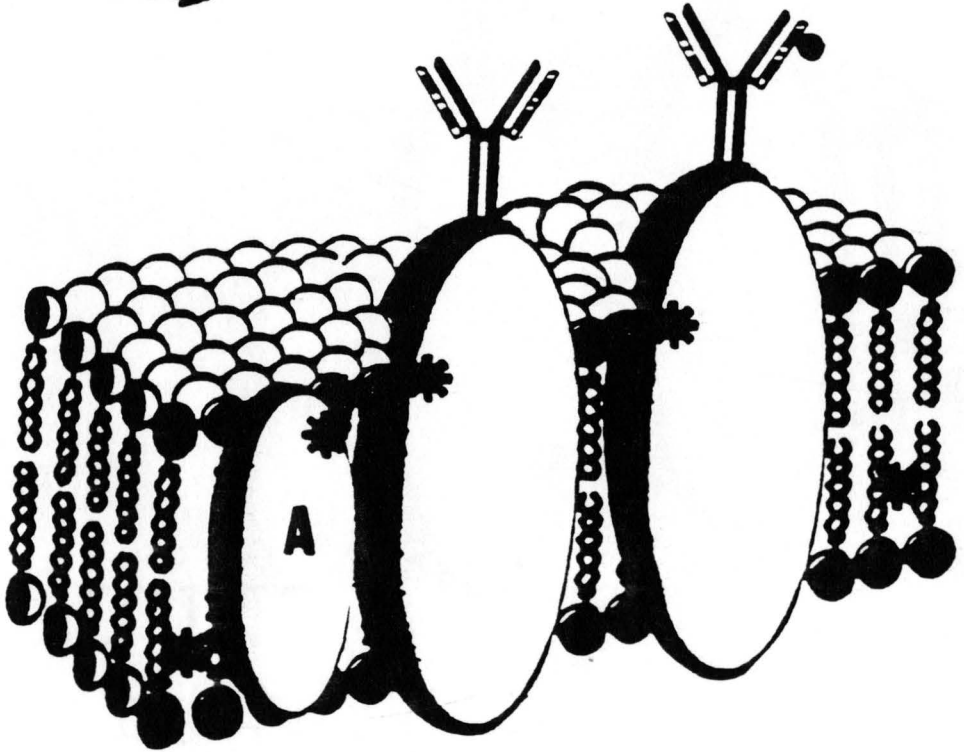


Figure 39. A schematic representation of the IgE molecule binding to the type I Fc_{ϵ} receptor on the RBL cell surface.

IgE

LIGHT
514nm →

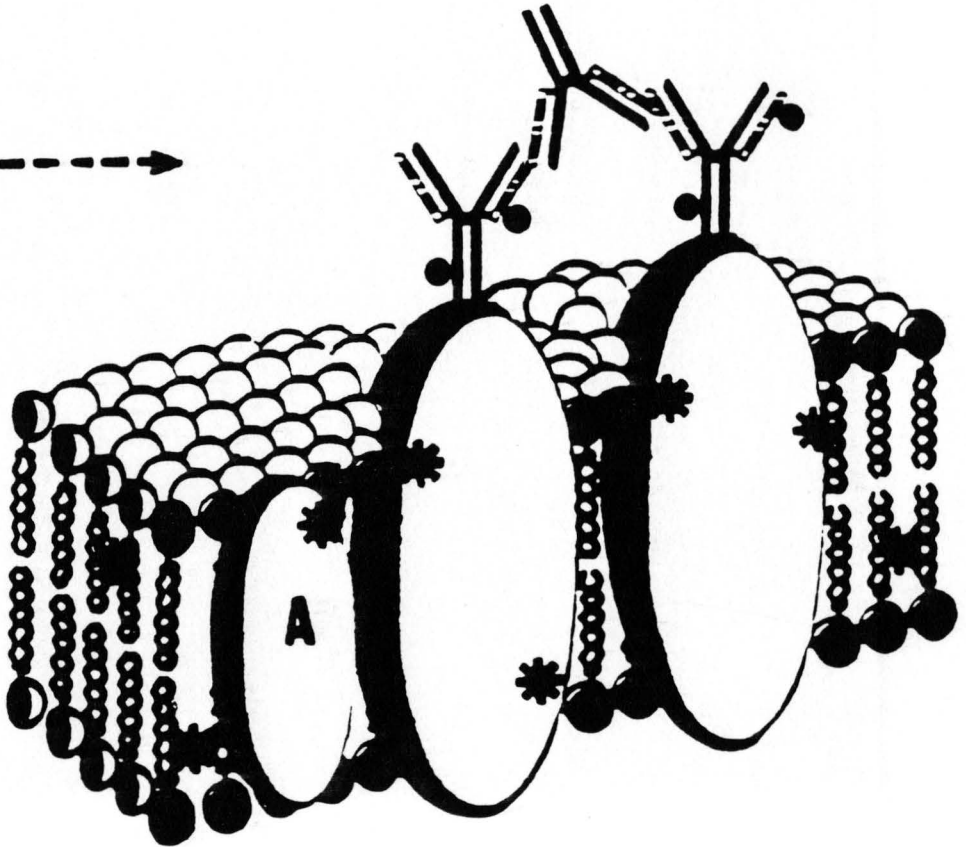


Figure 40. A schematic representation of the RBL cell surface being crosslinked using an anti-IgE antibody.

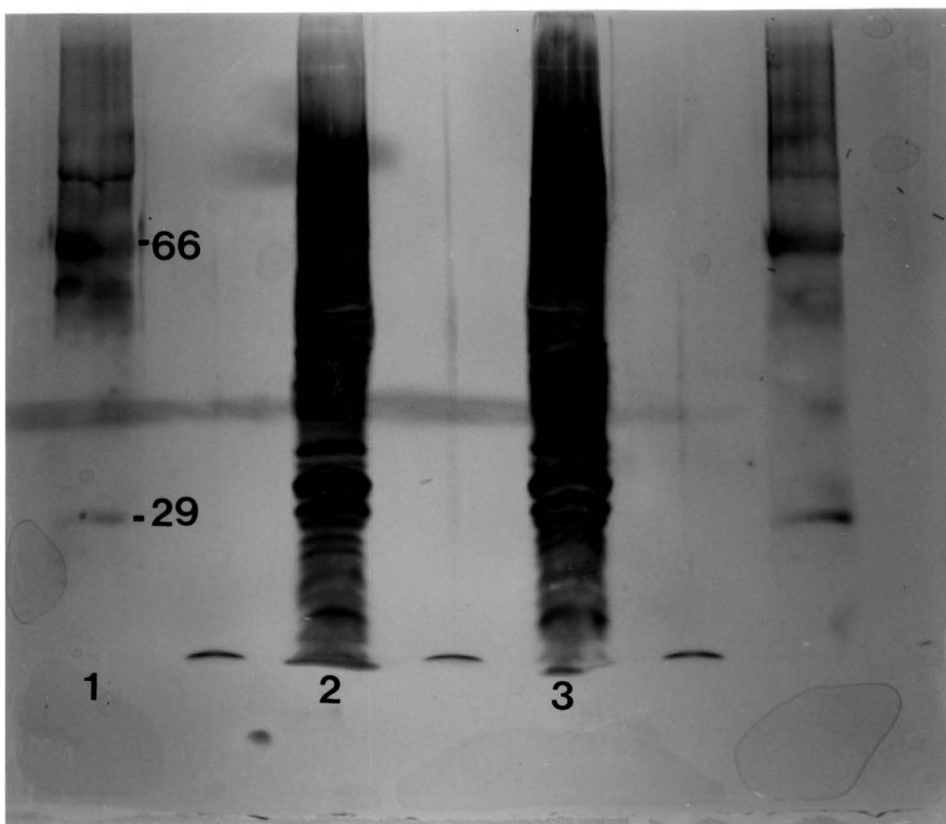


Figure 41: Silver stain of the proteins isolated in both crosslinked and non-crosslinked energy transfer system. The molecular weight standards are in lanes one and four Bovine Serum Albumin (BSA, 66 kDa) and Carbonic Anhydrase (C.A., 29 kDa). In lane two is the non-crosslinked and lane three is the crosslinked system.



Figure 42: The autoradiograph of the SDS-gel for RBL cells INA labeled via energy transfer. Lane one is the standard containing BSA (66 kDa) and carbonic anhydrase (29 kDa). Lane two is the non-crosslinked system while lane three is the crosslinked system.

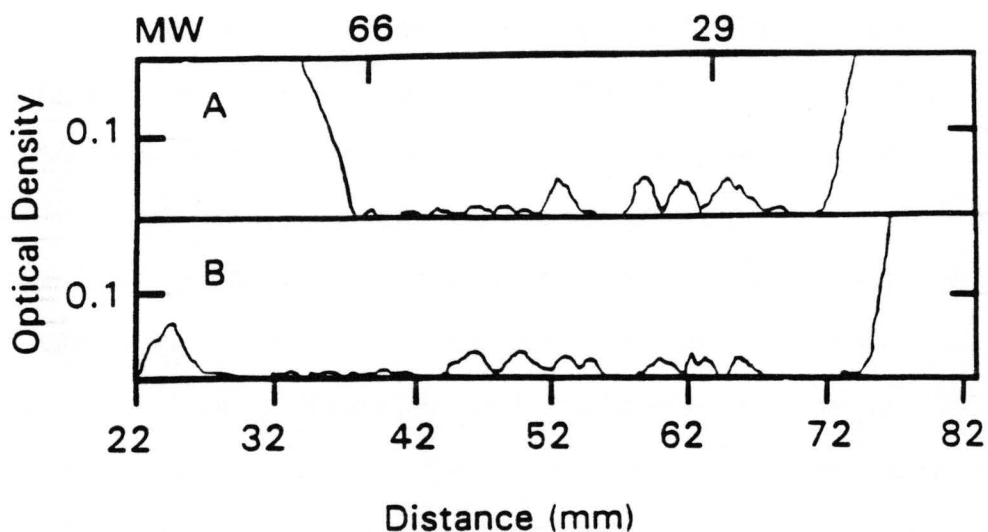


Figure 43: The gel scan of the autoradiograph for RBL cells INA labeled by energy transfer. The non-crosslinked system labelled four proteins (29, 34, 38, and 49 kDa) with the photoprobe (Lane A). The crosslinked system labeled a additional three proteins (43, 54, and 60 kDa) (Lane B).

this analysis. In the non-crosslinked system (Figure 43, lane A) four proteins were labeled with the photoprobe. These proteins had molecular weights of 29, 34, 38, and 49 kDa and correlated with the α chain, α subunit, β chain, and the 63 kDa associated protein of the Fc receptor. The 63 kDa protein dissociated into two 29 kDa protein bands on SDS reducing gels (10). In the crosslinked system (Figure 43, lane B), we observed three additional proteins of molecular weights of 43, 55, and 60 kDa. These three proteins were evidently recruited into the region of the IgE Fc_ε receptor during or after crosslinking. Their function might be to help in the release of histamine from the cell. A comparison of the molecular weights for both systems is found in Table 10. It should be noted that molecular weights of under 12 kDa were impossible to identify. This was due to the large background signal caused by free photoprobe and lipid-photoprobe in the moving solvent front. These results showed that we were able to effectively probe the differential recruitment of proteins into the region of the Fc_ε receptor upon crosslinking the receptors.

Table X

The Molecular Weights of the 2H3 RBL cells INA labeled by energy transfer from IgE.

 STANDARD

PROTEIN #		MW (Da)
1	BSA	66,000
2	CARBONIC ANHYDRASE	29,000

CROSSLINKED

PROTEIN #		MW (Da)
a		60,000
b		54,000
c		49,000
d		43,000
e		38,000
f		34,000
g		29,000

NON-CROSSLINKED

PROTEIN #		MW (Da)
c		49,000
e		38,000
f		34,000
g		29,000

A summary of the molecular weights of the proteins labelled with the photoprobe in both the crosslinked and non-crosslinked systems.

Chapter IV

DISCUSSION

Photoaffinity probes have been used extensively in the study of protein function. These lipophilic probes are relatively easy to synthesize, and are reactive with functional groups on molecules available within the membrane. The aromatic azides are a popular group of photoaffinity probes which, when irradiated with ultraviolet light, will form an active nitrene in the excited singlet state. It has been observed that azides can be photo-decomposed through the use of both singlet sensitizers (aromatic hydrocarbons) and triplet sensitizers (aromatic ketones) (32). Both sensitized mechanisms can work simultaneously with one of them contributing more heavily than the other to the major photo-activation. If the azide is generated via a sensitizing agent, the newly formed nitrene can exist in the excited triplet state (63,64). Following formation of the nitrene, two probable reactions can occur: the abstraction of a proton from a solvent molecule or insertion into a covalent bond (24). The weakly electrophilic nature of nitrenes causes them to preferentially insert into an O-H bond rather than a C-H bond (22). If the nitrene is generated in a membrane, insertion will occur with a proximal lipid or protein. It has

been observed that probes of this type have difficulty in labeling proteins with low hydrophobicity (28). However, the reactivity of the nitrene group can be increased by substitution of the aromatic ring with an electron withdrawing group (31). Addition of nitro groups increases reactivity and also causes a shift in absorbance maximum to a longer wavelength. This has considerable advantage in studies of biological molecules including DNA and proteins which undergo degradation upon UV exposure (65). For example, pyrimidines can dimerize or undergo hydrolysis at the 5-6 double bond (30). Exposure to longer wavelengths reduces damage to membrane proteins (24). Arylazides were first used by Knowles and colleagues (66) to identify the antibody binding site of 2-nitro-4-azidophenyl. Since then aromatic photoprobes have been used to label membrane proteins including insulin receptors, the lactose transport system, and ATPase (22). The probe naphthalene azide, which partitions in the hydrophobic lipid bilayer, (27) can be activated at wavelengths above 300nm and is capable of labeling membrane components. Naphthalene azide reactivity can be increased by substitution of the naphthalene ring with iodide to form 5-iodonaphthyl-1-azide (INA) (26). This photoprobe was synthesized through a series of steps in which 1,5-diaminonaphthylene was derivatized to form 5-iodo-naphthyl-1-azide with an overall yield of 68%. The yield might have been greater if the extraction of the photoprobe from the mud-like slurry was more

efficient. The photoprobe once isolated, was dissolved in ethanol, a saturated solution at 25°C being approximately $2.5 \times 10^{-3}M$ and used in the energy transfer experiments. INA has an absorbance maximum of 310 nm and an extinction coefficient of $21,400 M^{-1}cm^{-1}$. Although INA, activated via UV emission, was originally used to label intrinsic proteins in biological membranes (35), later studies showed that it was possible to activate the probe at considerably higher wavelengths. Gitler and coworkers (50) used fluorescein as an INA sensitizing agent, imbedding it into the membrane together with INA. Upon irradiation with 480 nm light, only INA in the proximity of fluorescein was activated (50). In our studies we used eosin to activate INA embedded in RBC membranes. We feel that because eosin is structurally similar to an aromatic ketone, the majority of energy transfer we observed could be the result of triplet sensitization. Direct activation of INA with a UV lamp produced the highest level of protein derivatization. Activation at 514 nm, resulted in a 7-fold higher incorporation of [^{125}I]-INA into the membrane in comparison to background and suggested that INA activation occurred.

Allowing the fluorochrome to insert in the membrane is useful for examining the organization of membrane proteins in the lipid bilayer. Only those proteins in contact with membrane lipids are derivatized with INA. Gitler (48) used FITC-bean lectin to probe both frog retina membranes and mouse

lymphoma cells. Although INA randomly derivatized some membrane proteins, it appeared that an 88 kDa protein in the retina and a 56 kDa protein in the mouse lymphoma cells were specifically labeled with the photoprobe. Raviv and coworkers (47) have also used doxorubicin as a agent to study a multidrug transporter in human KB carcinoma cells (47). Doxorubicin is actively transported across the sarcoplasmic reticulum membrane and, when activated by 450 nm light, the probe attaches to a 170 kDa protein. Gitler suggested that the activation by fluorescein required close proximity between the two molecules and that energy transfer was the result of charge transfer complexes (32).

In the experiments we describe here, energy transfer was accomplished using eosin as a donor molecule, and from experiments on murine B-cells and 2H3 cells, it appears that a majority of the sensitized energy transfer occurs as a result of energy exchange from the triplet state of a donor eosin molecule to a neighboring INA in the singlet ground state. The azide is promoted to the triplet state and becomes chemically active after loss of nitrogen. Triplet-triplet energy transfer occurs over distances of up to 50 to 100 Å (37,38). Maximal efficiency of triplet-triplet energy transfer requires proper molecular orientation and similar triplet energy levels between the donor and acceptor molecules (38). Eosin was selected as the donor for these experiments because approximately 70 percent of eosin molecules in the

excited singlet state undergo intersystem crossing into the triplet state (40). In comparison, only five percent of excited singlet fluorescein molecules enter the triplet state (40). The triplet lifetime of eosin was also important in increasing the probability of acceptor molecule activation (38). Energy transfer efficiency can be increased by lengthening the triplet lifetime. Oxygen, as well as other molecules such as phenol (67), are excellent triplet energy acceptors. Under aerobic conditions EITC-BSA had a triplet lifetime of approximately 10 μ s which was increased to 1 msec upon removal of oxygen using glucose oxidase and catalase (Figure 44).

Glucose oxidase is a flavoenzyme that catalyzes the oxidation of β -D-glucose in the presence of oxygen to form δ -D-gluconolactone and hydrogen peroxide. Catalase catalyzes the reduction of hydrogen peroxide to water and oxygen. The overall reaction of the enzymes is the oxidation of two glucose molecules to remove one oxygen from solution (Figure 44). Characterization of the energy transfer between the photoprobe and eosin donor was first obtained in solution to demonstrate that the system worked. Later labeling experiments were performed in biological membranes. Experiments were designed to monitor the energy transfer until half of the original photoprobe concentration was depleted.

GLUCOSE OXIDASE



CATALASE



Figure 44. Enzyme deoxygenation system for INA activation via energy transfer. Glucose oxidase and catalase will remove O_2 from the system in the presence of glucose.

The transfer efficiency was measured as a function of exposure time, laser power, eosin concentration, and INA concentration. To assure the solubility of the hydrophobic photoprobe and to better mimic conditions that exist in the lipid bilayer the experiments were performed in a solution of 70 % ethanol in water. It should be noted however, that ethanol has been reported to lower the overall efficiency of energy transfer (67). This was undesirable in our system. But fortunately, the efficiency was not greatly affected by the use of ethanol.

A 514 nm wavelength beam of light from an argon ion laser was used to excite the donor eosin molecules. The beam was passed through a 514 nm band pass filter and a solution of 0.1 M potassium ferricyanide at pH 12.5. The solution of ferricyanide served two purposes. Firstly, it was used as a wavelength filter because it absorbs strongly in the near ultraviolet. Second, the ferricyanide solution was cooled to 10 °C and circulated through the jacketed cuvette in which the experiments were performed to avoid heating from the laser which would result in thermo-decomposition of the photoprobe. Once the beam was filtered, it was expanded to approximately 1 cm in diameter using a 8X galileon telescope. This increased the cross section of solution interacting with the laser beam.

Two methods were used for the identification of membrane proteins labeled with the photoprobe. First, the probe was radiolabeled with [¹²⁵I]-INA and proteins were analyzed by

liquid scintillation counting. Second, an antibody was developed that recognized the photoprobe. In the latter method, the samples were incubated with the anti-INA antibody and the proteins were then analyzed to determine which of them had the antibody attached. The antibody detection method was utilized for experiments in which proteins were heavily labeled since it was desirable to avoid the use of ^{125}I . The antibody method did not have the sensitivity of the radiolabeling method. Thus the radiolabeling had to be employed in situations where the proteins were lightly labeled.

In order to develop a working antibody against the probe, the probe was injected intramuscularly into a rabbit. Because the photoprobe was too small to be recognized by the immune system the photoprobe was attached to a larger carrier protein, rabbit immunoglobulin. The animal's immune system recognized this as a foreign particle and produced antibody against it. In these experiments, the water soluble molecule, an N-hydroxy sulfosuccinamide ester derivative of the photoprobe, was coupled to the rabbit IgG molecule in an aqueous solution. Presumably, by using rabbit IgG, more antibodies would be produced that were specific for the photoprobe rather than for the carrier protein. Another commonly used carrier protein is bovine serum albumin (BSA). However, this protein has a strong immune response of its own in rabbits and was not useful.

The method of photoprobe attachment to carrier protein was important for proper presentation to the immune system and subsequent antibody production. To provide the correct photoprobe-carrier protein attachment, a linker arm was attached to the probe. This made the INA ring system more accessible to the antibody binding site, making it more immunogenic. Generally, the more mobile proteins epitope, the greater the immune response against it. Additionally, the linker arm helped lessen the extent to which the hydrophobic photoprobe associated with and folded onto the backbone protein. This also increased the probability of recognition by the immune system.

In order to assure the production of an antibodies that recognize our photoprobe it is important to mimic the photochemistry of the INA attachment to the protein. Secondary amines result from the carbon-hydrogen insertion into proteins. To accomplish this we performed an alkylation of the aromatic amine derivative of the photoprobe. This resulted in the formation of an amide. This amide form of the photoprobe derivative was injected into the rabbits. Because the amide group is known to be highly immunogenic, the resulting antibodies had to be carefully screened to determine specificity.

Therefore, antibodies generated by the rabbits were affinity purified and tested for specificity. The results of the tests showed that the affinity purified antibodies

recognized the photoprobe exclusively. The animals may have produced antibodies against the linker arm and carrier protein, but they did not interact with the affinity column and were discarded with the rest of the serum. The purified antibodies recognized the photoprobe that was both photochemically and chemically attached to protein. This assured us that the difference in the functional group used in the immunization had little effect. It should be noted that the antibodies had a stronger response to the chemically attached photoprobe in comparison to the photochemically attached photoprobe. This is probably due to the slight chemical difference between the amine and amide.

The second method for detection was radiolabeling the photoprobe. After the proteins were extracted from the membrane, the rate of beta particle emission by the probe was determined using a scintillation counter. This reflected the number of photoprobe molecules attached to the proteins. Autoradiographic methods also were used to determine specific protein labeling after separation of the proteins by electrophoresis.

After characterization in solution, we determined that it was possible to transfer energy from an eosin donor to a photoprobe acceptor that was embedded into the lipid bilayer of the cell. Our model cellular system used was the red blood cell. Cells were reacted with the photoprobe and then placed in a solution of eosin. We observed that direct conversion of

our photoprobe by 310 nm light had the highest amount of reaction. The photoprobe molecules that were in close proximity of membrane proteins were activated and covalently to neighboring proteins. The antibody method describe earlier also demonstrated the strongest response to direct conversion indicating that proteins were heavily labeled. Samples exposed to 514nm laser light but not containing eosin demonstrated no significant increase in counts over background. This proved that there was no conversion due to thermal decomposition or ultraviolet plasma glow. Also, the spontaneous reaction of the probe with proteins was insignificant. The effect of oxygen had on the transfer efficiency of energy across membranes was observed in samples exposed to laser light and containing eosin. The deoxygenated sample was labeled at a level approximately four times greater than the oxygenated sample. Both samples gave positive test for INA using the anti-INA antibody method. However, the deoxygenated sample consistently produced considerably stronger results. This suggests that the transfer of energy via a triplet-triplet pathway is more efficient.

We learned from the RBC experiment that it was possible to transfer energy from a donor molecule outside a cell membrane to an acceptor molecule within the membrane. It should be considered, however, that the eosin molecule, being hydrophobic, could also partition itself into the membrane.

To further study the mechanism and general usefulness of energy transfer, we next used our technique on murine B-cells. We examined the INA labeling of sIgM by energy transfer between EITC-conjugated anti-IgM and INA on murine B-cells. Surface IgM has two identical heavy chains with a molecular weight of 68 kDa and one transmembrane domain of 26 amino acids (68) which serves to anchor the IgM molecule in the membrane. EITC-anti-IgM antibody binds to the extracellular portion of the IgM molecule. Unlike the RBC experiments it is unlikely that eosin is able to insert into the membrane in this configuration. Therefore, any transfer of energy would have to occur at distances greater than those explained by charge transfer (10-15 Å) (38). Following exposure to 514nm light, only the heavy chain on the IgM molecule reacted with INA. Silver stained SDS gels of B-cell membrane proteins suggest that this method was indeed selective. Of the many proteins appearing on the SDS gel only one was labeled with [¹²⁵I]-INA. We concluded that energy transfer via a triplet-triplet activation mechanism rather than collisional energy transfer might be occurring in the eosin-INA system.

Finally, we attempted INA activation using energy transfer in the study of the more complex RBL cell type I Fc_ε receptor. These receptors are known to have a molecular weight of approximately 130 kDa (9), and are composed of three different peptides - the α (30 kDa), β (34 kDa), and γ (7 kDa) chains (6). The receptor binds IgE, a 180 kDa protein

(Figure 45) (68), on the surface of the RBL cell (8,69). Crosslinking of IgE on the surface ultimately results in degranulation of the basophil cell. Energy transfer was used to probe the membrane for the possible protein recruitment into the region of the receptor upon crosslinking of the Fc receptor.

The donor chromophore eosin, was covalently attached to IgE bound to the Fc_ε receptor of the RBL cell plasma membrane. The membranes were studied withh the Fc_ε receptor in both crosslinked and isolated states.

In our laboratory, we have previously performed rotational diffusion measurements on the type I Fc_ε receptor to determine its hydrodynamic size in isolated and aggregated states (70). Our rotational diffusion measurements of the Fc_εR probed with EITC-derivatized IgE gave suggested a molecular weight consistent with monomeric Fc_ε receptor. Probing using anti Fc_ε receptor, however, gave a molecular weight somewhat greater than that expected for the monomer-dimer distributions. Studies by Ortega et al. (71) suggest that dimerizing the Fc_εR results in a subsequent recruitment of a proximal protein which may be necessary for signal transduction (72). In our experiments we attempted to INA label this proximal protein following Fc receptor aggregation and extract it from the membrane for characterization. In the non-crosslinked experiment the photoprobe labeled four proteins. These proteins had molecular weights 49, 38, 34,

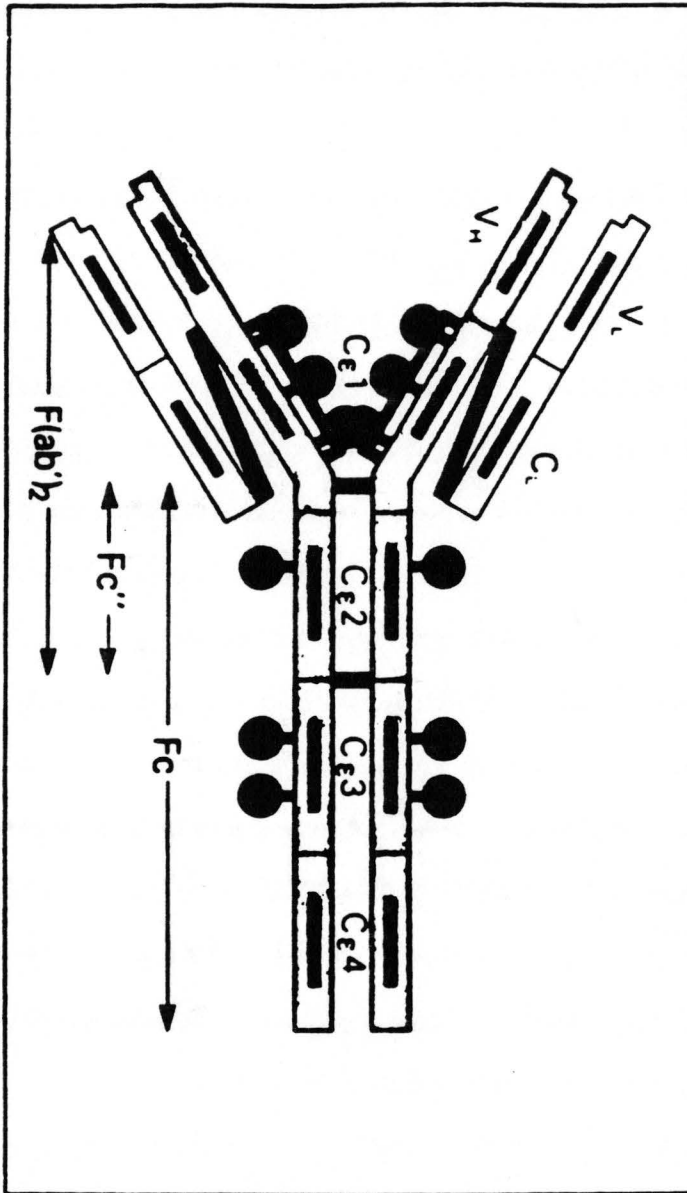


Figure 45.

The IgE molecule consists of two heavy chains and two light chains. The molecule contains an Fc region which binds to the Fc receptor on the rat basophil cell.

and 29 kDa which corresponded to those that are expected to be within the Fc_ϵ receptor. A 63 kDa protein had been previously reported to associate with the Fc_ϵ receptor (10). This molecule dissociates into two monomers having a molecular weight of 29 kDa in reducing SDS gels (I. Pecht, personal communication). The fourth protein labelled at 29 kDa was probably the dissociated 63 kDa protein. Slight differences in molecular weight from those expected were probably due to the latitude of migration determination inherent in the use of SDS-electrophoretic gels.

An antibody that binds to the IgE heavy chain was used to crosslink Fc_ϵ receptors on the surface of RBL. This antibody was selected because it was capable of binding to the membrane bound IgE. The crosslinked experiment labeled the same four proteins as the non-crosslinked experiment. In addition three new proteins were labeled with the photoprobe. These proteins had molecular weights of 43, 54, and 60 kDa. To confirm INA attachment all seven bands were also recognized by anti-INA antibodies on immunoblots. These three proteins may be involved in the Fc receptor function and in triggering basophil degranulation upon crosslinking of the membrane.

Although, photoaffinity labeling techniques are capable of identifying primary and associated proteins in intact cells under physiological conditions (47,48,50), this techniques has several limitations. To activate the nitrene through energy transfer mechanism requires long exposure times. For example,

Fc_γ receptor labeling required one hour to obtain detectable results on the autoradiographies. Also, once formed the nitrene can have a relatively long lifetime 200 μs in the membrane (73,74). Because membrane proteins can traverse from 200 to 1400 nm/s within the membrane (16), some random labeling of proteins with the photoprobe probably occurs. The use of more reactive compounds such as a carbenes may help to lower such random labeling of membrane proteins (29,75). Further, due to the relatively low levels of labeling, radioisotopes are often employed in detection systems, but these may cause degradation of the photoprobe. Radiolabeled anti-photoprobe antibodies (e.g. the anti-INA antibody that we developed) can be used to identify photo-labeled membrane components, thus avoiding degradation of the photoprobe. The ability to label membrane proteins selectively should allow for future researchers to probe deeper into the function and physiological make up of membrane structures.

REFERENCES

- (1) Kahn, C.; Bair, K.; Jarrett, D.; Flier, J. *Proc. Natl. Acad. Sci. USA* 1978, 75(9), 4209-13.
- (2) Schechter, Y.; Hernaez, L.; Schlessinger, J.; Cuatrecasas, P. *Nature* 1979, 278, 835-8.
- (3) Conn, P.; Rogers, D.; McNeil, R. *Endo.* 1982, 111(1), 335-7.
- (4) Schreiber, A.; Schlessinger, J.; Edidin, M. *J. Cell Biol.* 1984, 98, 725-31.
- (5) Phillips, M. L.; Moule, M. L.; Delovitch, T. L.; Yip, C. C. *Proc. Natl. Acad. Sci. USA* 1986, 83, 3474-8.
- (6) Alcaraz, G.; Kinet, J.-P.; Liu, T.-Y.; Metzger, H. *Biochem.* 1987, 26, 2569-75.
- (7) Orloff, D.; Ra, C.; Frank, S.; Klausner, R.; Kinet, J.-P. *Nature* 1990, 347, 189-91.
- (8) Rossi, G.; Newman, S.; Metzger, H. *J. Biol. Chem.* 1977, 252(2), 704-11.
- (9) Newman, S.; Rossi, G.; Metzger, H. *Proc. Natl. Acad. Sci. USA* 1977, 74(3), 869-72.
- (10) Ortega, S. F.; Pecht, I. *J. Immunol.* 1988, 141(12), 4324-32.
- (11) Schreiber, A.; Haimovich, J. *Meth. Enzym.* 1983, 93, 147-55.
- (12) Sevier, E.; David, G.; Martinis, J.; Desmond, W.; Bartholomew, R.; Wang, R. *Clin. Chem.* 1981, 27(11), 1797-806.
- (13) Monroe, D. *Anal. Chem.* 1984, 56(8), 920-31.
- (14) Klausner, R.; Van Renswoude, J.; Rivnay, B. *Meth. Enzym.* 1984, 104, 340-7.

- (15) Wold, F. In "Enzyme Structure"; Hirs, C.; Timasheff, S., Eds.; Academic Press: New York, 1972; Vol. 25.
- (16) Kiehm, D.; Ji, T. *J. Biol. Chem.* 1977, 252(23), 8524-31.
- (17) Peters, K.; Richards, F. *Ann. Rev. Biochem.* 1977, 46, 523-51.
- (18) Wang, K.; Richards, F. *J. Biol. Chem.* 1974, 249(24), 8005-18.
- (19) Steck, T. *J. Mol. Biol.* 1972, 66, 295-305.
- (20) Huang, C.-K.; Richards, F. *J. Biol. Chem.* 1977, 252(15), 5514-21.
- (21) Wang, K.; Richards, F. *Isr. J. Chem.* 1974, 12(1-2), 375-89.
- (22) Bayley, H.; Knowles, J. *Eur. J. Biochem.* 1975, 55, 69-115.
- (23) Bayley, H.; Knowles, J. *NYAS* 1980, 45-58.
- (24) Knowles, J. *Accounts of Chemical Research* 1972, 5, 155-60.
- (25) Klip, A.; Gitler, C. 1973, 315-25.
- (26) Gitler, C.; Bercovici, T. *NYAS* 1980, 199-211.
- (27) Klip, A.; Gitler, C. *Biochem. Biophys. Res. Commun.* 1974, 60(3), 1155-62.
- (28) Bayley, H.; Knowles, J. *Biochem.* 1978, 17(12), 2414-9.
- (29) Shih, L.; Bayley, H. *Anal. Biochem.* 1985, 144, 132-41.
- (30) Johns, E. In "Methods in Enzymology"; Kustin, K., Ed.; Academic Press: New York, 1969; Vol. 16.
- (31) Reiser, A.; Leyshon, L. *J. Am. Chem. Soc.* 1970, 92, 7487.
- (32) Leyshon, J. L.; Reiser, A. *J. Chem. Soc. Faraday Trans. 2* 1972, 68, 1918-27.

- (33) Lewis, F.; Saunders, W., Jr. 1967, 645-7.
- (34) Lwowski, W., Ed. "Nitrenes"; Wiley & Sons (Interscience): New York, 1970.
- (35) Bercoici, T.; Gitler, C. *Biochem.* 1978, 17(8), 1484-9.
- (36) Lewis, F.; Saunders, W., Jr. *J. Am. Chem. Soc.* 1968, 90(25), 7033-8.
- (37) Lower, S.; El-Sayed, M. 1965, 199-241.
- (38) Calver, J.; Pitts, J., Jr., Eds. "Photochemistry"; John Wiley & Sons, Inc.: New York, 1966.
- (39) Lessing, H.; Von Jena, A.; Reichert, M. *Chem. Phys. Lett.* 1976, 42(2), 218-22.
- (40) Johnson, P.; Garland, P. *Biochem. J.* 1982, 203, 313-21.
- (41) Garland, P.; Johnson, P. In "Enzymes of Biological Membranes", 2nd ed.; Martonosi, A., Ed.; Plenum Press: New York, 1985; Vol. 1.
- (42) Zwicker, E.; Grossweiner, L. 1963, 67, 549-55.
- (43) Rollie, M.; Ho, C.-N.; Warner, I. *Anal. Chem.* 1983, 55, 2445-8.
- (44) Swoboda, B.; Massey, V. *J. Biol. Chem.* 1965, 240(5), 2209-15.
- (45) Bright, H.; Appleby, M. *J. Biol. Chem.* 1969, 244(13), 3625-34.
- (46) Wiebel, M.; Bright, H. *J. Biol. Chem.* 1971, 246(9), 2734-44.
- (47) Raviv, Y.; Pollard, H.; Bruggemann, E.; Pastan, I.; Gottesman, M. *J. Biol. Chem.* 1990, 265(7), 3975-80.
- (48) Raviv, Y.; Bercovici, T.; Gitler, C.; Salomon, Y. *Biochem.* 1989, 28, 1313-9.
- (49) Saxena, B.; Dattatreya Murty, B.; Ota, H.; Milkov, V.; Rathnam, P. *Biochem.* 1986, 25, 7943-50.
- (50) Raviv, Y.; Salomon, Y.; Gitler, C.; Bercovici, T. *Proc. Natl. Acad. Sci. USA* 1987, 84, 6103-7.

- (51) Garland, P. B.; Moore, C. H. *Biochem. J.* 1979, 183, 561-72.
- (52) Ayyangar, N.; Kalkote, U.; Lugade, A.; Nikrad, P.; Sharma, V. *Bull. Chem. Soc. Jpn.* 1983, 56, 3159-64.
- (53) Von Scholl, R. *Nach Beilstein und Kuhlberg*, A 1873, 169(37).
- (54) Yip, C.; Yeung, C.; Moule, M. *J. Biol. Chem.* 1978, 253(6), 1743-5.
- (55) Anderson, G.; Callahan, F.; Zimmerman, J. *J. Am. Chem. Soc.* 1967, 89(1), 178.
- (56) Denny, J.; Blobel, G. *Proc. Natl. Acad. Sci. USA* 1984, 81, 5286.
- (57) Hawkes, R.; Niday, E.; Gordon, J. *Anal. Biochem.* 1982, 119, 142-7.
- (58) Yoshida, T.; Barisas, B. *Biophys. J.* 1986, 50, 41-53.
- (59) Laemmli, J. *Nature* 1970, 222, 680.
- (60) Mishell, B.; Shiigi, S., Eds. "Selected methods in cellular immunology"; W.H. Freeman and Company: San Francisco, 1980.
- (61) Harlow, E.; Lane, D., Eds. "Antibodies: A laboratory manual"; Cold Spring Harbor Laboratory: Cold Spring Harbor, New York, 1988.
- (62) de Alwis, W.; Hill, B.; Meiklejohn, B.; Wilson, G. *Anal. Chem.* 1987, 59(22), 2688-91.
- (63) Brunner, J. *Meth. Enzym.* 1989, 172, 628-87.
- (64) Eftink, M. R.; Ghiron, C. A. *Anal. Biochem.* 1981, 114, 199-227.
- (65) McLaren, A. D.; Shugar, D. "Photochemistry of Protein and Nucleic Acids"; Macmillan: New York, 1964.
- (66) Fleet, G. W.; Porter, R. R.; Knowels, J. R. *Nature* 1969, 224, 511.
- (67) Grossweiner, L.; Zwicker, E. *J. Chem. Phys.* 1961, 34(4), 1411-7.

- (68) Roitt, I. M.; Bristoff, J.; Male, D. K. "Immunology"; Gower Medical Publishing, Ltd.: London, 1985.
- (69) Kulczycki, A., Jr.; McNearney, T.; Parker, C. J. *Immunol.* 1976, 117(2), 661-5.
- (70) Barisas, B. G.; Rahman, N. A.; Yoshida, T. M.; Roess, D. A. *SPIE* 1989, 1204, 765-74.
- (71) Oretaga, E.; Schweitzer-Stenner, R.; Pecht, I. *The EMBO Journal* 1988, 7, 4101-9.
- (72) Oretaga, E.; Schweitzer-Stenner, R.; Pecht, I. *Biophys. J.* 1989, 1989:500a.
- (73) Matheson, R., Jr.; Van Wart, H.; Burgess, A.; Weinstein, L.; Scheraga, H. *Biochem.* 1977, 16(3), 396-403.
- (74) Reiser, A.; Willets, F.; Terry, G.; Williams, V.; Marley, R. *Trans. Faraday Soc.* 1986, 64, 3265-75.
- (75) Bayley, H.; Knowles, J. *Biochem.* 1978, 17(12), 2420-3.

ABBREVIATIONS

Eosin isothiocyanate	EITC
Bovine Serum Albumin	BSA
5-iodo-naphthyl azide	INA
Immunoglobulin M	IgM
Immunoglobulin E	IgE
Immunoglobulin G	IgG
Sodium Dodecyl Sulfate	SDS
Polyacrylamide gel electrophoresis	PAGE
Rat basophilic leukemia	RBL
Kilo dalton	kDa
Major Histocompatible Class I	MHC-I
Luteinizing hormone	LH
phosphate buffered saline	PBS
ethanol	ETOH
cystalizable fraction	fc
balanced salt solution	BSS
dimethyl sulfoxide	DMSO
B lymphocyte	B-cell
red blood cell	RBC
carbonic anhydrase	CA